

THE  
LONDON, EDINBURGH, AND DUBLIN  
PHILOSOPHICAL MAGAZINE  
AND  
JOURNAL OF SCIENCE.

---

[SEVENTH SERIES.]

FEBRUARY 1934.

XVII. *Investigation of Thin Films of Organic Substances by Electron Diffraction.* By C. A. MURISON, M.A.\*

[Plates VIII. & IX.]

OF recent years much work has been done in the investigation of thin films of long chain organic compounds. Adam †, Langmuir, Rideal, and others have studied the properties of monomolecular films of these substances on water and other liquids. They have found that if the molecules have a water-attracting group at one end this group is fixed in the surface of the water, and if the length of the molecules makes the lateral adhesion between them great enough then they are closely packed together side by side and oriented with their long axes at a steep angle to the surface of the water. On the other hand, if the molecules have a water-attracting group at each end, and are so short that their lateral attraction is small, then they will lie flat on the surface of the water and will move about independently if the film is not compressed into a small area. These two types of film are the two-dimensional analogues of the solid and gaseous states respectively. There are other kinds of films with properties intermediate between these two extremes, but we need not consider them in

\* Communicated by Prof. G. P. Thomson, M.A., F.R.S.

† See Adam's 'Physics and Chemistry of Surfaces,' Chaps. II. & III.

detail. We are here interested primarily in the solid or "condensed" films where the molecules are packed closely together.

Using the method of X-ray diffraction \* Müller, Shearer, Trillat, and others have investigated the structure of rather thicker films of these substances. The method they adopt is to put a thin film of the substance on a glass or mica sheet either by melting, pressing, or evaporation from solution. They then take a reflexion photograph, oscillating the specimen through about  $10^\circ$ . The patterns obtained show that the molecules are arranged so that their ends lie in sheets parallel to the surface on which the specimen is mounted. For some substances, such as the normal hydrocarbons, the molecules are normal to the sheets, but in the case of others, *e. g.*, the fatty acids, alcohols, etc., the molecules are tilted at an angle to the normal. It is found that if the molecule has an oxygen-containing group at or near one end then the distance between the sheets corresponds to two molecules instead of one. The oxygen groups attract each other and the molecules are arranged in pairs, the two members of each pair pointing in opposite directions.

For any one chemical series it is found that the spacing of the sheets increases uniformly with the number of carbon atoms in the molecule, but the increase in spacing for the addition of one carbon atom is not the same for all series. This is due to the molecules being tilted at different angles in the different series, for it has been shown that the hydrocarbon chain has the same structure in every case. The carbon atoms are arranged in a flat zigzag such that the angle between the carbon bonds is approximately equal to the tetrahedral angle as found in the diamond structure. The distance between consecutive  $\text{CH}_2$  groups on the chain is approximately  $1.9 \text{ \AA.}$ , while that between alternate groups is  $2.54 \text{ \AA.}^*$ . The area of cross-section of the chain is  $18.5 \text{ sq. \AA.}$ , which agrees closely with the value found in the work on monomolecular films if allowance is made for the angle of tilt.

#### *Method.*

In the work described here the type of structure shown by various long-chain mixtures is investigated by the

\* Müller, Proc. Roy. Soc. A, cxx. p. 437 (1928).

method of electron diffraction. For purposes of comparison some pure substances are also studied. The diffraction apparatus used is very similar to that described by Prof Thomson \*. A fine beam of fast electrons (about 30,000 volts) passes from the discharge-tube through two small pin-holes in the anode, and is incident at a small grazing angle on the substance to be investigated, which is spread out in a thin film on some form of backing. The diffracted rays are received on a willemite screen or photographic plate. The materials used for the backing are copper, oxidized copper, steel, or glass, and most of the substances investigated are solid at ordinary temperatures, though some are liquids and some greases.

From the point of view of chemical purity they fall into three classes : (1) various mixtures, including oils, greases, and waxes ; (2) some fairly pure but not specially purified substances, liquids or solids ; (3) some very pure substances obtained from Dr. N. K. Adam, all solid and mostly crystalline.

The choice of substances was limited in various ways. Most of them were partially insulating, so charging up took place if the film was made too thick. If the backing used was non-conducting this effect was, of course, greatly increased. Some substances were too volatile, and evaporated off, either because of the low pressure in the apparatus or bombardment by the electron beam, or both.

#### *Preparation of Films.*

The oils and greases were spread into a thin film either by smoothing them over the surface of the block which acted as backing with a clean glass rod or by putting a little of the substance on tissue-paper and rubbing the block to-and-fro through it till a thin uniform film was obtained. The solid substances were generally prepared by heating the metal block on which the film was to be formed until the substance melted, and then smoothing it out with a glass rod while it was still in a liquid or semi-liquid state.

The films varied in thickness over a fairly wide range. Some appeared too thin to give interference colours, while others were as much as 1 mm. thick. This latter

\* Thomson and Fraser, Proc. Roy. Soc. A, cxxviii. p. 641 (1930).

figure was obtained by weighing films prepared from pure substances.

### *Types of Patterns.*

In the case of X-rays the patterns obtained from those long-chain compounds are most easily explained by considering the length of the molecule as containing uniform density of scattering matter. The drop in density at the gap between the ends of the molecules is then the periodic discontinuity which gives rise to the diffraction pattern. For electrons, owing to the shortness of the wave-length (for 30 kv. electrons  $-\lambda=0.07 \text{ \AA.}$ ), the spacing corresponding to the length of the molecule is so great that the rings will fall too close to the central spot to be distinguished. The patterns actually obtained are considered in detail below. There are six different kinds :—

- (a) A straight-line-pattern. Figs. 1 and 2 (Pl. VIII.).
- (b) A straight-line-pattern with spots on the lines. Fig. 3 (Pl. VIII.).
- (c) Sharp rings.
- (d) Diffuse rings or lines curved at the ends. Fig. 4 (Pl. IX.).
- (e) Diffuse rings. Fig. 5 (Pl. IX.).
- (f) Diffuse rings with one spot just inside the second ring. Fig. 6 (Pl. IX.).

### *Patterns (a) and (b).*

Patterns (a) and (b) may be considered together as they are very similar. The line-pattern (a) is obtained from tallow, lard, cetyl alcohol, and tripalmitin. Of these the first two are "mixtures," the third is fairly pure, and the last is one of the very pure substances obtained from Dr. Adam. Pattern (b) is given by tap-grease, vaseline, picein, paraffin-wax, and one liquid—a heavy oil. Two normal hydrocarbons obtained from Dr. Adam also give this pattern. Patterns (a) and (b) together will be referred to as the "grease-pattern."

The lines in this pattern are not evenly spaced on account of the inner potentials of the substances. If allowance is made for this it is found that the spacing ( $d$ ), corresponding to the distance between two lines,

agrees fairly well with the value of  $2\cdot54 \text{ \AA}$ . found by Müller for the distance between alternate carbon atoms in the flat zigzag structure of a long-chain molecule. We shall see that for this pattern the molecules are orientated normal to the free surface.

The values of the spacing ( $d$ ) and the inner potential  $\Phi$  for the various substances are shown in Table I.

It is obvious from the similarity of the patterns obtained from these substances that they are all due to the same structure. We are therefore justified in averaging the values of ( $d$ ) obtained for the different substances.

TABLE I.

Substance.	$d$ .	$\Phi$ .
	$\text{\AA.}$	volts.
Everett's thin tap-grease .....	2.54	5.3
Everett's thick tap-grease .....	2.55	7.2
Vaseline .....	2.48	6.7
Paraffin-wax .....	2.57	1.3
Thermostat oil .....	2.58	5.5
$C_{33}H_{66}$ .....	2.59	1.2
$C_{22}H_{42}$ .....	2.59	1.5
Picein .....	2.59	6.7
Tallow .....	2.62	4.2
Lard .....	2.59	3.1
Tripalmitin.....	2.51	6.5
Average .....	2.56	

The wide variations in the values of  $\Phi$  are probably due to the presence of different amounts of "impurities." This view is supported by the fact that the value for paraffin-wax, which is the least "impure" mixture, containing only hydrocarbons and no fatty acids, agrees within experimental error with the values for the two pure hydrocarbons.

#### Orientation.

The patterns obtained from most of these substances show that the orientation is very complete, although in the case of the first-order line of paraffin-wax the spots show a tendency to be drawn out into short arcs. The pure hydrocarbons are not orientated so perfectly as

the "mixtures," all the spots being drawn out into short arcs. Indeed, in the case of  $C_{22}H_{46}$  faint arcs may be seen crossing between the first and second order lines, showing that there is a certain amount of random arrangement. This is not observed for  $C_{30}H_{62}$ , so it is probable that the longer the molecule the greater is the tendency for orientation, perhaps due to the greater lateral adhesion between molecules.

The sharp pattern of spots obtained with the mixtures is rather surprising, but we must remember that the substances forming these mixtures are all of the long-chain type and, given sufficient lateral adhesion between the molecules, it is natural that these should arrange themselves parallel to each other. There is less chance of small crystals breaking away and lying at random under the influence of mechanical treatment, so that the orientation for the mixtures is more complete than for the pure substances.

#### *Effect of Backing used.*

It was found in the case of tap-grease that patterns obtained from a specimen prepared by rubbing on tissue-paper were generally sharper than those prepared by smoothing out the grease with a glass rod. This is due either to the greater amount of rubbing in the first case giving more perfect orientation or to the orientating effect of the backing being more marked in the case of the thinner film. To test whether the backing has any effect tap-grease specimens were prepared on different substances—rock-salt, glass, and rough copper—but the patterns obtained were not markedly different.

In the case of rock-salt one film of tap-grease was prepared so thin that a strong rock-salt pattern appeared on the plate along with a faint tap-grease pattern. The spacings of the lines were not altered, so it seems that the crystal structure of the backing used has no effect on the orientation of such substances. This agrees with the results of Trillat \*, who decided that the effect of the backing is due more to its chemical nature, whether acid or alkaline, than to its crystal structure.

With rough copper as backing a fairly thick grease film (about .2 mm.) was prepared, but the pattern,

\* Trillat, *Ann. de Physique*, vi. p. 5 (1926).

though not very sharp, was the same as usual. It is not likely that orientation of the molecules could extend through such a thick film, and the effect would also be complicated by the roughness of the copper. In order to test how well-marked the tendency to orientation is, a specimen of tap-grease was prepared on copper, and, to avoid any effects due to rubbing, the grease was melted on to the copper, where it solidified in a drop which was found to be .6 mm. thick where the electrons struck it. The pattern obtained from this specimen was practically the same as the normal tap-grease-pattern. The orientation was as complete as ever, though the background scattering was rather more pronounced. This is strong evidence that the discontinuity at the grease-air interface is sufficient to cause orientation of the molecules, for it is most improbable that any orientation effect due to the backing could be transmitted through so great a distance as .6 mm. Therefore in such a grease film it is possible that there is a thin completely orientated layer at both the grease-metal and grease-air interfaces, while between the two the molecules are arranged at random. Probably rubbing the film increases the thickness which is completely orientated, thus giving a sharper pattern. This would also explain why the friction of such a film decreases with rubbing. It is really impossible to say what thickness of film is orientated without using X-rays.

#### *Explanation of Patterns (a) and (b).*

If the long-chain molecules in a substance are all arranged parallel to each other and normal to the free surface, but otherwise at random, and a plane wave is incident on the substance, then each molecule will scatter independently and the effects of the various molecules will be additive. The directions of maximum intensity of the radiation scattered by the carbon atoms in a molecule will lie on cones with the molecule as axis. The cones intersect the photographic plate in hyperbolæ, but since the incident radiation is almost normal to the molecules, the semi-vertical angles of the cones corresponding to the first few orders are so large that the curves on the plate are not distinguishable from straight lines. The sharpness of the lines will depend on the number of carbon atoms in the molecule.

If now some of the molecules are packed closely together in small groups, the strongest spots corresponding to the side-by-side spacings of the chains will appear. Of these the most important in the hydrocarbon structure is the 110 plane with a spacing of 4.17 Å. This spacing ( $11k$ , see below) corresponds to the strong side-spots on the second order line of the pattern. When these strong side-spots appear the central spot on this line also appears, and is relatively more intense, showing that when the chains are close-packed the carbon atoms of the different molecules are arranged in planes parallel to the surface. This is to be expected from the crystal structure of the hydrocarbon chain. The spacing of this set of planes is the distance between consecutive atoms in the molecule measured parallel to the chain axis, *i.e.*, 1.27 Å. The spots arising from these planes will thus lie in the plane of incidence on the even-order lines.

As the process of packing continues the groups of close-packed molecules become larger and larger; more spots appear on the lines, and the lines themselves become progressively weaker. They never entirely disappear, showing that the molecules do not all form into close-packed groups. The substance is then for the most part a collection of probably rather imperfect crystals which have their long axes all parallel to each other but are orientated at random about that axis. The pattern obtained is thus very similar to that given by a single crystal rotated about its long axis.

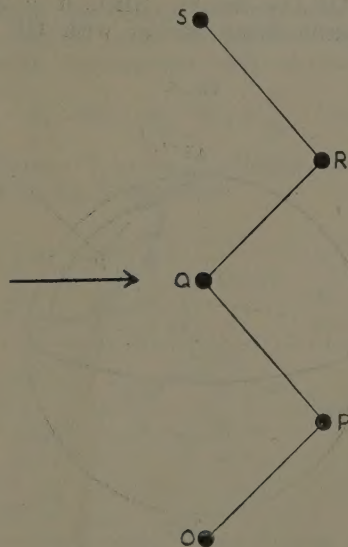
Consider the case where the molecules are all scattering independently. The carbon atoms in a long-chain molecule are arranged in two parallel rows. For simplicity we may suppose one of these rows fixed and different azimuths of the plane of the molecule with respect to the incident beam obtained by rotation about this row as axis. The carbon atoms on the other row will then describe circles lying in planes normal to this axis.

Consider the arrangement of scattering centres O, P, Q, R, S, shown in fig. 7, where the incident radiation is normal to O, Q, S. Let the phase difference between the waves scattered by O and Q in the direction considered be  $\alpha$ , while that between O and P is  $\beta$ . Then the phase difference between the waves scattered by O and R is obviously  $\alpha+\beta$ . If  $\psi_R$  and  $\delta$  are the resultant

amplitude and phase respectively and there are  $n$  scattering centres in each row, then

$$\begin{aligned}\psi_R e^{i\delta} = & \psi + \psi e^{i\alpha} + \psi e^{2i\alpha} + \dots + \psi e^{i(n-1)\alpha} + \psi e^{i\beta} + \psi e^{i(\beta+\alpha)} \\ & + \psi e^{i(\beta+2\alpha)} + \dots + \psi e^{i(\beta+n-1)\alpha},\end{aligned}$$

Fig. 7.



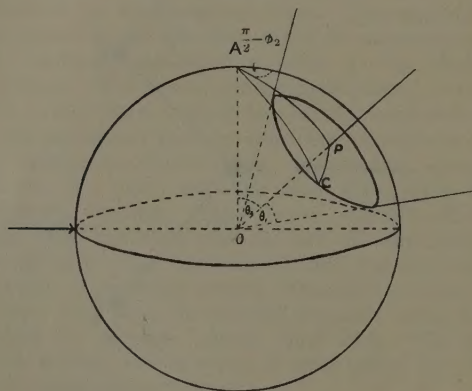
where  $\psi$  is the amplitude of each scattered wave;

$$\begin{aligned}\therefore \psi_R e^{i\delta} = & \psi(1+e^{i\beta}) \frac{1-e^{in\alpha}}{1-e^{i\alpha}} \\ = & \psi \frac{\sin \frac{n\alpha}{2}}{\sin \frac{\alpha}{2}} \cdot e^{i(n-1)\alpha/2} \cdot (1+e^{i\beta}),\end{aligned}$$

whence  $\psi_R^2 = 2\psi^2 \cdot \frac{\sin^2 \frac{n\alpha}{2}}{\sin^2 \frac{\alpha}{2}} (1+\cos \beta).$

In the present case the plane containing the scattering centres may make any angle with the incident beam. Using polar coordinates let OP have direction  $\theta_2\phi_2$ . Then  $\theta_2$  is a constant for the molecule, while  $\phi_2$  may have any value from 0 to  $2\pi$ . Let the incident beam have direction  $\frac{\pi}{2}, \frac{\pi}{2}$ , and let the diffracted ray  $\theta\phi$  make an angle  $\theta_1$  with OP (see fig. 8). Then, if  $\chi$  is the angle that the incident beam makes with OP, the phase

Fig. 8.



difference between the waves scattered from O and P in the direction  $\theta\phi$  is

$$= \frac{2\pi l}{\lambda} (\cos \theta_1 - \cos \chi), \quad \text{where } OP = l.$$

Also  $\cos \chi = \sin \theta_2 \sin \phi_2$ .

From the spherical triangle APC

$$\cos \theta_1 = \cos \theta \cos \theta_2 + \sin \theta \sin \theta_2 \cos \phi - \phi_2$$

$\therefore$  the phase difference  $\beta$

$$= \frac{2\pi l}{\lambda} \{ \cos \theta \cos \theta_2 + \sin \theta \sin \theta_2 \cos \phi \cos \phi_2 \\ + (\sin \theta \sin \theta_2 \sin \phi - \sin \theta_2) \sin \phi_2 \}.$$

The phase difference between the waves scattered from O and Q in the direction  $\theta\phi$

$$\begin{aligned} &= \frac{2\pi}{\lambda} \cdot 2l \cos \theta_2 \cdot \cos \theta \\ &= \frac{4\pi l}{\lambda} \cdot \cos \theta_2 \cos \theta = \alpha. \end{aligned}$$

If there are N molecules whose long axes are all parallel and whose planes make all possible angles with the incident beam, the number with an azimuth between

$$\phi_2 \text{ and } \phi_2 + \delta\phi_2 = \frac{N}{2\pi} \cdot \delta\phi_2;$$

$\therefore$  the intensity I of the radiation scattered in the direction  $\theta\phi$  by the N molecules

$$\begin{aligned} &= \int_0^{2\pi} 2\psi^2 \frac{\sin^2 \frac{n\alpha}{2}}{\sin^2 \frac{\alpha}{2}} (1 + \cos \beta) \cdot \frac{N}{2\pi} \cdot d\phi_2 \\ &= 2N\psi^2 \frac{\sin^2 \frac{n\alpha}{2}}{\sin^2 \frac{\alpha}{2}} + \frac{N\psi^2}{\pi} \frac{\sin^2 \frac{n\alpha}{2}}{\sin^2 \frac{\alpha}{2}} \int_0^{2\pi} \cos \beta d\phi_2 = A + B \text{ say.} \end{aligned}$$

$$\begin{aligned} B &= \frac{N\psi^2}{\pi} \cdot \frac{\sin^2 \frac{n\alpha}{2}}{\sin^2 \frac{\alpha}{2}} \int_0^{2\pi} \cos \left[ \frac{2\pi l}{\lambda} \{ \cos \theta \cos \theta_2 + \sin \theta \sin \theta_2 \right. \\ &\quad \left. \cos \phi \cos \phi_2 + (\sin \theta \sin \theta_2 \sin \phi - \sin \theta_2 \sin \phi_2) \} \right] d\phi_2 \end{aligned}$$

$$= \frac{N\psi^2}{\pi} \cdot \frac{\sin^2 \frac{n\alpha}{2}}{\sin^2 \frac{\alpha}{2}} \int_0^{2\pi} d\phi_2 \cos \left( \frac{2\pi l}{\lambda} \cos \theta \cos \theta_2 \right) \cdot \cos \frac{2\pi l}{\lambda}$$

$$\begin{aligned} &\{ \sin \theta \sin \theta_2 \cos \phi \cos \phi_2 + (\sin \theta \sin \theta_2 \sin \phi - \sin \theta_2 \sin \phi_2) \\ &\quad \sin \phi_2 \} \\ &- \sin \left( \frac{2\pi l}{\lambda} \cos \theta \cos \theta_2 \right) \cdot \sin \frac{2\pi l}{\lambda} \{ \sin \theta \sin \theta_2 \cos \phi \cos \phi_2 \\ &\quad + (\sin \theta \sin \theta_2 \sin \phi - \sin \theta_2 \sin \phi_2) \sin \phi_2 \}. \end{aligned}$$

On integration the second term disappears \* ;

$$\therefore B = \frac{N\psi^2}{\pi} \cdot \frac{\sin^2 \frac{n\alpha}{2}}{\sin^2 \frac{\alpha}{2}} \cdot \cos \frac{\alpha}{2} \cdot \int_0^{2\pi} \cos \left[ \frac{2\pi l}{\lambda} \{ \sin \theta \sin \theta_2 \right.$$

$$\left. \cos \phi \cos \phi_2 + (\sin \theta \sin \theta_2 \sin \phi - \sin \theta_2) \sin \phi_2 \} \right] d\phi_2.$$

An integral of this type has been evaluated \* :

$$B = \frac{N\psi^2}{\pi} \cdot \frac{\sin^2 \frac{n\alpha}{2}}{\sin^2 \frac{\alpha}{2}} \cdot \cos \frac{\alpha}{2} \cdot 2\pi \left\{ 1 + \sum_1^\infty \frac{(-1)^m}{(m!)^2} \left( \frac{p^2 + q^2}{4} \right)^m \right\},$$

where  $p = \frac{2\pi l}{\lambda} \sin \theta \sin \theta_2 \cos \phi,$

$$q = \frac{2\pi l}{\lambda} (\sin \theta \sin \theta_2 \sin \phi - \sin \theta_2);$$

$$\therefore I = 2N\psi^2 - \frac{\sin^2 \frac{n\alpha}{2}}{\sin^2 \frac{\alpha}{2}} \left[ 1 + \cos \frac{\alpha}{2} \left\{ 1 + \sum_1^\infty \frac{(-1)^m}{(m!)^2} \left( \frac{p^2 + q^2}{4} \right)^m \right\} \right].$$

This expression has to be evaluated for the values of  $\theta$  corresponding to the lines of different order. We have already found that these lines correspond to a spacing of  $2.54 \text{ \AA.}$ , so that if  $\theta'$  is the glancing angle and  $n_1$  the order

$$\sin \theta' = \frac{n_1 \lambda}{2d}, \text{ where } d = 2.54. \text{ Also } \theta = \frac{\pi}{2} - 2\theta'.$$

Suppose that  $V = 30,000$  volts, so that  $\lambda = .07 \text{ \AA.}$  The angle  $\theta_2 = 48^\circ$  and  $l = 1.9 \text{ \AA.}$

It is found that the values depend to some extent on whether  $n$  is even or odd, so they have been worked out for  $n=7$  and  $n=8$ . They have been calculated both for the plane of incidence and for a value of  $\phi$  corresponding to a distance of 1 cm. (on the photographic plate) from this plane. The orders considered are the second, third, and fourth, these being the orders of the lines generally obtained (see fig. 1, Pl. VIII.). The intensity of these lines in the plane of incidence was measured by a microphoto-

\* de Haan, 'Tables of Definite Integrals,' p. 143 (Amsterdam, 1858).

meter. In the calculation  $\psi$  has been considered constant, though actually it decreases fairly rapidly with increasing deviation of the diffracted beam. This would help to explain the discrepancy between the measured and calculated values.

The values are given in Table II., where  $I=2N\psi^2I_0$  and  $r_1$  is the distance from the plane of incidence.

TABLE II.  
Intensities of Lines.

$n_1$ .	$r_1 = 0.$		$r_1 = 1 \text{ cm.}$		
	Measured intensity.	$I_0(n=7).$	$I_0(n=8).$	$I_0(n=7).$	$I_0(n=8).$
2	100	100	100	64	64
3	6	.2	1.3	0.2	1.7
4	25	40	30	31	24

### Side-Spots.

The spots on the lines in pattern (b) are measurable only in the case of four substances—tap-grease, paraffin-wax, and the two pure normal hydrocarbons. Owing to the effect of refractive index it is not possible to calculate the effective spacings of the planes giving rise to these spots by measuring their distances from the undeviated central spot. Since refractive index has no effect parallel to the surface of the specimen, the method was adopted of measuring the distances of the spots from the plane of incidence and calculating the spacings corresponding to these distances.

For the small angles occurring in practice we have for any spot \*

$$\frac{d}{n} = \frac{L\lambda}{r}, \text{ i.e., } r = L\lambda \cdot \frac{n}{d},$$

where  $r$ =distance between the spot and the point where the undeviated beam meets the photographic plate.

$L$ =distance between plate and specimen.

$\lambda$ =wave-length.

\* Thomson and Fraser, *loc. cit.*

$d$ =spacing of the planes giving rise to the spot.

$n$ =the order of reflexion.

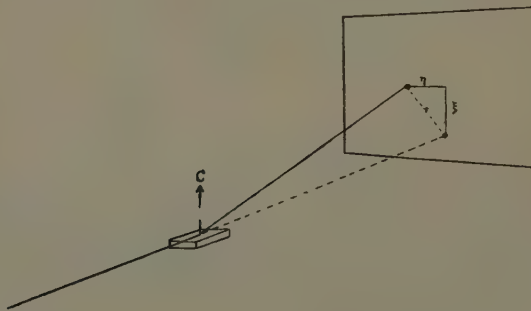
Then, since the axes of the hydrocarbon cell are rectangular,

$$r = L\lambda \sqrt{\frac{h^2}{a^2} + \frac{j^2}{b^2} + \frac{k^2}{c^2}},$$

where  $a, b, c$  are the lengths of the axes of the unit-cell and the order  $n$  is included in the indices  $(h, j, k)$  of the set of planes giving rise to the spot.

Let the spot on the photographic plate have co-ordinates  $\xi\eta$ , where  $\xi$  is measured normal to the shadow edge.

Fig. 9.



If we have a substance in which the crystals are so arranged that the  $c$ -axis is always normal to the free surface, the orientation about it being at random, then with the present experimental arrangement  $\xi$  is measured in a direction parallel to the  $c$ -axis and is a function of  $k/c$  alone (fig. 9).

Actually

$$\xi = L\lambda \cdot \frac{k}{c}, \quad \eta = L\lambda \cdot \sqrt{\frac{h^2}{a^2} + \frac{j^2}{b^2}}.$$

The method used here is equivalent to measuring  $\eta$  alone, and the spacing so obtained is therefore independent of the index  $k$ . The calculated spacings in the table below are derived using Müller's values for " $a$ " and " $b$ ," namely,  $a=7.45 \text{ \AA}$ ,  $b=4.97 \text{ \AA}$ .

TABLE III.

Spacings corresponding to the Side-Spots on the Lines.

*Tap-grease.**Second-order Line :*

Experimental spacing .....	4.00 v.s.	2.46 s.	2.10 f.	1.23 f.
Calculated spacing .....	4.13	2.48	2.06	1.24
Plane .....	11 k.	02 k.	22 k.	04 k

*Third-order Line :*

Experimental spacing .....	5.02 m.	4.04 m.	2.31 f.
Calculated spacing .....	4.97	4.13	2.36
Plane .....	01 k.	11 k.	12 k.

*Fourth-order Line :*

Experimental spacing .....	..	4.09 m.	
Calculated spacing .....	..	4.13	
Plane .....	..	11 k.	

*Paraffin-wax.**First-order Line :*

Experimental spacing .....	5.23 s.	4.20 m.	3.07 f.	2.36 m.
Calculated spacing .....	4.97	4.13	2.98	2.36
Plane .....	01 k.	11 k.	21 k.	12 k.

*Second-order Line :*

Experimental spacing .....	..	4.19 v.s.	2.43 s.
Calculated spacing .....	..	4.13	2.48
Plane .....	..	11 k.	02 k.

 $C_{22} H_{46}$ .*First-order Line :*

Experimental spacing .....	4.80 s.	3.97 m.	3.05 f.	2.36 m.
Calculated spacing .....	4.97	4.13	2.98	2.36
Plane .....	01 k.	11 k.	21 k.	12 k.

*Second-order Line :*

Experimental spacing .....	..	4.05 vs.	
Calculated spacing .....	..	4.13	
Plane .....	..	11 k.	

 $C_{30} H_{62}$ .*First-order Line :*

Experimental spacing .....	..	5.07 s.	2.57 m.
Calculated spacing .....	..	? 4.97	? 2.48
Plane .....	..	? 01 k.	? 02 k.

*Second-order Line :*

Experimental spacing .....	..	4.85 s.	2.36 f.
Calculated spacing .....	..	4.97	2.36
Plane .....	..	01 k.	12 k.

The distances on the plate corresponding to the largest spacings are of the order of 5 mm., so that if we take into account the fact that the spots are not very sharp most of the discrepancy may be considered as due to error in measurement. This view is supported by the smaller spacings being in much better agreement with the calculated values.

The spacings of  $C_{30} H_{62}$  do not agree with those found for all the other substances. The pattern it gives is very similar to the others, the only marked difference being that the central spot on the second-order line is only as strong as the two side-spots near it on either side, instead of being much more intense. No explanation can be given of this difference.

### *Pattern (c) Sharp Rings.*

With the method of preparation generally used (heating and smoothing out with a glass rod) this pattern was obtained with only one pure substance— $\alpha$ -bromostearic acid. It is obviously due to the substance having crystallized out as a large number of small crystals arranged at random. It is strange that this pattern did not occur more frequently for the pure substances, but although they are very pure they do not crystallize very readily, and this method of preparing the film is not likely to promote crystallization.

In the pattern obtained from  $\alpha$ -bromostearic acid the rings are sharp and show no sign of orientation, but owing to the large amount of background scattering they are not easily measurable, and the spacings do not agree very well with the calculated values.

The structure of this substance has been worked out by Müller. He finds

$$a = 11.04 \text{ \AA}, \quad b = 4.90, \quad c = 52.88, \quad \beta = 43^\circ 17'.$$

The experimental and calculated spacings are shown below:—

### *$\alpha$ -bromostearic Acid.*

Experimental spacing.	4.58 v.s.	2.52 m.	2.05 m.	1.72 f.	1.26 f.
Calculated spacing ...	4.11	2.45	2.06	1.89	1.22
Plane .....	110	020	220	400	040

## Pattern (d) Curved Lines.

In this pattern there are a few rings of small radius which show marked orientation. The outer rings are so strongly orientated that they appear only in a small region in and near the plane of incidence. As a result of this it is impossible to say whether they are actually parts of rings or lines slightly curved. They appear rather too straight to be parts of rings. To distinguish them from the inner rings in this pattern they will be described as "curved lines."

Many long chain compounds, mostly alcohols and fatty acids, gave this pattern, but there was so much background scattering that only in the case of two substances,

TABLE IV.

*Stearic Acid :*

Measured spacings . . .	4.21 s.	2.55 m.	..	2.10 m.	1.40 v.s.	.887 f.	.846 f.
Measured angles . . .	0°	28°	..	0°	0°	0°	0°

*Palmitic Acid :*

Measured spacings . . .	3.80 s.	2.46 m.	2.24 m.	2.06 m.	1.29 v.s.	.857 f.	.849 f.
Measured angles . . .	0°	30°	30°	0°	0°	0°	0°

*Stearic Acid :*

Calculated spacings . .	4.12	2.48	2.22	2.06	..	..	..
Calculated angles . . .	0°	34°	25°	0°	..	..	..
Plane . . . . .	110	200	130	220	..	..	..

palmitic and stearic acid, was the pattern measurable. The inner rings all show marked orientation, and the angles between the intense parts of the rings are compared with the angles between the planes giving rise to them. Since palmitic and stearic acid belong to the same chemical series, their crystal structures are the same except for the long spacings, which do not come in here.

The values given by Müller for stearic acid are therefore used in the calculations.

The "measured angles" give the positions of the intense parts of the rings with the plane of incidence taken as 0°. It follows therefore that some of the molecules are lying flat on the surface of the film with the 110 plane parallel to the surface. According to Müller the 110 and 020 planes with spacings of 4.12 and

3.64 Å. respectively give the two strongest rings. No sign of the 020 ring was seen, but the plane makes an angle of about  $60^\circ$  with the 110 plane, so that the maxima on the plate would be more or less on the shadow edge. In the case of palmitic acid the 200 and 130 rings are so close together that it is impossible to differentiate between the positions of their intensity maxima. The spacings are not in very good agreement, but from consideration of the spacings of the curved lines it would appear that in the case of stearic acid at least there is a refractive-index effect.

The three curved lines farther out do not seem to be due to the side-spacings of the chain, as the very strong line is far too intense to arise from any of these. As we shall see, it is very probable that these lines are caused by molecules tilted at an angle to the surface in the manner already described. It may seem improbable that molecules should be arranged in both positions in the film, but in some of his work Trillat \* comes to the conclusion that molecules lying flat are present along with the tilted molecules, and that the two orientations may be mixed to a certain extent. To work out the effect of the tilted molecules we shall consider the simplest possible arrangement where the carbon atoms are taken as being distributed in a straight line along the axis of the molecule, while the molecules themselves are tilted at a constant angle to the normal to the surface but are distributed at random about that normal. If they are considered as scattering independently, the same effect will be obtained by taking a single molecule with one end fixed and allowing it to have all possible positions about the normal. The molecule can then coincide with any generator of the cone whose axis is normal to the free surface and whose semi-vertical angle equals the angle of tilt.

Using polar coordinates, let the molecule have direction  $\theta_2 \phi_2$ .  $\theta_2$  is then equal to the angle of tilt and is constant, while  $\phi_2$  may vary from 0 to  $2\pi$ . Let the wave be incident along  $\frac{\pi}{2}$ ,  $\frac{\pi}{2}$ , and let the distance between the carbon atoms on the axis of the molecule be  $l$ . Then the path difference

\* Trillat, *loc. cit.*

between the rays scattered in the direction  $\theta\phi$  by two adjacent carbon atoms is, as already shown,

$$=l\{\cos\theta\cos\theta_2+\sin\theta\sin\theta_2\cos\phi\cos\phi_2 \\ +(\sin\theta\sin\theta_2\sin\phi-\sin\theta_2)\sin\phi_2\}$$

(see fig. 8, p. 210).

The directions of the diffraction maxima are the generators of cones with the molecule as axis.

For a maximum

$$n\lambda=l\{\cos\theta\cos\theta_2+\sin\theta\sin\theta_2\cos\phi\cos\phi_2 \\ +(\sin\theta\sin\theta_2\sin\phi-\sin\theta_2)\sin\phi_2\}. \dots , \quad (\text{A})$$

In practice  $\theta$  and  $\phi$  are approximately equal to  $\frac{\pi}{2}$ , so that

$$\sin\theta=\sin\phi=1.$$

Let the point where the incident beam strikes the photographic plate have coordinates (0, 0), and let the point of intersection of the molecule produced and the plate be  $(x_2y_2)$ . L is the distance from the specimen to the plate, and  $(xy)$  is the point where a diffracted ray meets the plate,  $x$  and  $y$  being small compared with  $x_2, y_2$  and L :

$$\cos\phi=\frac{x}{L}, \quad \cos\theta=\frac{y}{L}.$$

$$(\text{A}) \text{ becomes } \frac{n\lambda}{l}+\sin\theta_2\sin\phi_2=\cos\theta\cos\theta_2 \\ +\sin\theta_2(\cos\phi\cos\phi_2+\sin\phi_2);$$

$$\therefore \frac{n\lambda}{l}=\frac{y}{L}\cos\theta_2+\frac{x}{L}\sin\theta_2\cos\phi_2;$$

$$\therefore x+(y-\frac{n\lambda L}{l}\sec\theta_2)\cot\theta_2\sec\phi_2=0.$$

This is the equation of a family of parallel straight lines and is the pattern for a definite value of  $\phi_2$ . Owing to the limited number of carbon atoms in the molecule the line will not be very sharp. The complete pattern will be obtained by superposing the lines corresponding to all values of  $\phi_2$ . It is to be noted that all the lines pass

through the point  $(0, \frac{n\lambda L}{l}\sec\theta_2)$ .

From considerations of the atom form-factor of the carbon atom it is obvious that each line will be most intense at the point on it nearest the central spot—that is, at the foot of the perpendicular drawn on it from the centre—and the intensity will fall along the line as the distance from this point increases. The intensity distribution along such a line will depend on its distance from the central spot. A model was prepared in the following way:—The lines for different values of  $\phi_2$  form a divergent pencil passing through the common point. A line in the middle of this pencil was taken, and the intensity distribution along it calculated. A strip of photographic plate 0.2 mm. wide and 6 cm. long was then prepared with approximately this intensity distribution, and exposures were made with this strip placed on a photographic plate in the positions corresponding to values of  $\phi_2$  taken at intervals of  $3^\circ$ . The curve thus obtained was similar to the “curved lines” of fig. 4 (Pl. IX.).

It may be thought that these “curved lines” are rather blurred, considering that they are obtained from very pure substances which X-rays show to be fairly likely to crystallize. It is very likely that the units which are tilted at a fixed angle to the normal are small crystals and not single molecules. In such crystals the gap between the molecules placed end to end is not equal to the spacing of the carbon atoms along the axis of the molecule. There are thus two periodicities present in which the larger is not a multiple of the smaller. Hence at a maximum for the smaller spacing several maxima for the larger spacing will appear, but owing to lack of homogeneity of the electron beam etc. these are not resolved, so that a broad ring is formed.

#### *Patterns (e) and (f).*

These two patterns, namely, blurred rings and blurred rings accompanied by a spot, may be considered together, as some substances gave either pattern, depending on the method of forming the film. Of the substances giving these patterns only one—benzyl phthalate—was fairly pure, all the others being oils. Most of these oils were obtained from Shell-Mex and B. P. Ltd.

According to Rupp \* and Trillat † in liquid long-chain

\* Rupp and Bühl, *Zeits. für Physik*, lxvii. p. 572 (1931).

† Trillat, *Journ. Chim. Phys.* xxvii. no. 10 (1930).

substances the molecules at or near the free surface are orientated normal to it. Rupp reflected electrons of from 100 to 400 volts from the surface of various liquids, keeping the angle of incidence fixed and varying the accelerating voltage. He obtained peaks in his curves, and the spacings calculated from these agree in the case of the pure substances tested with the lengths of the molecules as found by other methods; so he concludes that the molecules are arranged normal to the surface, with their ends lying in planes parallel to it. For some of the oils he obtains more than one spacing, which is to be expected, as they contain molecules of different lengths. The highest spacing he gives is 12.3 Å. for triolein; but some of the spacings, namely, 3 to 6 Å., seem rather small for the length of a long-chain molecule. In the case of paraffin-oil especially his spacing of 4 to 5 Å. corresponds closely to the value of 4.6 Å. found by Müller \* for normal hydrocarbons just above their melting-points, but Müller considers this spacing as being the distance between the hydrocarbon chains, and not the length of the molecule, which is invariably much greater. However, for this oil Rupp states that there are signs of larger spacings.

In his experiments Trillat uses the "tangent-drop" method, in which the X-ray beam is incident tangentially on the surface of a drop of liquid. The curvature of the drop gives the necessary variation in the angle of incidence, so that the specimen does not have to be rotated or oscillated in any way. He finds that liquid fatty acids and alcohols give the most marked orientation effects when the molecules contain nine to twelve carbon atoms. He suggests that the shorter molecules will have less tendency to orientate, while the longer ones probably become twisted. The molecules are orientated normal to the surface instead of being tilted, and the layers are only one molecule thick instead of two as in the solids.

The blurred rings obtained here show no sign of any orientation, but the oils tested by Rupp are without exception heavy oils, and, as has already been stated, such an oil gives a line-pattern similar to that of tap-grease. Within limits the thickness of such an oil film has no effect on the pattern, and Rupp also finds this to be the case.

\* Müller, Proc. Roy. Soc. A, cxxvii. p. 417 (1930).

For all the oils tested, except that which gives the line-pattern, if a thick film is prepared by putting a drop on a copper block and merely allowing it to drain off, then the blurred rings alone are obtained; but in some cases if a thin film of oil is prepared by rubbing on tissue paper then, in addition to the blurred rings, a sharp spot appears on the pattern in the plane of incidence just inside the second ring. We are led to the conclusion that in the case of a thin film, as a result of irregularities in the surface of the backing, some parts are only a few molecules thick, and here the orientation due to the backing extends to the free surface. In other places the film is so much thicker that the orientation is destroyed before the surface is reached. The former region gives rise to the spot, the latter to the blurred rings. On this view the sharpness of the spot should depend on the backing used, and it was in fact observed that the patterns obtained with oxidized copper as backing were sharper than those with copper. Such a comparison is not very rigid, as the appearance also depends on the film thickness, and it is impossible to make this the same for every specimen. In the case of those oils which do not give a spot even in a thin film the tendency of the molecules to orientate must be so slight that nowhere does the orientation extend to the free surface.

It is to be expected that the tendency of the molecules to arrange themselves parallel to each other will depend on the lateral adhesion between them—that is, on their length. In order to test this a series of four oils distilled from one crude were obtained from Shell-Mex and B. P. Ltd. These are of different molecular weights, and it was found that the three of lowest molecular weight show only blurred rings even when prepared in a thin film, while the highest member of the series shows blurred rings when prepared in a thick film, but a spot and two side-spots as well as the rings when the film is thin. Measurement shows that these three spots correspond to the strong spot in the plane of incidence and the two side-spots on the second-order line of the grease-pattern. In the grease-pattern these three are the most intense, so that the spots obtained from this oil may be regarded as the first traces of this pattern. Presumably with an oil containing longer molecules these spots would become more pronounced and the rest of the pattern would appear,

while the rings would grow correspondingly fainter. With molecules of sufficient length the discontinuity at the air-oil interface would be sufficient to cause orientation, and we then arrive at the case of the heavy oil already mentioned, where the orientation shown is independent both of the backing and of the film thickness.

### *Blurred Rings.*

The Bragg spacings of the two blurred rings are very nearly the same for all the specimens tested, the average for twelve liquids being 2.55 and 1.39 Å. respectively. It was thought that these rings might arise from the spacings of the carbon atoms in the molecule. Accordingly the formula of Mark and Wierl \* for the scattering of electrons by organic vapours was applied to the structure of a hydrocarbon chain with eight carbon atoms. The formula for the intensity distribution is

$$I = k \sum_i^n \sum_j^n \psi_i \psi_j \frac{\sin \chi_{ij}}{\chi_{ij}}, \quad \text{where } \chi_{ij} = 4\pi l_{ij} \frac{\sin \theta/2}{\lambda};$$

$\theta$ =angle of deviation of the beam;

$\lambda$ =wave-length;

$l_{ij}$ =distance between atom  $i$  and atom  $j$ ;

$\psi_i$ =scattering power of the atom  $i$ .

The maxima of the intensity curve so obtained are in good agreement with the positions of the two rings, so that, in spite of the approximation involved in applying this formula to a liquid, it seems certain that the rings are formed in this way.

### *Discussion.*

These experiments show that the orientation of long-chain compounds is of a very marked nature. The patterns obtained from the fatty acids do not bring to light any facts which were not previously known from X-ray work, but those given by the greases etc. are quite different from the X-ray patterns obtained with such substances. The line-pattern here obtained is due to the  $\text{CH}_2$  groups in the chain, and the length of the molecule which is the spacing observed in X-ray work is of importance only in so far as it affects the sharpness of the

\* *Ann. Physik*, viii. p. 521 (1931).

lines. With X-rays the spacing of the carbon atoms in the chain is deduced from the distribution of intensity, but here it is directly measurable.

It has been observed that the orientation of a pure hydrocarbon is more pronounced the longer the molecule, due to the greater lateral adhesion between the chains. It is even more marked for impure substances, since these, being composed of molecules of different lengths, are less liable to crystallize, and thus the formation of small crystals arranged at random is avoided.

The more marked orientation of grease as compared with pure substances is no doubt the reason why it acts better as a lubricant. The pure hydrocarbon crystallizes more or less completely, and the formation of random crystals will tend to cause interlocking and prevent relative motion between different parts of the substance. In the case of the grease there are always some molecules not attached to the close-packed groups, as is shown by the continued presence of the blurred lines in the diffraction pattern even when the spots are sharpest. The presence of these "free" molecules will make it easier for the groups to slide parallel to each other, a motion which will be necessary if the surface to be lubricated is very rough compared with molecular dimensions, and in practice this is always the case.

Furthermore, the orientation of the molecules at the grease-metal interface indicates the presence of a strong attractive force, and this attraction will help to prevent the grease from being squeezed out from between the surfaces by pressure.

As is well known there are two types of lubrication—complete or "film" lubrication, where the surfaces moving relative to each other are completely separated by a thick film of lubricant, and "boundary" or "adsorbed-layer" lubrication, where the surfaces are separated by a film either monomolecular or only a few molecules thick. In practice complete lubrication is aimed at, but it is not always possible, so it is desirable that the oil used should be a good "boundary" lubricant—that is, when in the form of a thin film it should be able to resist being squeezed out from between the surfaces by pressure. It is therefore natural to suppose that an oil which gives a diffraction pattern of the kind here described as a "grease"-pattern, will act well as a boundary lubri-

cant. It is found that the higher the molecular weight the greater is the tendency for the liquid to give this pattern when prepared as a thin film, so we may conclude that the lubricating power of such a film increases with the molecular weight. The work of Sir Wm. Hardy \* on the lubricating properties of thin films of pure long-chain compounds in the liquid state shows that their efficiency as a lubricant increases with increasing molecular weight, and thus supports this conclusion.

I wish to thank Messrs. Metropolitan-Vickers for permission to publish this paper. My thanks are also due to Dr. N. K. Adam for the highly purified substances, and to Mr. F. J. Slee, of Shell-Mex and B. P. Ltd., for the samples of the various oils tested. In conclusion, I would like to express my gratitude to Professor G. P. Thomson for his kindly interest and many helpful suggestions during the progress of the work.

#### *Summary.*

The method of electron diffraction was used to investigate a type of pattern obtained with films of certain "grease-like" mixtures spread on various types of backing. This pattern indicates orientation of the molecules normal to the surface of the film, and experiment shows that this orientation is present both at the vacuum-grease and "backing-grease" interfaces. A substance which gives this pattern is likely to act well as a lubricant.

---

**XVIII. The Constancy of the Viscosity of Strong Lithium Chloride Solutions at low Velocity Gradients.** By G. W. SCOTT BLAIR, M.A., and R. K. SCHOFIELD, M.A., Ph.D. (Physics Department, Rothamsted Experimental Station, Harpenden, Herts, England) †.

DATA were presented in an earlier paper ‡ which seemed to show that a strong solution of lithium chloride, when forced through a narrow tube, does not flow in exact conformity with Poiseuille's law. Parallel data for a glycerine-water mixture, having a similar viscosity,

\* Hardy, Proc. Roy. Soc. A, cviii. (1925).

† Communicated by the Authors.

‡ G. W. Scott Blair and R. K. Schofield, Phil. Mag. xi. p. 890 (1931).

revealed no anomaly, and therefore appeared to rule out the possibility that the discrepancies observed when using the lithium chloride solution were due to imperfections in the apparatus. The subsequent publication by Ostwald and Malss \* of data for a lithium chloride solution in which no anomaly is apparent led us to repeat and extend our earlier measurements. Using the same apparatus as before, anomalous flow was confirmed with several solutions of lithium chloride, and was also observed for strong solutions of potassium carbonate and magnesium chloride. Regular behaviour was again found when using glycerine-water mixtures, and, as a further check on the apparatus, mixtures of medicinal paraffin (kerosene) and benzene were used, and no anomaly was found.

An attempt was next made to demonstrate the inconstancy of the viscosity of strong salt solutions by an entirely different method. Two brass cylinders were drilled axially, and threaded on to a thin vertical rod attached by its upper end to a steel torsion wire, the system having a period of 28 sec. The lower cylinder (1.1 cm. radius and 7.5 cm. long) was surrounded by the solution contained in a wide boiling tube (3 cm. diameter), while the upper one (3.7 cm. radius and 7.7 cm. long) served to increase the inertia of the system. A scale of degrees was mounted on the large cylinder and observed through a low-power microscope with an eye-piece cross-wire. Rotational oscillations were started, and the logarithmic decrement of the amplitude determined. Even though the experiments were continued until the amplitude had fallen to half a degree (maximum velocity gradient  $0.003 \text{ sec.}^{-1}$ ), no variation in the logarithmic decrement was found exceeding what would be caused by an error of  $0.1^\circ$  in any single reading (*cf.* Table I.). This result, therefore, confirms and extends those of Ostwald and Malss in which the velocity gradient at the wall for the lowest stress used was  $0.6 \text{ sec.}^{-1}$ .

This being the case, the discrepancies observed with our capillary tube apparatus must be due to some imperfection in the instrument, though it is evident that the defect is a subtle one, seeing that it is selective—always appearing with strong salt solutions, and never with glycerine-water or paraffin-benzene mixtures.

\* Wo. Ostwald and H. Malss, *Koll. Zeits.* lxiii. p. 61 (1933).

TABLE I.

1.	2.	3.	4.	5.	6.	7.	8.	9.	10.	11.
Swing no.	Double amplitude (degrees).	Swing no.	Double amplitude (degrees).	Column 2 $\times 0.3253$ .	Column 2 $\times 0.3253$ .	Swing no.	Double amplitude (degrees).	Column 2 $\times (0.3253)^2$ .	Double amplitude (degrees).	Column 2 $\times (0.3253)^3$ .
1	71.7	41	23.3	23.3	81	7.6	7.6	121	2.4	2.5
6	62.2	46	20.2	20.2	86	6.8	6.6	126	2.1	2.1
11	53.8	51	17.4	17.5	91	5.8	5.7	131	1.8	1.9
16	46.6	56	15.2	15.2	96	5.0	4.9	136	1.6	1.6
21	40.7	61	13.2	13.2	101	4.4	4.3	141	1.4	1.4
26	35.5	66	11.5	11.5	106	3.8	3.8	146	1.2	1.2
31	30.8	71	10.1	10.0	111	3.2	3.3	151	1.1	1.1
36	26.8	76	8.6	8.7	116	2.8	2.8	156	1.0	0.9
41	23.3	81	7.6	7.6	121	2.4	2.5	161	0.8	0.8

A clue was obtained through our carrying out an experiment in which a burette was attached to one end of the capillary tube, the other end as usual being joined to a wide bulb. It was noticed that with the lithium chloride solution the zero showed a progressive fall, indicating an escape of some three cubic centimetres of fluid during a morning's experimentation. This experiment was repeated a number of times, a fall in zero *always occurring with the lithium chloride solution and never with the glycerine-water mixture*. The junctions between the capillary tube and the burette and bulb were made by grinding the ends flat and holding them together by means of sleeves of rubber tubing. The escape could only have occurred through a creep of the salt solution between the glass and the rubber. Further consideration shows that such an escape is more likely in the case of the salt solution, since, owing to its high density, it exerts a greater hydrostatic pressure although this is always below that of the thermostat water surrounding the junction. Quite apart from this, however, a chemical test showed, under equally favourable pressure conditions, a small but definite leakage in the case of lithium chloride and potassium carbonate, but none in the case of glycerine.

That the rubber junctions were responsible for the discrepancies was rendered even more probable by the complete disappearance of the anomalies when the capillary was fused on to the bulbs of the original apparatus. Data obtained for the lithium chloride solution in this way were in complete accord with Poiseuille's law. The dimensions of a capillary with ground ends can be determined more precisely than one which is fused on to a wide tube, and it was for this reason that rubber sleeve joints were originally used. The effective dimensions of a fused-in capillary can, however, be obtained by calibration with a true fluid of known viscosity. Using capillaries calibrated in this way, the deviations from the  $R^4$  law were found as usual with a clay suspension, so that the conclusions which the authors \* have drawn regarding such systems are not affected by the results here recorded.

\* R. K. Schofield and G. W. Scott Blair, Journ. Phys. Chem. xxxiv. p. 248 (1930); G. W. Scott Blair, Journ. Phys. Chem. xxxiv. p. 1505 (1930); R. K. Schofield and G. W. Scott Blair, Journ. Phys. Chem. xxxv. p. 1212 (1931).

Our natural regret that we should have been led to draw unwarranted conclusions about the viscous behaviour of a strong salt solution is tempered by satisfaction in that the flow-meter\*, which is the distinctive feature of our apparatus, was not to blame. In this device the pressure difference developed by allowing the air displaced by the flowing liquid to escape through a capillary tube is measured on an alcohol manometer set at one in ten. The range of the flow-meter can be altered by changing the air capillary. The flow-meter has been subjected to constant test and has proved itself thoroughly reliable. The reading of the flow-meter usually becomes steady after applying the pressure for a few seconds, so that it is very rapid in operation.

We are not aware that the peculiar ability of very strong salt solutions to "creep" between rubber and glass has been observed before, and we hope that by putting on record our own experience we may prevent others from being similarly misled.

#### *Summary.*

Measurements of the logarithmic decrement of a cylinder executing rotational oscillation while immersed in a strong lithium chloride solution revealed no inconstancy in the viscosity, even though the final amplitude was so small that the maximum velocity gradient was only  $0\cdot003 \text{ sec.}^{-1}$ .

The data confirm and extend that obtained by Ostwald and Malss using a capillary viscometer in which the velocity gradient at the wall for the lowest stress was  $0\cdot6 \text{ sec.}^{-1}$ .

The anomalies reported earlier by the authors appear to have been due to the ability of the strong salt solutions used to "creep" under the rubber sleeves which held the capillaries in place, a property not shared by the glycerine-water mixture used to check the standardization of the apparatus. On sealing the joints, the anomalies in the case of the lithium chloride solution disappear, but the clay pastes still show a characteristic behaviour including departure from the  $R^4$  law.

The flow-meter used in this work has proved itself both trustworthy and convenient in operation.

\* G. W. Scott Blair and E. M. Crowther, *Journ. Phys. Chem.* xxxiii. p. 321 (1929).

*XIX. Negative Lengths of Telephone Line.* By A. C. BARTLETT, M.A. (Communication from the Staff of the Research Laboratories of the General Electric Company, Limited, Wembley, England \*.)

#### SUMMARY.

IT is shown that with the help of negative resistance devices it is possible to construct networks which are equivalent to negative lengths of telephone line.

THE distance over which telephone communication can be carried on is limited by the attenuation and phase distortion of the line or cable used : many methods are in use to overcome these effects, but the simplest method would be to construct some device whose properties were those of a negative length of the line and to insert this in the line between transmitter and receiver.

It will be shown that such negative lengths of line can be designed with the help of negative resistance devices †.

Let the physical line under consideration have constants  $R$ ,  $L$ ,  $S$ , and  $C$  per unit length ; then its characteristic impedance will be

$$Z_0 = \sqrt{\frac{R+j\omega L}{S+j\omega C}},$$

and its propagation constant will be

$$\gamma = \sqrt{(R+j\omega L)(S+j\omega C)}.$$

To neutralize completely a length  $l$  of this line we require an artificial line which will have the same characteristic impedance  $Z_0$  as the physical line and a propagation constant equal to  $-Pl$ , i.e., equal and opposite to that of the physical line. Such an artificial line could be realized in a number of ways, three of which are shown in fig. 1, where

$$A = Z_0 \tanh Pl/2$$

and

$$B = Z_0 \coth Pl/2.$$

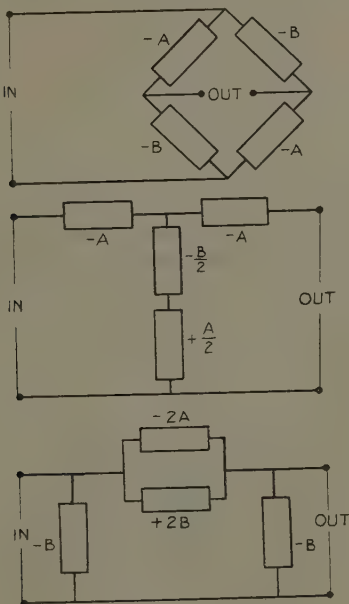
\* Communicated by C. C. Paterson, M.I.E.E.

† British Patent, No. 290,701.

The impedances A and B have physical meanings—they are the input impedances of a length  $l/2$  of the physical line with its far end short- and open-circuited respectively.

It has been shown previously \* that it is possible to construct networks in three different ways that can be made to approximate as nearly as may be desired to

Fig. 1.



both A and B; one type of network that can be used to approximate to A is shown in fig. 2.

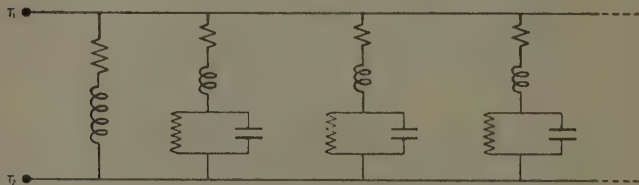
It remains to construct the impedances  $-A$  and  $-B$ . It is easily proved that the impedance of a network as fig. 3, which consists of two positive resistances  $r$ , a negative resistance  $-r$ , and a terminal impedance  $z$ , is equal to  $-r^2/z$ . Consequently if  $z$  is an inductance  $L$ , the impedance of the network is  $-r^2/j\omega L$ , which is equivalent

\* Phil. Mag. xlvi. p. 859 (Nov. 1924).

to that of a negative capacity of value  $-L/r^2$ ; similarly, if  $z$  is a capacity  $C$ , the impedance of the network is  $-jr^2C\omega$ , and is thus that of a negative inductance of value  $-r^2C$  \*. Hence, given a negative resistance device it is possible to construct negative inductances and negative capacities.

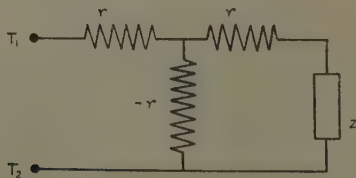
Thus, to obtain the negative impedances  $A$  and  $B$  we

Fig. 2.



could take the network such as fig. 2 for  $A$  or  $B$ , and replace each resistance, capacity, and inductance by its negative. There is, however, a simpler way which requires only one negative resistance for each negative  $A$  or  $B$ : in a well-known way we may derive from the networks for  $A$  and  $B$  reciprocal networks whose impedances

Fig. 3.



are  $r^2/A$  and  $r^2/B$ . If one of these networks, say  $r^2/A$ , is inserted in place of  $z$  in fig. 3, the impedance of the network will be  $-r^2/r^2/A = -A$ , which is the required negative impedance; similarly the impedance  $-B$  can be constructed.

\* Brit. Pat. No. 278,036, J. I. E. E., lxv, pp. 373-6 (1927).

*XX. The Rate of Heating of Wires by Surface Combustion.*  
*By W. DAVIES, B.Sc., Ph.D.\**

THE rate of reaction during the catalytic combustion of gases on solid surfaces is usually inferred from the rate of change in the composition of the gaseous mixtures, but in the case of a metallic wire it is possible to determine the rate of heating due to surface combustion directly by observing the rise of temperature in the wire when it is partially heated in the gaseous mixture by an electric current.

This method was recently adopted by the writer to investigate the errors arising from catalytic action on platinum resistance thermometers when used in researches on gaseous combustion and in internal combustion engine tests, and it has since been employed in a general investigation of the rate of heating of wires of different metals in mixtures comprising a large number of combustible gases and vapours.

The experiments described in this paper were carried out with platinum, palladium, gold and silver wires in mixtures of hydrogen, carbon monoxide and air. The results obtained with the platinum and palladium wires appear to be in accord with Langmuir's theory of the process of catalytic oxidation of gases on solids. The surface conditions for maximum reaction velocities are established on these metals at comparatively low temperatures, and a quantitative analysis of the results shows that the effective rate of combustion is then governed by the diffusive and convective processes which limit the rate of transfer of the reacting gases to the surface of the wire. The concentration of the combustible gas at the surface of the wire is very greatly reduced during reaction owing to the slowness of diffusion, and it is shown in the discussion that this has a very important bearing on the problem of the ignition of explosive gaseous mixtures by hot wires.

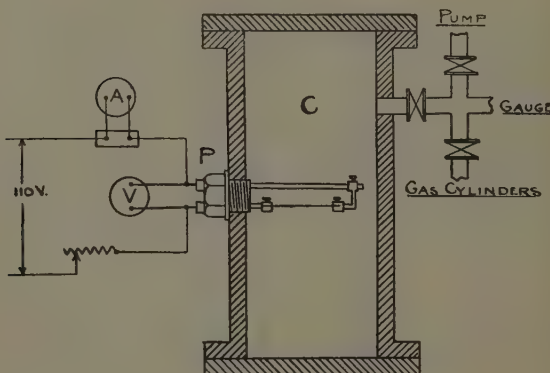
In the case of gold and silver wires there is no evidence of heating due to surface combustion in any mixture of hydrogen and air or carbon monoxide and air at temperatures below the ignition points of the gaseous mixtures.

\* Communicated by Prof. W. T. David, Sc.D., M.Inst.C.E.

*Apparatus and Experimental Procedure.*

The wires to be tested were stretched between two heavy clamps supported on thick brass rods which passed through insulating bushes in the screwed plug P shown in fig. 1. The cast-iron cylindrical vessel C had a capacity of 1 cubic foot, and it was fitted with the usual arrangements for the introduction of different gases in any desired proportion. The wire was connected through an ammeter shunt and rheostat to a source of D.C. supply provided with a number of voltage tappings up to a maximum of 110 volts. The P.D. across the

Fig. i.



terminals of the wire and the current passing through it were measured on a standard Weston instrument, and from these readings the resistance of the wire and the electrical energy supplied to it were determined. The temperature of the wire was deduced from its resistance by referring to a calibration curve based on data obtained by actual measurement of the temperature coefficient of the wire in an electric furnace up to 1100° C.

After filling the vessel with the required gaseous mixture the wire was heated electrically to a higher temperature than its surroundings, and the gases in contact with it were therefore continually renewed by convection. The volume of combustible gas consumed during the time required to take a complete set of

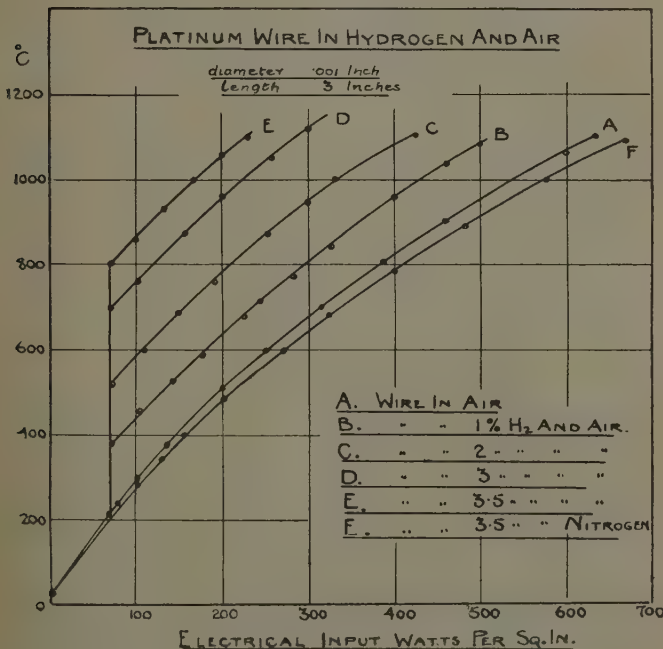
readings was very small compared with the total amount of gas present in the vessel, and the composition of the unburnt gases thus remained sensibly constant during any particular experiment.

### Experimental Results.

#### (1) Platinum Wires in Hydrogen and Air.

The results obtained with mixtures containing from 1 per cent. to 3·5 per cent. of hydrogen and air are shown

Fig. 2.

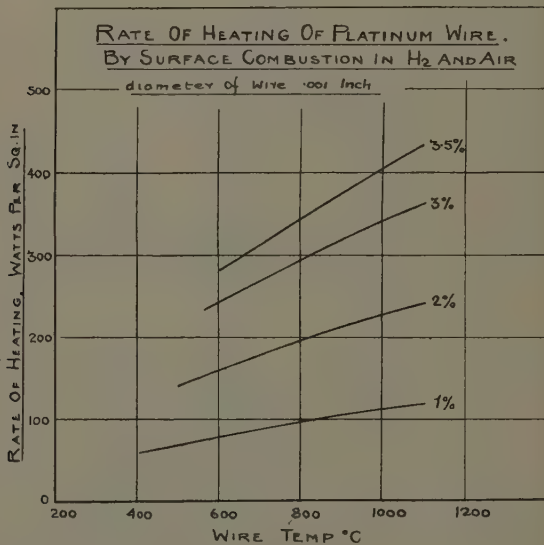


in fig. 2, in which the temperature of the wire is plotted against the electrical input in watts per square inch of wire surface. The rise of temperature in the wire when it is electrically heated in air alone is shown by the curve A. When hydrogen is added to the air the temperature rise for a given electrical input is slightly lower

during the initial stages of heating due to the higher thermal conductivity of the mixture, but at about 200° C. the wire is suddenly heated by surface combustion and its temperature is raised to higher levels, as shown by the curves B, C, D, and E.

In order to differentiate between the heat produced by surface combustion and that due to the electric current a series of experiments were carried out with mixtures containing nitrogen instead of air. The curve

Fig. 3.



F shows the temperature rise in the wire when heated by the current in a mixture of 3.5 per cent. hydrogen and nitrogen, and since the thermal conductivity of nitrogen is nearly equal to that of air, the difference between the electrical inputs shown by the curves E and F practically represents the heat produced on the wire by surface combustion in a similar mixture of hydrogen and air.

The results obtained in this manner for the various hydrogen mixtures are shown in fig. 3. At any given temperature the effective rate of combustion is directly

proportional to the concentration of hydrogen ; therefore the reaction velocity is high enough to enable all the hydrogen molecules which arrive at the surface of the wire to combine with oxygen.

It is evident that under these conditions the hydrogen concentration is lowered in the neighbourhood of the wire, and the rate of heating therefore depends on the rate of diffusion of the combustible gas towards the wire. If, however, the concentration gradient extended to any appreciable distance from the wire the rate of supply of hydrogen would diminish with time, but the observed rates of heating remained sensibly constant for several minutes ; therefore diffusion must be restricted to a very thin film of air surrounding the wire, at the outer boundary of which the concentration of hydrogen is maintained at a steady value by convection.

When this steady state has been attained the concentration gradient within the diffusion film varies inversely as the radius, since the total amount of hydrogen which flows inwards across any concentric shell in unit time must be constant. This consideration leads to the conclusion that the total rate of heating of a wire by surface combustion under these conditions is independent of its diameter, and the rate of heating per unit area therefore varies inversely as the diameter. Within certain limits this was found to be the case, as shown by the results given in Table I.

If very thin wires are used, as in the present instance, the method fails when the amount of hydrogen in air exceeds about 4 per cent., because the temperature rise in the wire due to surface combustion is then sufficient to cause ignition, and a partial or complete explosion ensues according to the mixture strength.

In all the experiments described in this paper the amount of oxygen available was greatly in excess of that required for combustion ; therefore the rate of heating depended only on the rate of diffusion of the combustible gas. Other experiments in which the diffusion of oxygen is also a governing factor will be described in another paper.

#### (2) *Platinum Wires in Carbon Monoxide and Air.*

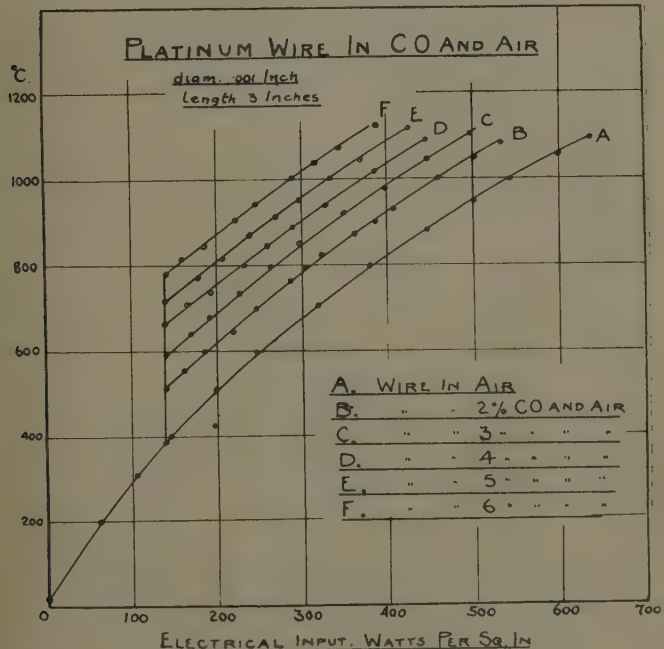
A platinum wire is not heated by surface combustion in carbon monoxide and air until its temperature is raised

TABLE I.  
Rate of heating by surface combustion in watts per sq. inch.

Per cent. $H_2$	Diam. of wire in inches.	Wire temperature °C.						1050	1100
		600	650	700	750	800	850		
1	.001	80	85	88	92	98	102	107	112
	.002	42	42	43	45	46	48	51	52
	.003	28	28	29	30	31	32	34	35
2	.001	160	165	180	182	200	202	215	223
	.002	80	83	86	90	96	100	106	110
	.003	56	58	60	64	66	68	70	73
3	.001	240	253	260	275	285	307	320	335
	.002	120	130	135	142	148	154	160	168
	.003	80	85	90	94	98	107	108	110

to about  $400^{\circ}\text{C}$ . , as shown in fig. 4 ; up to this point the rise of temperature is practically the same as in air, since the addition of carbon monoxide has no appreciable effect on the thermal conductivity of the gaseous mixture. The rates of heating due to surface combustion alone in mixtures containing from 2 per cent. to 6 per cent. of carbon monoxide and air, shown in fig. 5, are con-

Fig. 4.

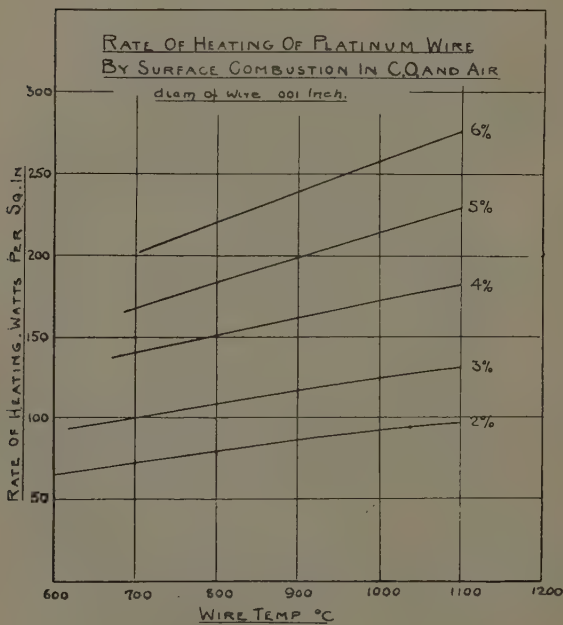


siderably less than those obtained with similar concentrations of hydrogen and air, but this difference is to be anticipated on account of diffusion.

Taking the rates of diffusion of hydrogen and carbon monoxide in air to be in the ratio of 3.83 to 1.115, and the heats of combustion as 57,290 and 68,000 calories per gram molecule respectively, the rates of heating for the same thickness of diffusion film should be in the

ratio of  $\frac{3.83 \times 57,290}{1.115 \times 68,000} = 2.9$ . The difference between this theoretical value and the mean value of the experimental results given in Table II. probably indicates that the diffusion film is somewhat thicker with hydrogen than with carbon monoxide.

Fig. 5.



The curves in fig. 3 and fig. 5 indicate that the effective rate of combustion increases very appreciably with the temperature of the wire, and the results given in Table III. show that the proportional increase in the rate of heating for a given rise of temperature is independent of the nature of the combustible gas and of the ratio of gas to air. This accords fully with the fact that the rate of supply of combustible gas to the wire is limited in each case by the same physical factors to

a value which falls far short of the reactive capacity of the wire.

TABLE II.

Per cent. comb. gas.	Wire temp. °C.	Rate of heating by surface combustion, watts per sq. in.		
		H <sub>2</sub> (a).	CO (b).	$\frac{a}{b}$
2.....	600	160	61	2.62
	700	180	70	2.57
	800	200	76	2.64
	900	215	80	2.69
	1000	230	85	2.71
	1100	240	92	2.61
3.....	600	240	88	2.73
	700	260	100	2.60
	800	285	110	2.59
	900	320	116	2.76
	1000	345	125	2.76
	1100	365	132	2.76
Mean....				2.67

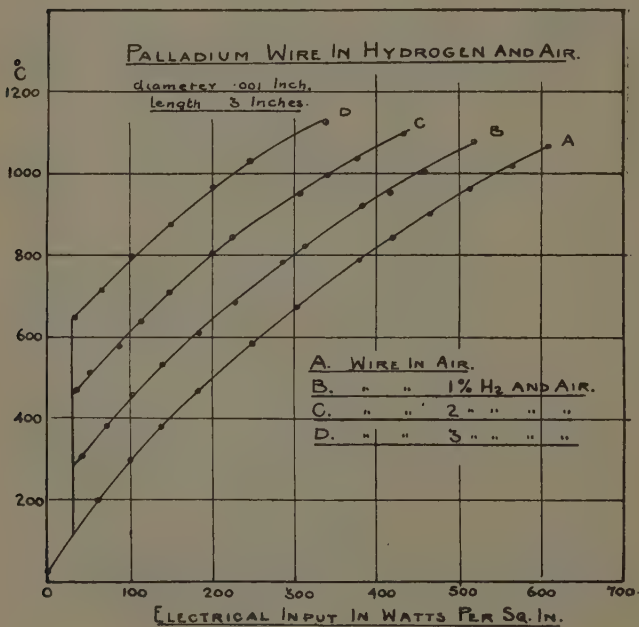
TABLE III.

Comb. gas in air.	Rate of heating in watts per sq. inch at		$\frac{b}{a}$
	600° C. (a).	1100° C. (b).	
1 p.c. H <sub>2</sub> ....	80	120	1.50
2 " H <sub>2</sub> ....	160	240	1.50
3 " H <sub>2</sub> ....	240	365	1.52
3.5 " H <sub>2</sub> ....	287	430	1.50
2 " CO ....	61	92	1.50
3 " CO ....	88	132	1.50
4 " CO ....	125	186	1.49
5 " CO ....	150	230	1.53
6 " CO ....	183	275	1.50

Convection naturally tends to reduce the thickness of the diffusion film, therefore a rise of temperature in

the wire has a twofold effect on the rate of heating, since it accelerates both diffusion and convection, but the extent to which the increase is due to either of these factors alone can only be conjectured. An upper limit to the effect of the acceleration of diffusion is given by

Fig. 6.



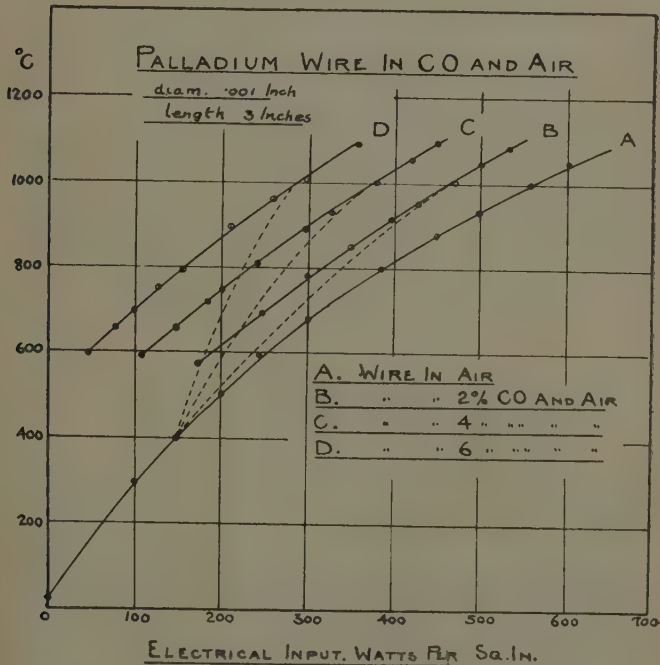
$\sqrt{\frac{1373}{873}} = 1.254$ , which corresponds to a percentage increase of only about half the observed value.

Experiments are now being made to determine whether the effective rate of combustion can be increased to the saturation limit of the active surface by streaming the gases over the wire at higher velocities than are produced by natural convection alone.

(3) *Palladium Wires in Hydrogen and Air and in Carbon Monoxide and Air.*

The results obtained with palladium wires in these mixtures are shown in figs. 6 and 7. In hydrogen and air the wire is first heated by surface combustion at about  $120^{\circ}$  C., as against  $200^{\circ}$  C. in the case of platinum, but

Fig. 7.



apart from this difference the curves in fig. 6 are similar to the corresponding curves for platinum wires shown in fig. 2.

With carbon monoxide, on the other hand, heating by surface combustion commences at about  $400^{\circ}$  C., as in the case of platinum, but the maximum rate is not attained until the temperature of the wire has been raised to a much higher value. During this transition

period the appearance of the wire when it glows suggests that it is heated unequally along its length; therefore the temperature, as inferred from the resistance at this stage, is a mean value to which no special significance can be attached, but it increases with the electrical input in a fairly consistent manner in different experiments, as roughly indicated by the dotted lines in fig. 7. After the maximum rate of heating has been attained surface combustion then proceeds normally, as shown by the full lines, which are exactly similar to the corresponding curves for platinum wires shown in fig. 4. This continues until the temperature is lowered to  $600^{\circ}\text{C}.$ , at this point the wire begins to revert to its initial state, and the rate of heating falls off accordingly.

These results show that above certain temperatures the rate of heating of a palladium wire by surface combustion is the same as that of a platinum wire in similar gaseous mixtures, but it does not necessarily follow from this that the chemical processes are the same on the two metals. The results merely indicate that in both cases the reaction velocity is sufficiently high to bring the same physical factors into effective control.

#### (4) *Platinum and Palladium Wires in Mixtures of Hydrogen, Carbon Monoxide, and Air.*

In mixtures containing both hydrogen and carbon monoxide the latter appears to suppress the hydrogen reaction at low temperatures, since, as shown in fig. 8, the wires are not heated by surface combustion until the temperature approaches that at which carbon monoxide itself begins to react, and in the case of the palladium wire the characteristics of the transition stage are similar to those observed with carbon monoxide alone. The maximum rate of heating is the same on both wires, and the results given in Table IV. show that it is equal to the sum of the rates previously obtained with equivalent concentrations of the combustible gases separately. It appears therefore that above certain temperatures the hydrogen and carbon monoxide reactions proceed concurrently on the surfaces of these wires without hindrance.

Fig. 8.

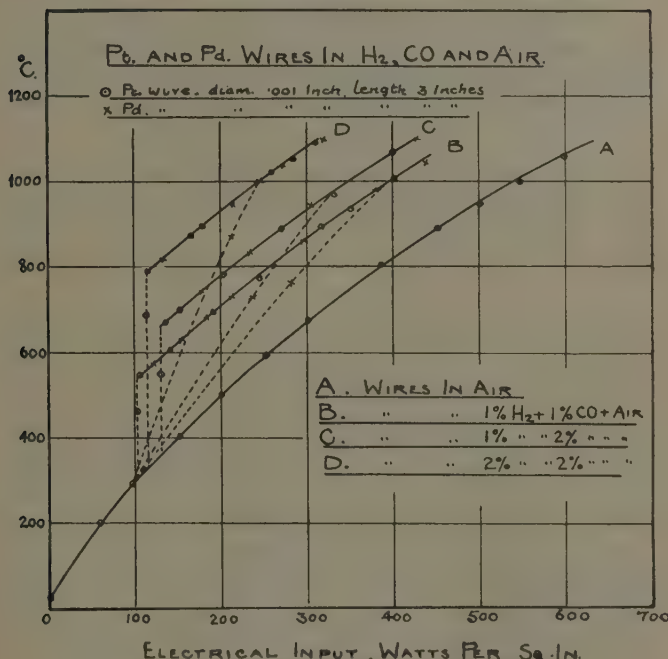


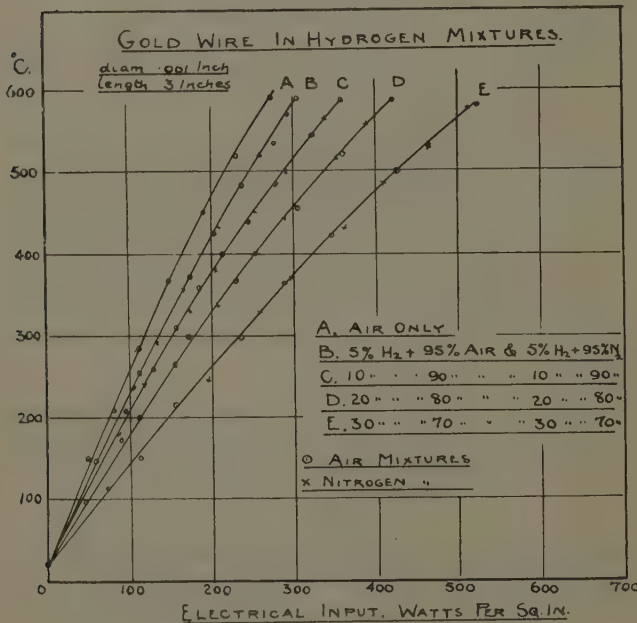
TABLE IV.

H <sub>2</sub> per cent.	CO per cent.	Wire temp. °C.	Rate of heating by surface combustion in watts per sq. in.		
			H <sub>2</sub> .	CO.	Mixture.
1	1	{ 800 1100	98	39	138
			120	45	166
1	2	{ 800 1100	98	76	174
			120	2	212
2	2	{ 800 1100	200	76	273
			240	92	330

## (5) Gold and Silver Wires in Hydrogen and Air and in Carbon Monoxide and Air.

The curves in fig. 9 show that up to about 600° C. the temperature rise in a gold wire in hydrogen and nitrogen is the same as in hydrogen and air; therefore there is no evidence of heating due to surface combustion

Fig. 9.



in the air mixtures at any temperature below the ignition point of the gaseous mixtures. Similar results were obtained with silver wires, and they are equally well represented by the curves in fig. 9, because the rise of temperature for a given electrical input is practically the same in both cases since the heat lost by radiation from wires of this size is negligibly small and differences in emissivity, therefore, have no appreciable effect on the total rate of heat loss.

In the case of these wires hydrogen merely increases the rate of cooling ; thus, with 30 per cent. of hydrogen and air the electrical input for any given rise of temperature is approximately twice that required in air alone.

There is also no evidence of heating due to surface combustion on gold and silver wires in carbon monoxide and air. The temperature rise in any of these mixtures is therefore practically the same as that shown by the curve A in fig. 9, since the thermal conductivity of carbon monoxide does not differ materially from that of air.

### *Discussion.*

According to the adsorption activation theory, which has been developed chiefly by Langmuir, catalytic reactions on solid surfaces are necessarily preceded by the adsorption of one or more of the reactants. Metals of the platinum group adsorb certain gases, including hydrogen, carbon monoxide, and oxygen specifically. Maxted \* states that "the adsorption of oxygen on platinum differs from that of hydrogen and resembles to a certain extent the formation of a non-dissociating chemical compound on account of its non-reversibility, adsorbed oxygen being only removable by degassing if a high temperature is used." Langmuir † has shown that platinum acts as a powerful oxidation catalyst only when its surface is covered by an adsorbed layer of oxygen. In some experiments carried out at very low pressures he found that when a "clean" platinum wire is exposed to a mixture of hydrogen and oxygen, or carbon monoxide and oxygen, at ordinary temperatures its surface is normally covered by an adsorbed layer of the combustible gas in a relatively inactive state, but with rise of temperature a point is reached at which the combustible gas leaves the surface and is replaced by a monomolecular film of oxygen which, in the process of adsorption, becomes extremely active towards the combustible gas. After this transition has taken place every hydrogen or carbon monoxide molecule which

\* 'Catalysis and its Industrial Applications' (1933, J. and A. Churchill).

† Trans. Far. Soc. xvii. p. 621 (1922).

strikes the surface combines with an adsorbed oxygen atom, and the reaction velocity then becomes independent of any further rise of temperature in the wire.

The point at which the wire is initially heated by surface combustion evidently coincides with this transformation on its surface, and one of the advantages of the present experimental method is that it gives a clear indication of the temperature at which the change occurs.

According to the theory the transition temperature depends only on the adsorptive properties of the metal in relation to the combustible gas provided that oxygen is adsorbed at higher temperatures. It would appear from the results that adsorbed carbon monoxide remains stable on platinum and palladium at atmospheric pressure up to about 400° C., but hydrogen at the same pressure is disorbed from platinum at about 200° C. and from palladium at about 120° C. or less.

As regards these temperatures a good deal naturally depends on the initial state of the surface of the wire. Occasionally a new wire was found to be inactive, or more frequently active only along certain portions of its length, until it had been "cleaned" by heating to about 500° C. or more in hydrogen and air. Heating by surface combustion started almost invariably on clean platinum wires at the temperatures shown, but it is to be observed that these wires were all drawn from the same ingot. With palladium wires heating by surface combustion in hydrogen and air sometimes occurred at temperatures as low as 60° C., but these appear to have been exceptional cases.

The results of the experiments with mixtures containing both hydrogen and carbon monoxide, shown in fig. 8, suggest that the surface of the wire is initially covered by carbon monoxide to the exclusion of hydrogen, and the hydrogen reaction is therefore suppressed until the carbon monoxide begins to leave the surface. This appears to be in agreement with the results of Taylor and Burns \*, who found that in the case of platinum and palladium hydrogen, in the presence of carbon monoxide, can only be adsorbed on the surface of a carbon monoxide film and not directly on the metal.

Nitrogen and the products of combustion appear to have no effect on the reaction rates on platinum and

\* J. Am. Chem. Soc. xlvi. p. 1283 (1921).

palladium wires, but Langmuir has shown that nitrogen and carbon dioxide are not adsorbed in measurable quantities by platinum at any temperature, and presumably this applies also to water vapour at high temperatures. It also seems probable that palladium behaves more or less in a similar way in relation to these gases and to water vapour.

Gold and silver evidently do not act as oxidation catalysts to a sufficient extent to produce a measurable rise of temperature in the wires under the condition described, but Bone and Wheeler\* have shown that hydrogen and oxygen combine slowly on the surfaces of these metals at comparatively low temperatures. Sieverts† has shown that oxygen is not sorbed by gold, but Johnson and Larose ‡ found that it diffuses in silver in measurable quantities between 352° C. and 607° C. If, however, specific adsorption of the type which occurs on platinum and palladium does not take place it is to be inferred from Langmuir's theory that high reaction velocities are impossible.

When the conditions for the maximum reaction velocity are established on a platinum or palladium wire of .001 inch diameter the rate at which the combustible gas arrives at the surface is reduced by diffusion to something of the order of 1 per cent. of the rate at which it would strike the wire without restriction.

The rate at which the gas comes into contact with the wire when no reaction is taking place is given by

$$m = p \sqrt{\frac{M}{2\pi RT}},$$

where  $m$  is the mass of gas which strikes the surface in grams per sq. cm. per sec.,  $p$  is the partial pressure of the gas,  $M$  its molecular weight,  $R$  the gas constant, and  $T$  the absolute temperature.

The values of  $m$  given by this expression for some of the mixtures used in the experiments are shown in column 5 of Table V., and the actual values calculated from the observed rates of heating are shown in column 4. The ratios in column 6 indicate that hydrogen and carbon

\* Phil. Trans. A, i, p. 206 (1906).

† Z. Physik. Chem. ix, p. 129 (1907).

‡ J. Am. Chem. Soc. xlvi, p. 1377 (1924); xlix, p. 312 (1927).

monoxide strike the surface of the wire during reaction at only 0·66 per cent. and 0·84 per cent. respectively of the rates given by the formula.

It is evident that the concentration of the combustible gas at an infinitesimal distance from the wire is reduced in the same ratio during reaction, and this enormous dilution probably accounts for the well-known fact that a fine wire must be heated in an explosive mixture of any combustible gas and air to a much higher temperature than the ignition point before a flame is produced and an explosion can take place.

In cases where catalytic combustion occurs the explanation seems obvious. When, for example, a platinum wire

TABLE V.

Comb. gas.	Wire temp. °C.	Rate of heating in calories per sq. cm. per sec.	Mass of combustible gas striking the wire in grams per sq. cm. per sec.		$\frac{a}{b}$
			With reaction (a).	Without reaction (b).	
3 p.c. H <sub>2</sub> . .	800	10·6	·000368	·0566	·0065
1 p.c. H <sub>2</sub> . .	800	3·63	·000126	·01887	·0067
6 p.c. CO . .	800	8·76	·00358	·4234	·0084
2 p.c. CO . .	800	2·89	·00119	·1411	·0084

of ·001 inch diameter is heated up in a mixture of 30 per cent. of hydrogen and air the concentration of hydrogen near its surface is reduced to less than 0·2 per cent. before it reaches the ignition point of the gas, and although the temperature of the wire is now rising extremely rapidly, due to surface combustion, ignition does not occur until just before or after the wire melts.

Even when no catalytic action is involved, as in the case of gold and silver wires, combustion in the gas phase must actually begin on the surface of the wire, and by the time the temperature in the immediate neighbourhood of the wire has been raised to the ignition point the concentration of combustible gas in this region has been reduced to such an extent that it will not propagate

the flame. Explosion will therefore not take place until the temperature gradient is such that the mixture, at a greater distance from the wire, which is rich enough to be inflamed has been raised to the ignition point.

This conception of the mechanism of ignition by hot wires is strongly supported by the fact that any mixture of combustible gas and oxygen in their combining proportions is readily inflamed by a wire as soon as the latter reaches the ignition point, because it is clear that the ratio of combustible gas to oxygen in these mixtures must remain constant right up to the surface of the wire.

My thanks are due to Professor W. T. David for his encouragement and for granting me every facility to carry out this work.

Engineering Department,  
The University, Leeds.

---

*XXI. Steady States produced by Radiation with Application to the Distribution of Atmospheric Ozone. By OLIVER R. WULF, Fellow of the John Simon Guggenheim Memorial Foundation \*.*

THERE are numerous cases where radiation is absorbed in long paths of gas, producing a physical or chemical change which progresses until limited by a reverse process. The latter acts to destroy the product formed by the action of radiation, and to reconvert it to the original absorbing substance. This reverse process may be brought about also by radiation, or, on the contrary, it may depend only on thermal collisions. The system attains a condition, under the constant inflow of radiation, which does not change with time, the rate of production being equal to the rate of destruction, thus causing a steady state. Examples of this are to be found in the atmospheres of planets and stars, involving the processes of photoionization, photo-dissociation, and the photochemical formation of other

\* Communicated by Prof. S. Chapman, M.A., D.Sc., F.R.S.

molecules, such as the formation of ozone in the earth's atmosphere.

In all these cases there are present factors which act to disturb the normal steady state through the mechanical transport of the gases, such as the stirring by winds, convection, and diffusion. These are, however, usually so complicated that it is very difficult to treat their influence with any degree of certainty, and therefore it seems expedient to study the undisturbed steady state first, and afterwards to consider how far the disturbing factors modify it. The present work has to do principally with the undisturbed steady state.

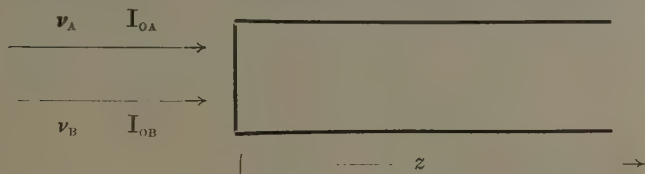
Three quantities usually possess special interest under such conditions. The first is the concentration of the product at any particular depth in the gas-space. The second is the change in this quantity as a function of depth, and therewith, naturally, the position of its maximum, if it possesses such in the distribution which results. The third, which is perhaps of primary importance, is the total amount of product in a column of unit cross-section through the gas-space. Thus in the case of the ionization of the earth's atmosphere it is the total number of ions over one square centimetre of earth's surface. This work deals with these three quantities in steady states where the radiation is absorbed in very long paths. This last condition is important, for under this condition frequencies of radiation possessing a wide range of absorption coefficient values will be totally absorbed in the gas-space. It is the purpose of the present work to point out that there is a marked difference between the distribution of the absorbed radiation and the distribution of the material formed in the steady state, and, in particular, that for the latter the more weakly absorbed deeply penetrating radiation plays an important rôle.

Let us first consider a tube of indefinite length containing a gas A at constant density, and irradiated with light of the frequencies  $\nu_A$  and  $\nu_B$  of initial intensities  $J_{OA}$  and  $I_{OB}$ . These are absorbed in the gases A and B with absorption coefficients  $\alpha$  and  $\beta$  respectively, carrying out thereby the reactions



The tube contains principally A. The molecule B is

produced by the action of light, and the reverse reaction, as well as the forward reaction, is carried out by light.



The absorption of the two frequencies may be represented by the differential equations

$$-dI_A = \alpha \cdot n_A \cdot I_A \cdot dz, \dots \dots \dots \quad (1)$$

$$-dI_B = \beta \cdot n_B \cdot I_B \cdot dz, \dots \dots \dots \quad (2)$$

where  $n_A$  and  $n_B$  represent the number of molecules per unit volume of the two kinds.

Considering the case in which the concentration of A is not appreciably depleted at any point by the radiation process \*, we may integrate (1), obtaining

$$I_A = I_{0A} \cdot e^{-\alpha \cdot n_A \cdot z}. \dots \dots \dots \quad (3)$$

Beside these equations we need only the equation defining this steady-state condition which results from the absorption of light by the molecules A and B.

$$\frac{\gamma_B \cdot \beta \cdot n_B \cdot I_B}{h\nu_B} = \frac{\gamma_A \cdot \alpha \cdot n_A \cdot I_A}{h\nu_A}, \dots \dots \dots \quad (4)$$

where  $\gamma_B$  and  $\gamma_A$  represent the respective quantum efficiencies. This is simply a statement that at any depth the number of molecules of B decomposing per cubic centimetre per second is equal to the number of molecules of B that are formed per cubic centimetre per second, where  $I_B$  and  $I_A$  are the respective intensities.

A further simplification can be made for the present purpose by considering frequency regions over which, despite large variation in the absorption coefficient, the quantum efficiencies remain constant. Thus, for instance, the production of iodine atoms by light absorption in iodine vapour would have the same quantum efficiency over the region 4900–4000 Å., with, however, an

\* Where this is not true it is usually possible to see from the following results approximately what will happen. Failure of this assumption acts to distribute the effect, i.e., as a lower effective value of  $\alpha$ .

enormous variation in the absorption coefficient. Making this simplification we set the ratio  $\frac{\gamma_A \nu_B}{\gamma_B \nu_A} = q$  (a constant).

The equations of interest may now be obtained directly. From equations (3) and (4) we may write

$$\beta \cdot n_B \cdot I_B = q \cdot \alpha \cdot n_A \cdot I_{OA} \cdot e^{-\alpha \cdot n_A \cdot z} \dots \dots \quad (5)$$

Introducing this expression into equation (2), we have

$$dI_B = -q \cdot \alpha \cdot n_A \cdot I_{OA} \cdot e^{-\alpha \cdot n_A \cdot z} dz \dots \dots \quad (6)$$

Upon integration over  $z$  from 0 to  $\infty$  this yields

$$I_B = q \cdot I_{OA} \cdot e^{-\alpha \cdot n_A \cdot z} + C \dots \dots \quad (7)$$

The integration constant is evidently the intensity of  $\nu_B$  remaining after infinite path-length, *i.e.*,  $C = I_{\infty B}$ . It is then also evident that  $I_{OB} = q \cdot I_{OA} + I_{\infty B}$ . Consequently we may write for the final expression for  $I_B$

$$I_B = I_{OB} - q \cdot I_{OA} (1 - e^{-\alpha \cdot n_A \cdot z}) \dots \dots \quad (8)$$

Attention should be called to the fact that no case can properly arise in which  $C = I_{\infty B}$  can have a negative value or can become zero before  $z = \infty$ . If  $I_B$  becomes negligibly small at some finite value of  $z$ , then for greater values of  $z$  the gas is practically 100 per cent. B, and the total amount of B in an infinite path would be infinite. Such a case would lie outside the present treatment, in which it is assumed that  $n_A$  is essentially constant, or somewhat less rigorously, that an appreciable amount of decomposing radiation always remains after the nearly complete absorption of the radiation forming B.

Equation (8) gives the course of the intensity of  $\nu_B$  as a function of depth  $z$ . Substituting this in equation (5), and rearranging, we obtain an expression for  $n_B$ , the number of molecules of B per unit volume as a function of  $z$ ,

$$n_B = \frac{q \cdot \frac{\alpha}{\beta} \cdot n_A \cdot I_{OA} \cdot e^{-\alpha \cdot n_A \cdot z}}{I_{OB} - q \cdot I_{OA} (1 - e^{-\alpha \cdot n_A \cdot z})} \dots \dots \quad (9)$$

This is one of the three desired expressions. It is perhaps clearest to repeat here what was said in the last paragraph, that we are considering that class of cases

in which the denominator of (9) approaches a constant finite positive value as  $z$  approaches infinity.

Differentiation of (9) leads to an expression for the manner in which  $n_B$  changes with the depth  $z$ . It may be written in the form

$$\frac{dn_B}{dz} = -\alpha \cdot n_A \cdot n_B + \beta \cdot n_B^2 \quad \text{or} \quad \frac{d \log n_B}{dz} = -\alpha \cdot n_A + \beta \cdot n_B. \quad \dots \quad (10)$$

Thus  $n_B$  falls away steadily from  $z=0$ , passing through no maximum.

Lastly, the most important expression, that for the total number of B molecules,  $N_B$ , in an indefinitely long path of unit cross-section, may be obtained by integration of (9) from  $z=0$  to  $z=\infty$ . This yields

$$N_B = \frac{1}{\beta} \log \frac{I_{OB}}{I_{OB} - q \cdot I_{OA}}. \quad \dots \quad (11)$$

Thus the total  $N_B$  is inversely as  $\beta$ . It is independent of  $\alpha$ , since  $n_A$  is completely absorbed. If the ratio of  $\frac{\alpha}{\beta}$  is held constant equation (9) shows that the value of  $n_B$  at  $z=0$  remains constant for changing  $\alpha$  and  $\beta$  values, while equation (10) shows that the rate of decrease of  $n_B$  with  $z$  is smaller the smaller are  $\alpha$  and  $\beta$ , since the term in  $n_B^2$  will be very small. The result contained in equation (11), that the weakly absorbed radiations are most effective in producing total B, is then to be expected.

To make this somewhat clearer we may consider the conditions existing under the action of two sets of frequencies  $\nu_A'$  and  $\nu_A''$ , and  $\nu_B'$  and  $\nu_B''$ , such that  $\alpha'$  and  $\beta'$  are much greater than  $\alpha''$  and  $\beta''$ . Such a circumstance could readily exist, for instance, if these frequencies lay in respective continuous absorptions of A and B,  $\nu_A'$  and  $\nu_B'$  lying where the continuous is strongest,  $\nu_A''$  and  $\nu_B''$  where it has fallen to very low values (e. g., as in iodine at 4900 Å. and 4000 Å.). Except for the condition that  $I_{OB} > q \cdot I_{OA}$ , the intensities may all be taken as of the same order. After a very small distance of penetration,  $z$ , the action due to  $\nu_A'$  and  $\nu_B'$  will be essentially ended except for the residual intensity of  $I_B'$ , which is equal to  $I_{OB}' - q \cdot I_{OA}'$ . The total

$B'$  produced so far will have been relatively small, because of the large value of  $\beta''$  (equation 11). This residual intensity of the frequency  $\nu_n'$  will be absorbed by the  $B''$  molecules originating from the action of  $\nu_A''$  and  $\nu_B''$ . The  $B''$  molecules will be somewhat reduced by this, but  $N_B''$  is large because of the low value of  $\beta''$ .

It is clear from this that the decrease in  $n_B$  will not be like the steep short decrease to be expected for strongly absorbed radiations from equation (10), but, on the contrary, will be very gradual, the formation of appreciable amounts of  $B$  being extended over a large distance. This is quite important, for, translated into the case of absorption of radiation incident from outside in an atmosphere distributed in a gravitational field, it means that there will be little tendency toward a layer-like distribution of the product  $B$ .

At this point it may be mentioned that an illustration of such conditions is to be found in the formation of ozone in the earth's atmosphere \*. Solar radiation absorbed by oxygen leads to ozone formation, while radiation absorbed by ozone leads to its decomposition. The above indicates that this ozone will not possess a sharp layer-like distribution, but will be spread over a range of heights, in contrast to the amount of radiation absorbed per unit volume, which is distributed in a rather sharp layer-like fashion. That weakly absorbed ozonizing radiation leads to important quantities of ozone at relatively low altitudes has already been shown † in a somewhat different way in connexion with the absorption of solar radiation in the region of 2200 Å.

Steady states produced by very weakly absorbed radiation are, of course, maintained by very slow processes of formation and decomposition, and hence are the more readily subject to mechanical disturbances such as diffusion, convection, and stirring by winds. These constitute ultimately the limiting factors to such steady states when the absorption of the maintaining radiations grows very weak.

If, instead of being induced by radiation the reverse

\* For recent work in this field see S. Chapman, Phil. Mag. x. p. 369 (1930); Helge-Peterson, 'Communications Magnetique,' No. 13 (Kopenhagen); Mecke, Trans. Farad. Soc. xxvii. p. 375 (1931); Z. physik Chem. Bodenstein Festband; Chalonge, Journ. de physique et le radium, iii. p. 21 (1932).

† Wulf, Phys. Rev. xli. p. 375 (1932).

process is independent of radiation, certain simple cases of this are of interest, and are really more common in experience than the former; for instance, where the initial process is simple excitation by radiation the reverse process depends upon the spontaneous decay of the excited state plus deactivation by collision. Under the simplest conditions equations (4), (9), (10), and (11) then read

$$k \cdot n_B + k' \cdot n_B \cdot n_A = \frac{\alpha \cdot n_A \cdot I_A}{h\nu_A}, \quad \dots \quad (12)$$

$$n_B = \frac{\alpha \cdot n_A \cdot I_{OA} \cdot e^{-\alpha \cdot n_A \cdot z}}{(k + k' \cdot n_A) h\nu_A}, \quad \dots \quad (13)$$

$$\frac{dn_B}{dz} = -\alpha \cdot n_A \cdot n_B, \quad \dots \quad (14)$$

$$N_B = \frac{I_{OA}}{(k + k' \cdot n_A) h\nu_A}. \quad \dots \quad (15)$$

Thus, as was rather obvious at the start, the total number of molecules in the excited state is independent of the magnitude of the absorption coefficient, and increases with decreasing gas density until the frequency of deactivating collisions is small compared to the reciprocal mean life, after which it is independent of gas density. Aside from simple excitation, however, such a case is not often encountered.

Recombination following photodissociation and photoionization is a collision process usually involving a third body. For such cases, letting  $n^v$  represent the concentration of atoms or ions respectively, equations (4), (9), (10), and (11) may be written in a slightly simplified form as

$$k \cdot n_B^2 \cdot n_A = \frac{\alpha \cdot n_A \cdot I_A}{h\nu_A}, \quad \dots \quad (16)$$

$$n_B = \left( \frac{\alpha I_{OA}}{k h\nu_A} \right)^{\frac{1}{2}} e^{-\frac{\alpha \cdot n_A \cdot z}{2}}, \quad \dots \quad (17)$$

$$\frac{dn_B}{dz} = -\frac{\alpha \cdot n_A}{2} \cdot n_B, \quad \dots \quad (18)$$

$$N_B = \left( \frac{4 I_{OA}}{k \cdot \alpha \cdot n_A^2 \cdot h\nu_A} \right)^{\frac{1}{2}}. \quad \dots \quad (19)$$

Thus here the more weakly absorbed radiation produces more of the product than strongly absorbed radiation. Low gas density is, of course, also favourable. To cite an imaginary experiment, if one wished to observe the absorption of iodine atoms produced by photodissociation in a tube of iodine vapour at some constant pressure irradiated with a wave-length lying in the region between 4900 and 4000 Å., it would be advantageous to choose a wave-length which is weakly absorbed by the iodine molecule, say at 4300 Å., instead of one in the vicinity of 4900 Å., up to the point where it ceased to be practical to work with a path long enough to give nearly complete absorption of the dissociating light.

It can be seen from the above that only where the reverse process depends upon the first power of  $n_b$  will the total amount of product be independent of  $\alpha$ , and that for powers of  $n_b$  greater than unity, thus for the majority of cases actually encountered, the weakly absorbed radiation will possess this characteristic advantage because of the sparse but extended distribution of the product which it produces. Thus in the case of atmospheric ozone, in whatever part it may decompose independent of radiation but dependent upon its concentration to a power greater than unity, the radiations which are more weakly absorbed by oxygen possess still an advantage in the total ozone they produce.

Where radiation is incident from outside on an atmosphere distributed in a gravitational field, such as the earth's atmosphere, the amount of effective radiation absorbed per unit volume possesses a layer-like distribution. This is true, for instance, of the radiation absorbed by oxygen which produces ozone and of the ionizing radiation which produces the Heaviside layer. The steady state of ozone produced will, on the contrary, not be layer-like in comparison with the absorbed radiation, but will be spread out over a range of altitudes. In principle this applies as well to the photoionization and photodissociation in the atmosphere, though in these last cases there are factors which act to restrict these phenomena to high altitudes. One is evidently the rapid increase in pressure with depth. There is also the important possibility of step-wise ionization, occurring in two or more processes involving radiation in a much more favourable part of the spectrum

than the extreme ultra-violet. The formation of excited molecules and atoms in metastable states by radiation at high altitudes, where collisions are very infrequent, may mean that the principal part of the photoionization is due to the absorption of radiation of frequencies not far removed from the sun's maximum of intensity by these metastable states.

The conditions in stellar atmospheres, adopting an obviously simplified model for the discussion of the point involved, are, however, the reverse of this. Here radiation streams from within outward through the outer gases \*. The strongly absorbed radiation is absorbed at low altitudes and high pressures where the reverse reaction proceeds rapidly and where the conditions are favourable for the conversion of the absorbed energy into heat. The weakly absorbed radiation, on the contrary, penetrates to the outer layers, and is in part absorbed there where the reverse reaction is slow and the conditions favourable for the maintenance of a high degree of photoionization. Thus in the outer part of stellar atmospheres there should be an excess of ions over that which one would expect from thermal ionization. Since it is also evident that the existence of excited states is favoured by low pressure where deactivating collisions are infrequent, the more weakly absorbed exciting radiations which penetrate to the outer layers of stellar atmospheres should produce an excess of excited states there over that which one would expect from thermal excitation. This has, of course, a limit, in that an appreciable amount of radiation must be absorbed, but in comparison with the very strongly absorbed radiation which is already absorbed at low altitudes, where the gas density is high, those cases of excitation where the absorption coefficient is smaller should lead to an excess of these excited atoms in the high altitudes.

In view of the fact that the case of the earth's atmosphere is of special interest, the formulæ devised for the experimental tube with gas at constant density will be derived for the case of the atmosphere. In proceeding from the surface of the earth outward

\* Equations similar to the above and following can be set up for these conditions.

the intensity of solar radiation increases, and letting  $z$  represent height, equations (1) and (2) take the form

$$dI_A = \alpha \cdot n_A \cdot I_A \cdot dz, \dots \quad (1a)$$

$$dI_B = \beta \cdot n_B \cdot I_B \cdot dz, \dots \quad (2a)$$

Expressing the oxygen distribution with height as  $n_A = n_{OA} e^{-p \cdot z}$ , where  $p$  is a constant and  $n_{OA}$  the number of molecules per cubic centimetre at any height  $z=0$  arbitrarily taken as a base, equation (1a) becomes

$$dI_A = \alpha \cdot n_{OA} \cdot e^{-p \cdot z} \cdot I_A \cdot dz, \dots \quad (1b)$$

which upon integration yields

$$I_A = I_{\infty A} \cdot e^{-\frac{\alpha \cdot n_{OA} \cdot e^{-p \cdot z}}{p}}, \dots \quad (3a)$$

where  $I_{\infty A}$  is the intensity of  $v_A$  outside the atmosphere.

The equation defining the steady state remains the same, namely

$$\frac{\gamma_B \cdot \beta \cdot n_B \cdot I_B}{h\nu_B} = \frac{\gamma_A \cdot \alpha \cdot n_A \cdot I_A}{h\nu_A}, \dots \quad (4)$$

Substituting in (4) we obtain the equation analogous to equation (5),

$$\beta \cdot n_B \cdot I_B = q \cdot \alpha \cdot n_{OA} e^{-p \cdot z} I_{\infty A} e^{-\frac{\alpha \cdot n_{OA} \cdot e^{-p \cdot z}}{p}}. \dots \quad (5a)$$

Introducing this expression into equation (2a) we have

$$dI_B = q \cdot \alpha \cdot n_{OA} e^{-p \cdot z} I_{\infty A} \cdot e^{-\frac{\alpha \cdot n_{OA} \cdot e^{-p \cdot z}}{p}} dz. \dots \quad (6a)$$

Upon integration this yields

$$I_B = q \cdot I_{\infty A} e^{-\frac{\alpha \cdot n_{OA} \cdot e^{-p \cdot z}}{p}} + C. \dots \quad (7a)$$

Setting  $I_B = I_{\infty B}$  for  $z = \infty$ , we find  $C = I_{\infty B} - q \cdot I_{\infty A}$ , and thus finally

$$I = I_{\infty B} - q \cdot I_{\infty A} \left( 1 - e^{-\frac{\alpha \cdot n_{OA} \cdot e^{-p \cdot z}}{p}} \right). \dots \quad (8a)$$

Here again it should be remarked that, despite the constant  $C$ ,  $I_B$  can never be negative nor become zero before  $z = -\infty$ . If  $I_B$  becomes negligibly small at some finite value of  $z$ , then for greater values of  $z$  the gas is

practically 100 per cent. B. Such cases lie outside these equations, which apply to the group in which an appreciable intensity of  $\nu_B$  remains after the nearly complete absorption of  $\nu_A$ . In the case of the production of atmospheric ozone this latter condition holds.

Continuing as before, we may substitute this expression for  $I_B$  into equation (5a), obtaining the expression for the number of molecules of B per unit volume as a function of the height  $z$ .

$$n_B = \frac{q \cdot \frac{\alpha}{\beta} \cdot n_{OA} \cdot e^{-p \cdot z} \cdot I_{\infty A} \cdot e^{-\frac{\alpha \cdot n_{OA} \cdot e^{-p \cdot z}}{p}}}{I_{\infty B} - q \cdot I_{\infty A} \left( 1 - e^{-\frac{\alpha \cdot n_{OA} \cdot e^{-p \cdot z}}{p}} \right)} \quad \dots \quad (9a)$$

Differentiation of this expression with respect to  $z$  leads to

$$\frac{dn_B}{dz} = -p \cdot n_B + \alpha \cdot n_{OA} \cdot e^{-pz} \cdot n - \beta \cdot n_B^2. \quad \dots \quad (10a)$$

Here, because of the character of the distribution of the absorbing gas with height, we do obtain a maximum for  $n_B$ , and setting expression (10a) equal to zero, find for the height of the maximum

$$z_{\max.} = -\frac{1}{p} \log \frac{p + \beta \cdot n_B}{\alpha \cdot n_{OA}}$$

The expression for  $n_B$  (equation 9a) represents a sharp layer-like distribution of B when  $\alpha$  and  $\beta$  are large, but the height of the maximum falls with decreasing  $\alpha$  (the term in  $n_B^2$  may be neglected where  $n_B$  is very small compared to  $n_A$ ), and it is clear that for sufficiently small  $\alpha$  values the maximum will not yet be reached at the earth's surface. Thus, where there are frequencies present with a very wide range of  $\alpha$  values (which is almost invariably the case in molecular absorption), the layer-like distribution of the product is to a large extent lost. Extremely weakly absorbed radiation loses, of course, its practical importance because of disturbing factors, such as diffusion and winds, especially since the position of the maximum falls as  $\log \alpha$ , but this does not affect the principle involved. Substituting in (9a) the expression for  $z_{\max.}$  for the case of  $n_B \ll n_A$ , we see that for a series of pairs of  $\alpha$  and  $\beta$  values of constant ratio but decreasing absolute values (say  $\frac{\alpha}{\beta} = 1$

for the sake of discussion) the concentration of B at each respective maximum is greater, with the maxima lying progressively lower and lower and the concentration of B falling thereafter slower and slower. This is perhaps the simplest way of illustrating the absence of the sharp layer-like characteristic in the resultant distribution.

Integration of (9a) leads to the final expression for  $N_B$ , the total number of molecules over unit area of earth's surface. Integrated from  $-\infty$  to  $+\infty$  this gives

$$N_B = \frac{I}{\beta} \log \frac{I_{\infty B}}{I_{\infty B} - q \cdot I_{\infty A}}, \quad \dots \quad (11a)$$

which is identical with equation (11). Thus the deeply penetrating radiation of small  $\alpha$  values is able to produce large amounts of B in the deep layers under the levels where the decomposing radiation with large  $\beta$  values is already absorbed.

In accordance with a remark made earlier regarding the rates of the processes maintaining the steady state, the action of the very weakly absorbed radiations may be largely obliterated where there are strong disturbing factors that effect the mechanical transport of the gases, and this may result in the establishment of a somewhat more layer-like distribution, since the more strongly absorbed frequencies are least affected.

In the case of a steady state which is maintained in both directions by radiation a moderate decrease in the initial intensity of the decomposing radiation may produce a large increase in the substance produced in the steady state. In accord with remarks made following equations (8) and (8a) it is clear that a transition from the condition in which  $n_A$  is at no point greatly depleted to that in which A is transformed more or less completely into B may occur if the initial intensity of  $v_B$  is sufficiently weakened, for then  $I_B$ , the denominator in equations (9) and (9a), will be negligibly small after passing through a first very short distance of  $z$ . Just such a situation occurs in the oblique entry of radiation into the earth's atmosphere. The radiation received by the outer layers of the atmosphere over the polar regions during the polar night is deflected in toward the earth due to refraction. The more refrangible radiation in the vicinity of the oxygen absorption will be bent inward and absorbed,

while the less refrangible radiation of longer wave-length in the vicinity of the ozone absorption will be less strongly deflected, and hence in part lost to the atmosphere. This should lead to a strengthening of the ozone existing in the steady state over the polar regions, and such seems from observation to be the case. Similar conditions exist as the atmosphere passes from day into night and from night into day, which should tend to leave the ozone quantity greater during the night than during the day. Here, however, the rates of the processes maintaining the steady state play an important rôle, and it is quite possible that in this last case the effect is quantitatively small. The effect depends also upon the extent to which the destruction of ozone is due to other causes than radiation, and is further complicated by the existence of the ozone itself, whose absorption of course affects directly the dispersion of the frequencies lying in this region. The effect has, however, in principle interesting possibilities, and in at least one case seems to act in a direction which is in accord with observation.

*Summary.*

Where steady states are produced by the absorption of radiation in very long paths of gas weakly absorbed radiation plays an important rôle because of its ability to produce large amounts of product in very dilute form—that is to say, sparsely but widely distributed. Such cases arise in the atmospheres of planets and stars. In the instance of the ozone of the earth's atmosphere, which in this paper is worked out in some detail as an example, these considerations show that the ozone will not be distributed as a layer, but will be spread out over a considerable range of altitudes. In the case of stellar atmospheres photoionization and photoexcitation should produce in the high altitudes an excess of ions and excited states over that to be expected from the temperature alone.

I wish to thank the John Simon Guggenheim Memorial Foundation for the opportunity to carry on this work.

**XXII. A Modification of Brillouin's Unified Statistics.**  
*By R. B. LINDSAY, Brown University, Providence,  
Rhode Island, U.S.A.\**

THE fundamental problem in the application of statistics in physics may be said to involve the distribution of certain particles over certain cells with respect to a given property or set of properties. An important case is that in which the latter is the energy. Thus, imagine that we have  $N$  particles of various energies in a physical space of volume  $V$ . A three-dimensional phase space is constructed and divided into shells in such a fashion that the  $i$ -th shell corresponds to energy values lying in the interval from  $E_i$  to  $E_i + dE_i$ , or momentum values in the interval from  $p_i$  to  $p_i + dp_i$ , where, if the energy is kinetic only, as we shall here assume it to be,  $p_i = \sqrt{2mE_i}$ . This shell contains cells of volume  $\hbar^3/VG$  to the number  $\dagger n_i = 4\pi VG/\hbar^3 \cdot p_i^2 dp_i$ , where  $G$  is a numerical factor whose value depends on the statistical aggregate being studied (usually unity for physical gases, but two for photons and electrons). It is now supposed that the  $N$  particles are distributed over the shells so that there are  $N_i$  in the  $i$ -th shell; these, in turn, are to be distributed over the  $n_i$  cells in this shell. The fundamental problem is the evaluation of the ratio  $N_i/n_i$  as a function of  $E_i$ . This constitutes the distribution function, and its form depends on the choice of statistics. The three principal cases are those corresponding to the classical, Bose-Einstein, and Fermi-Dirac statistics indicated below by (A), (B), and (C) respectively in eq. (1).

$$\left. \begin{array}{l} (A) \quad N_i/n_i = e^{\alpha - E_i/kT} \\ (B) \quad N_i/n_i = \frac{1}{-1 + e^{-\alpha + E_i/kT}} \\ (C) \quad N_i/n_i = \frac{1}{1 + e^{-\alpha + E_i/kT}} \end{array} \right\} . . . . . \quad (1)$$

Here  $T$  is the absolute temperature and  $k$  is Boltzmann's gas constant. The quantity  $\alpha$  is a parameter dependent

\* Communicated by the Author.

† See, for example, L. Brillouin, 'Les Statistiques Quantiques,' i. pp. 119, 138.

on T, N, and V. Its value differs with the statistics used and also with the so-called state of degeneracy of the aggregate.

Brillouin \* has lately proposed a unified point of view with respect to these types of statistics. He assumes, contrary to the fundamental assumption of classical statistics, that the capacity of each cell is dependent on the number of particles in it. In particular, for a cell with  $p$  occupants the capacity is  $1-pa$ , where  $a$  is a parameter. Brillouin then shows that for  $a=0$  we are led to the classical distribution function (A), while the choice of  $a=-1$  leads to the Bose-Einstein law (B) and that of  $a=+1$  to the Fermi-Dirac law (C).

It is the purpose of the present paper to examine the consequences of allowing  $a$  to remain to a certain extent unrestricted. The statistical probability for the distribution, *i.e.*, the number of ways of distributing N objects so that there are  $N_i$  in the  $i$ -th shell (further divided among the  $n_i$  cells in this shell) is now readily seen to be

$$W = \frac{N!}{\prod_i N_i!} \cdot \prod_i a^{N_i} (n_i/a)! / (n_i/a - N_i)! \quad . \quad (2)$$

Inquiring for the distribution corresponding to maximum W, subject to the usual constancy of N and the total energy  $E = \sum_i N_i E_i$ , we obtain in the customary manner

the general distribution law

$$\frac{N_i}{n_i} = \frac{1}{a + e^{-\alpha + \bar{E}_i/kT}}, \quad . \quad . \quad . \quad . \quad . \quad (3)$$

which reduces to (A), (B), or (C) according as  $a=0$ ,  $-1$ , or  $+1$ . However, it is not dependent for its validity on these specific choices of  $a$ . In view of the considerable success of the Fermi-Dirac distribution law ( $a=1$ ) it seems pertinent to investigate some of the results of applying the more general formula (3). By varying  $a$  in the neighbourhood of unity we may introduce the physical result of tightening or loosening the Fermi restriction, while at the same time implying less freedom of cell occupancy than on the classical theory. Of course the real physical significance of the various values of  $a$  is here left as an open question.

\* Loc. cit. i. p. 167 ff.

Fortunately the mathematical analysis involved in working with (3) is no more difficult than that used in the usual discussions of the Bose or Fermi statistics. Thus to consider the case of a degenerate aggregate, where  $a \sim e^{-\alpha + E_i/kT}$ , we can evaluate the parameter  $\alpha$  as follows. Using  $E_i/kT = z_i$ , we rewrite (3) in the form

$$\frac{N_i/n_i}{1 \pm e^{-(\alpha + \log(\pm a)) + z_i}} = \dots \quad (4)$$

where the plus or minus sign is to be used according as  $a$  is positive or negative. Confining our attention for simplicity to the case of positive  $a$ , we have, using the proper expression for  $n_i$ ,

$$\begin{aligned} N = \sum N_i &= \frac{2\pi GV}{h^3} (2mkT)^{3/2} \int_0^\infty \frac{\sqrt{z} dz}{a + e^{-\alpha + z}} \\ &= \frac{2\pi GV}{ah^3} (2mkT)^{3/2} \int_0^\infty \frac{\sqrt{z} dz}{1 + e^{-(\alpha + \log a) + z}}. \end{aligned} \quad (5)$$

The integration can now be effected by the usual formulas \*, and yields the result (to the second approximation)

$$\begin{aligned} N &= \frac{4GV}{3\sqrt{\pi ah^3}} (2\pi mkT)^{3/2} (\alpha + \log a)^{3/2} \\ &\quad \left[ 1 + \frac{\pi^2}{8(\alpha + \log a)^2} + \dots \right]. \end{aligned} \quad (6)$$

Solving for  $\alpha$ , we obtain

$$\begin{aligned} \alpha + \log a &= \frac{h^2}{2mkT} \left( \frac{3aN}{4\pi GV} \right)^{2/3} \\ &\quad \left[ 1 - \frac{(2\pi mkT)^2}{12h^4} \left( \frac{3aN}{4\pi GV} \right)^{-4/3} + \dots \right]. \end{aligned} \quad (7)$$

This differs from the corresponding Fermi value only in the presence of the  $\log a$  on the left side and the  $a$  in the factor  $(3aN/4\pi GV)^{2/3}$  on the right.

\* Brillouin, *loc. cit.* ii, p. 384 ff.

In entirely similar fashion we find for the total energy of the degenerate aggregate

$$\begin{aligned} E &= \frac{2\pi GVkT}{h^3} (2mkT)^{3/2} \int_0^{\infty} \frac{z^{3/2} dz}{a + e^{-\alpha z}} \\ &= \frac{3N h^2}{10m} \left( \frac{3aN}{4\pi GV} \right)^{2/3} \left[ 1 + \frac{5\pi^2 m^2 k^2}{3h^4} \left( \frac{3aN}{4\pi GV} \right)^{-4/3} T^2 + \dots \right]. \quad (8) \end{aligned}$$

Again the only difference from the Fermi formula lies in the presence of the  $a$ . The zero-point energy now becomes

$$E_0 = \frac{3Nh^2}{10m} \left( \frac{3aN}{4\pi GV} \right)^{2/3}. \quad . . . . \quad (9)$$

For  $0 < a < 1$ , corresponding to a loosening of the Fermi restriction of at most one particle to a cell,  $E_0$  is smaller than the Fermi zero-point energy. This is easily understood physically from the fact that at absolute zero more particles may now crowd into the cells of lower energy.

One of the early triumphs of the Fermi statistics came in its application to the specific heat of metals. Whereas on the classical statistics the contribution of the free electrons to the specific heat is comparable with that due to the atoms, and hence leads to disagreement with experimental values, on the Fermi statistics the contribution of the electrons is negligible at ordinary temperatures. It is desirable to see how this result is affected by the use of arbitrary  $a$ . Consulting the expression for  $E$  (eq. (8)), we have for the specific heat per electron to the first approximation

$$\frac{1}{N} \frac{dE}{dT} = \frac{\pi^2 mk^3}{h^2} \left( \frac{3aN}{4\pi GV} \right)^{-2/3} T. \quad . . . . \quad (10)$$

This again differs from the corresponding Fermi formula only in the presence of the parameter  $a$ . For  $a > 1$  the contribution of the electrons to the specific heat is even smaller than in the Fermi statistics, while for  $0 < a < 1$  the contribution is greater. It is, however, interesting to note that even for  $a = 1/10$  the electron contribution to the specific heat is still only about 7 per cent. of the classical value at room temperature. It is clear then that the success of the new statistics in handling the specific heat problem does not depend on having  $a = 1$  precisely.

Another test is provided by the application to the electrical and thermal conductivity of metals where the Fermi statistics has proved rather satisfactory, particularly in its deduction of the Wiedemann-Franz law. Here again it is easy to apply the more general distribution law (3). Referring to Brillouin (*loc. cit.* ii. p. 209), we have for the electrical conductivity

$$\sigma = \frac{8\pi e^2 m G k T V_0}{3h^3}, \quad \dots \quad (11)$$

where  $e$  is the electronic charge, and now

$$V_0 = \int_0^\infty \frac{\partial(zL)}{\partial z} \frac{dz}{a + e^{-\alpha+z}} = \frac{1}{a} \int_0^\infty \frac{\partial(zL)}{\partial z} \frac{dz}{1 + e^{-(\alpha+\log a)+z}} \quad \dots \quad (12)$$

in place of the corresponding expression on the Fermi statistics with  $a=1$ . (We are again taking  $a$  with positive sign.) Here it may be recalled that  $L$  (a function of  $z$  and  $T$ ) is the mean free path of the electrons in the metal. The evaluation of  $V_0$  follows the usual procedure for the degenerate case, and we get as the first approximation

$$V_0 = \frac{1}{a} (\alpha + \log a) L(\alpha + \log a), \quad \dots \quad (13)$$

where  $L(\alpha + \log a)$  is the value that the mean free path takes when  $\alpha + \log a$  is substituted for  $z$ . The form (13) replaces  $V_0 = \alpha L(\alpha)$  of the Sommerfeld theory based on Fermi statistics.

The thermal conductivity is similarly obtained as

$$\kappa = \frac{16\pi m G k^3 T^2}{3h^3} V_1 (3V_2/V_1 - 2V_1/V_0) \quad \dots \quad (14)$$

with

$$\left. \begin{aligned} V_1 &= 1/2! \cdot \int_0^\infty \frac{\partial(z^2 L)}{\partial z} \frac{dz}{a + e^{-\alpha+z}}, \\ V_2 &= 1/3! \cdot \int_0^\infty \frac{\partial(z^3 L)}{\partial z} \frac{dz}{a + e^{-\alpha+z}}. \end{aligned} \right\} \quad \dots \quad (15)$$

Evaluation of the integrals yields finally (to an approximation of the same order as that involved in (13))

$$\kappa = \frac{16\pi m G k^3 T^2}{3h^3} \cdot \frac{\pi^2}{6a} \cdot (\alpha + \log a) L(\alpha + \log a), \quad \dots \quad (16)$$

whence for the ratio  $\kappa/\sigma T$  we obtain

$$\kappa/\sigma T = \pi^2/3 \cdot k^2/e^2, \dots \dots \quad (17)$$

which is the Wiedemann-Franz ratio in precisely the form obtained in the Sommerfeld theory based on the Fermi statistics. We have then the interesting result that the value of this ratio is independent of the value of  $a$  (assumed, of course, to be positive).

A further interesting test of the general distribution formula is provided by the calculation of the Thomson thermoelectric coefficient  $\mu$ , defined as the heat evolved or absorbed per second per unit volume of a metallic conductor per unit current density per unit temperature gradient \*. In the notation already used,

$$\mu = kT/e \cdot \frac{\partial}{\partial T} (2V_1/V_0 - \alpha), \dots \dots \quad (18)$$

On substituting the values of  $V_1$  and  $V_0$  given above (eqs. (13) and (15)) we get

$$\mu = -kT/e \cdot \pi^2/3(\alpha + \log a)^2 \cdot \frac{\partial}{\partial T} (\alpha + \log a), \dots \quad (19)$$

and, on further substitution, there finally results as a first approximation

$$\mu = 2\pi^2/3e h^2 \cdot m k^2 T \left( \frac{3aN}{4\pi G V} \right)^{-2/3}, \dots \dots \quad (20)$$

which again reduces to the expression obtained on the Fermi statistics when  $a = 1$ . For  $0 < a < 1$  the value of  $\mu$  given by eq. (20) is larger than the Fermi-Sommerfeld value. It is well known that the experimental values for  $\mu$  are in general much lower than the values calculated using classical statistics and in rather better order of magnitude agreement with those computed on the Fermi statistics. However, in many cases (*e.g.*, gold, copper, cadmium, zinc) the latter are too low to be satisfactory, and in these cases an adjustment of  $a$  less than unity brings about considerably better agreement. For example, in the case of gold the choice of about 0.75 for  $a$  makes the agreement excellent. A precise tabulation of values at this time, however, has been thought unwise partly

\* See again Brillouin, *loc. cit.* ii. p. 213. There is considerable divergence of usage in the definition of the Thomson coefficient. Cf. the comprehensive article of Sommerfeld and Frank, 'Reviews of Modern Physics,' iii. p. 1, 1931. The coefficient discussed above is called  $\mu_E$  by these authors.

because of the uncertainty in the experimental values and partly because the application of the theory is not yet complete. It will be recalled that in the simple form here being discussed the theory based on the Fermi statistics takes no account of differences in the sign of  $\mu$  which are observed experimentally. The introduction of the present discussion is merely for the purpose of pointing out that the general distribution formula is as successful in the study of the Thomson effect as that of Fermi, if not more so. The possibility that the value of  $a$  may depend on the metal in question can hardly be considered seriously without more careful investigation.

The calculation of the entropy using the general formula (2) is of some interest, though a trifle puzzling in its result. Calculating  $\log W$  to the usual approximation, we obtain finally the expression

$$\begin{aligned}\log W = N \log N - N - \sum N_i \log \frac{n_i - aN_i}{N_i} \\ - \frac{1}{a} \sum n_i \log \frac{n_i - aN_i}{n_i},\end{aligned}. \quad (21)$$

which becomes, on substituting for  $N_i/n_i$  from (3).

$$\log W = N \log N - N - \alpha N + \frac{E}{kT} + \frac{1}{a} \sum n_i \log (1 + ae^{\alpha - z_i}). \quad (22)$$

Utilizing the fact that

$$\begin{aligned}\frac{1}{a} \sum n_i \log (1 + ae^{\alpha - z_i}) \\ = \frac{4\pi GV}{ah^3} \int_0^\infty p^2 \log (1 + ae^{\alpha - p^2/2mkT}) dp,\end{aligned} \quad (23)$$

we obtain, on partial integration,

$$\log W = N \log N - N - \alpha N + \frac{E}{kT} + \frac{2}{3} \frac{E}{kT},$$

or for the entropy

$$S = k \log W = kN \log N - kN - k\alpha N + \frac{5}{3} \frac{E}{T}. \quad (24)$$

The substitution of  $\alpha$  from (7) and  $E$  from (8) finally yields to a first approximation for the case of positive  $a$

$$S = kN \log N - kN + kN \log a + \frac{\pi^2 k^2 m NT}{h^2} \left( \frac{3aN}{4\pi GV} \right)^{-2/3} + \dots \quad (25)$$

The zero-point entropy therefore becomes

$$S_0 = kN \log N - kN + kN \log a. \dots . \quad (26)$$

Now when  $a=1$  this should reduce to the value for the Fermi statistics, viz.,  $S_0=0$ . That it does not do so arises from the fact that in our general expression for  $W$  (eq.(2)) we have retained the factor  $N!$ , which does not appear in the Fermi expression for  $W$ . Indeed, it will be recalled that the latter is simply

$$W_F = \prod_i \frac{n_i!}{N_i!(n_i-N_i)!}, \dots . \quad (27)$$

viz., the expression (2) for  $a=1$  with the factor  $N!$  omitted. The omission of this factor in the general expression for  $W$  leads to

$$S_0 = kN \log a,$$

which, while reducing to the Fermi value for  $a=1$ , leads to negative  $S_0$  for  $a<1$ . Indeed, it would mean that at absolute zero  $W=a^N$ , or  $W<1$  for  $a<1$ . It is difficult to believe that the slightest alteration of  $a$  from unity should make the number of complexions at absolute zero less than unity ; hence it is probable that in computing the zero-point entropy for  $a$  different from unity the factor  $N!$  in  $W$  should be retained. This point needs further investigation. The significance of the factor for the special cases  $a=-1, 0, +1$  has already given rise to much discussion \*.

### XXIII On the Operability of a Salient-Pole Alternator on an Infinite Bus. By W. H. INGRAM, School of Engineering, Columbia University †.

A GENERALIZATION of Hopkinson's formula ‡, connecting power, voltage, and relative rotor angle to the case of salient-pole machines leads to a generali-

\* Cf. Brillouin, *loc. cit.* i. p. 171 ff.

† Communicated by the Author.

‡ The formula for a machine of constant armature inductance

$$pz^2 + e_0 e_0^* r = e_0 e_0^* z \sin (\psi + \tan^{-1}(r/x))$$

is due to J. Hopkinson, 'Original Papers,' i. p. 138.

zation of the power-angle diagram given elsewhere †. A three-phase star-connected orthocyclic alternating-current motor, dynamically specified by the functions

$$\left. \begin{aligned} T &= \frac{1}{2} \sum \sum l_{jk} \dot{q}_j \dot{q}_k + \frac{1}{2} \mathbf{L} i^2 + \frac{1}{2} L I^2 + \frac{1}{2} \Theta \dot{\theta}^2 \\ &\quad + \sum m_j(\theta) \dot{q}_j i + \mathbf{M} i \mathbf{I} + \sum M_j(\theta) I \dot{q}_j, \\ V &= 0, \\ S &= \frac{1}{2} r (\dot{q}_1^2 + \dot{q}_2^2 + \dot{q}_3^2) + \frac{1}{2} \mathbf{R} i^2 + \frac{1}{2} R I^2 + \frac{1}{2} s \dot{\theta}^2, \\ U &= \sum e_j \dot{q}_j + E I - f \dot{\theta}, \end{aligned} \right\} \quad (1)$$

where  $T$  is the kinetic energy,  $V$  the potential energy,  $S$  the Rayleigh dissipation, and  $U$  the activity of the external forces on the machine, for which the busbars are maintained at sinusoidal potentials  $e_1$ ,  $e_2$ , and  $e_3$  with respect to ground, which is connected to a shaft load which exerts a reactive torque  $f$  on the rotor, and whose field circuit contains a source of e.m.f.  $E$ , will be considered.

The equations of motion are given by the formula

$$\frac{\partial(U-S)}{\partial \dot{q}_r} = \frac{d}{dt} \left( \frac{\partial(T-V)}{\partial \dot{q}_r} \right) - \frac{\partial(T-V)}{\partial q_r}, \quad \dots \quad (2)$$

and are

$$\left. \begin{aligned} e_k &= r \dot{q}_k + \frac{d}{dt} [\sum l_{jk} \dot{q}_j + m_k i + M_k I], \\ 0 &= \mathbf{R} i + \frac{d}{dt} [\sum m_k \dot{q}_k + \mathbf{L} i + \mathbf{M} I], \\ E &= R I + \frac{d}{dt} [\sum M_k \dot{q}_k + \mathbf{M} i + L I], \\ -f &= \Theta \ddot{\theta} + s \dot{\theta} - \{ \sum m_k' \dot{q}_k i + \frac{1}{2} \sum \sum l_{jk}' \dot{q}_j \dot{q}_k + \sum k' \dot{q}_k I \}, \end{aligned} \right\} \quad . \quad (3)$$

where the self and mutual inductances of the armature circuits are given by

$$l_{jk} = l^* l_{jk} - l_m - l_\mu \cos(2\theta - (j+k)2\pi/3), \quad \dots \quad (4)$$

where  $l_{jk}$  is a quantity equal to unity when  $j=k$  and otherwise zero. The inductance mutual to the field

† Ingram, Proc. Camb. Phil. Soc. xxviii. p. 106 (1932); the factor  $\frac{1}{2}\sqrt{2}$  should be inserted on the right of the equality sign of the first two equations of (2) of this paper. Also, in the footnote on p. 108 read saturation for "armature reaction."

circuit and the  $k$ th armature circuit are assumed to have the form

$$M_k^* = M_0 \sin(\theta - 2k\pi/3), \dots \quad (5)$$

and the inductance mutual to the amortisseur circuit and the  $k$ th armature circuit to have the form

$$m_k = m_0 \sin(\theta + \alpha - 2k\pi/3), \dots \quad (6)$$

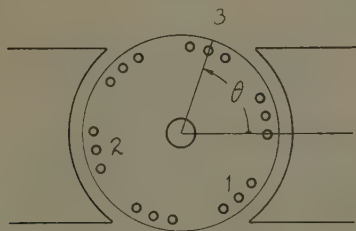
where  $\alpha$  is the inclination of the amortisseur to the field winding.

In the case of salient-pole machines it is more convenient to adapt the origin of time to the internal e.m.f.

$$e_k^* = \sqrt{2}e_0^* \cos \theta_k = \omega M_0 I_0 \cos \theta_k, \dots \quad (7)$$

where  $\theta_k = \theta - 2k\pi/3$ , rather than to the bus voltage, so the steady-state solution for rotor coordinate, field

Fig. 1.



current, amortisseur current, and armature currents are taken to be

$$\left. \begin{aligned} \theta &= \omega t, \\ I_0 &= E_0/R, \\ i &= 0, \\ \dot{q}_k &= \sqrt{2}q_0 \cos(\omega t - \gamma + \psi - 2\pi k/3), \end{aligned} \right\} \quad \dots \quad (8)$$

where  $\gamma$  is the angle of lag of the current and  $\psi$  the angle of lag of the internal e.m.f. behind the bus-voltage

$$e_k = \sqrt{2}e_0 \cos(\theta_k + \psi). \dots \quad (9)$$

The flux linking the field winding at synchronous running due to the armature currents is

$$\Sigma M_k \dot{q}_k = \frac{3}{2} \sqrt{2} M_0 q_0 \sin(\gamma - \psi), \dots \quad (10)$$

where  $\gamma - \psi$  is the angle of lag of the current behind the

internal electromotive force. This flux is constant, and may be ascribed to the fictitious current  $\xi$ , given by

$$\left. \begin{aligned} \dot{\xi} &= \dot{q}_1 \sin \theta_1 + \dot{q}_2 \sin \theta_2 + \dot{q}_3 \sin \theta_3, \\ \dot{\eta} &= \dot{q}_1 \cos \theta_1 + \dot{q}_2 \cos \theta_2 + \dot{q}_3 \cos \theta_3, \end{aligned} \right\} \quad \dots \quad (11)$$

where  $\eta$  is a constant current tending to produce flux in the transverse axis.

The system (11) is the transformation of variable peculiar to the Blondel view-point.

The star-point may be connected through an impedance  $z_s$  to ground, so that the current through this impedance is given by

$$\dot{\xi} = \dot{q}_1 + \dot{q}_2 + \dot{q}_3; \quad \dots \quad (12)$$

dynamically,  $\xi$ ,  $\eta$ ,  $\zeta$ , are quasi-coordinates.

The substitution of variable (11) and (12) may be inverted to give

$$\left. \begin{aligned} \dot{q}_1 &= \frac{2}{3}\dot{\xi} \sin \theta + \frac{2}{3}\dot{\eta} \cos \theta_1 + \frac{1}{3}\dot{\zeta}, \\ \dot{q}_2 &= \frac{2}{3}\dot{\xi} \sin \theta_2 + \frac{2}{3}\dot{\eta} \cos \theta_2 + \frac{1}{3}\dot{\zeta}, \\ \dot{q}_3 &= \frac{2}{3}\dot{\xi} \sin \theta_3 + \frac{2}{3}\dot{\eta} \cos \theta_3 + \frac{1}{3}\dot{\zeta}, \end{aligned} \right\} \quad \dots \quad (13)$$

and in terms of the currents  $\dot{\xi}$ ,  $\dot{\eta}$ , and  $\dot{\zeta}$  the activity function becomes

$$U = \Sigma e_k \dot{q}_k + EI - f\theta = e_d \dot{\xi} + e_i \dot{\eta} + \frac{1}{3} \epsilon \dot{\zeta} + EI - f\theta, \quad (14)$$

where, for the positive phase-sequent e.m.f.'s (9),

$$\left. \begin{aligned} \sqrt{2}e_d &\equiv \frac{2}{3}\Sigma e_k \sin \theta_k = -\sqrt{2}e_0 \sin \psi, \\ \sqrt{2}e_i &\equiv \frac{2}{3}\Sigma e_k \cos \theta_k = \sqrt{2}e_0 \cos \psi, \\ \sqrt{2}\epsilon &\equiv \frac{1}{3}\Sigma e_k = 0. \end{aligned} \right\} \quad \dots \quad (15)$$

Making use of (13), the first equation of (3) may be written

$$e_k = r\dot{q}_k + \frac{d}{dt} [\dot{\xi} l_d \sin \theta_k + \dot{\eta} l_i \cos \theta_k + \frac{1}{3}(l^* - 3l_m)\dot{\zeta} + m_k i + M_{ik} I] \quad \dots \quad (16)$$

This equation may be multiplied by  $\frac{2}{3} \sin \theta_k$  and  $\frac{2}{3} \cos \theta_k$  to yield the first two of the following system :

$$\left. \begin{aligned} \frac{2}{3}\Sigma e_k \sin \theta_k &= \frac{2}{3}r\xi - \dot{\theta}[l_t\dot{\eta} + m_0 \sin \alpha i] \\ &\quad + \frac{d}{dt}[l_d\xi + m_0 \cos \alpha i + M_0 I], \\ \frac{2}{3}\Sigma e_k \cos \theta_k &= \frac{2}{3}r\dot{\eta} + \dot{\theta}[l_d\xi + m_0 \cos \alpha i + M_0 I] \\ &\quad + \frac{d}{dt}[l_t\dot{\eta} + m_0 \sin \alpha i], \\ 0 &= \mathbf{R}i + \frac{d}{dt}[m_0(\xi \cos \alpha + \dot{\eta} \sin \alpha) \\ &\quad + \mathbf{L}i + \mathbf{M}I], \\ \mathbf{E} &= \mathbf{R}I + \frac{d}{dt}[M_0\xi + \mathbf{M}i + \mathbf{L}I], \\ -f &= \theta\ddot{\theta} + s\dot{\theta} - [m_0(\dot{\eta} \cos \alpha - \dot{\xi} \sin \alpha)i \\ &\quad + (l_d - l_t)\dot{\xi}\dot{\eta} + M_0I\dot{\eta}], \end{aligned} \right\}. \quad (17)$$

where the last three equations are obtained directly from (3) with the use of (8), and where

$$\left. \begin{aligned} l_d &= \frac{2}{3}l^* + l_\mu, \\ l_t &= \frac{2}{3}l^* - l_\mu. \end{aligned} \right\}. \quad \dots \quad (18)$$

Park† has employed Duhamel's integral‡ and operational methods, which are applicable when  $\dot{\theta}$  on the right is assumed to be constant, in a step-by-step process going back and forth from the first four to the last equation of (17) for the computation of electro-mechanical transients in numerical cases §.

Purely electrical transients may be computed by writing  $\theta = \omega t$ . The first four equations of (17) then become linear and their variations have the same form. The variational forces  $\delta e_d$ ,  $\delta e_t$ , and  $\delta E$ , with the Heaviside unit function as a factor, come in and the operational determinant is

$$\Delta = \begin{vmatrix} \frac{2}{3}r + l_d p & -\omega l_t & -m_0(\sin \alpha \omega - \cos \alpha p) & M_0 p, \\ \omega l_d & \frac{2}{3}r - l_t p & m_0(\cos \alpha \omega + \sin \alpha p) & M_0 \omega, \\ m_0 \cos \alpha p & m_0 \sin \alpha p & \mathbf{R} + \mathbf{L}p & \mathbf{M}p, \\ M_0 p & 0 & \mathbf{M}p & \mathbf{R} + \mathbf{L}p. \end{vmatrix} \quad (19)$$

† Park, Trans. Am. Inst. Elect. Eng. lii. p. 352 (1933).

‡ Vide Berg, 'Heaviside's Operational Calculus,' chap. xiv, p. 67.

§ Vide Crary and Waring, Trans. Am. Inst. Elect. Eng. li. p. 764 (1932).

This determinant is implicit in a paper by Park † and is essentially identical with one given elsewhere ‡.

The stability of the system (17) can be ascertained, as Kron § has noted, from an application of Routh's criteria|| to the linear system, derived from (17),

$$\left. \begin{aligned} 0 &= r^* \delta \dot{\xi} - \theta \dot{\delta} \phi_t - \phi_d \dot{\delta} \theta + \delta \dot{\phi}_d - \sqrt{2e_0} \cos \psi \delta \theta, \\ 0 &= r^* \delta \dot{\eta} + \theta \dot{\delta} \phi_d + \phi_d \dot{\delta} \theta + \delta \dot{\phi}_t - \sqrt{2e_0} \sin \psi \delta \theta, \\ 0 &= \mathbf{R} \delta i + \frac{d}{dt} [m_0 (\delta \dot{\xi} \cos \alpha + \delta \dot{\eta} \sin \alpha) + \mathbf{L} \delta i + \mathbf{M} \delta \mathbf{I}], \\ 0 &= \mathbf{R} \delta \mathbf{I} + \frac{d}{dt} [\mathbf{M}_0 \delta \dot{\xi} + \mathbf{M} \delta i + \mathbf{L} \delta \mathbf{I}], \\ 0 &= \theta \ddot{\delta \theta} + s \delta \dot{\theta} - \delta [\phi_d \dot{\eta} - \phi_t \dot{\xi}], \end{aligned} \right\} \quad (20)$$

where  $\phi_d = l_d \dot{\xi} + m_0 \cos \alpha i + \mathbf{M}_0 \mathbf{I}$ ,  
 $\phi_t = l_t \dot{\eta} + m_0 \sin \alpha i$ ,  
 $r^* = \frac{2}{3} r$ .

The first to employ coordinates of the Blondel type in a discussion of stability was B. Hopkinson ¶, who found that a single-phase motor without an amortisseur and without mechanical friction and with constant excitation is inherently unstable. The system (20) for the three-phase motor may be verified readily to be unstable under similar conditions.

A treatment of the stability problem from a different standpoint is given elsewhere \*\*.

In the steady state the first two equations of (17) reduce to

$$\left. \begin{aligned} \sqrt{2e_d} &= r^* \dot{\xi} - \omega l_t \dot{\eta}, \\ \sqrt{2e_t} &= r^* \dot{\eta} + \omega l_d \dot{\xi} + \sqrt{2e_0} *, \end{aligned} \right\} \quad . . . . \quad (21)$$

and the power transmitted is

$$\begin{aligned} P &= 3p = \frac{1}{2} \omega \sum L_k' \dot{q}_k q_k + \omega I_0 \sum M_k' q_k \\ &= 2l_u \omega \dot{\xi} \dot{\eta} + \sqrt{2e_0} * \dot{\eta}, \end{aligned} \quad . . . . \quad (22)$$

† Park, Trans. Am. Inst. Elect. Eng. xlvi, p. 716 (1929).

‡ Ingram, 'Electrician' for May 12th, 1933, p. 616.

§ Kron, 'Tensor Analysis of Rotating Machinery,' pt. ii. (privately mimeographed), p. 12 (1933).

|| Routh's criteria for stability have been put in determinantal form by Hurwitz, *Math. Annalen*, xlvi, p. 273 (1895), and by Frazer and Duncan, Proc. Roy. Soc. A, cxxiv, p. 642 (1929).

¶ B. Hopkinson, Proc. Roy. Soc. lxxii, p. 235 (1903).

\*\* Ingram, Proc. Camb. Phil. Soc. xxix, p. 1 (1933).

where  $p$  is the power per phase. From (21)

$$\left. \begin{aligned} \frac{1}{3}\sqrt{2z^2\xi} &= e_d r + e_t x_t - e_0^* x_t, \\ \frac{1}{3}\sqrt{2z^2\eta} &= e_t r - e_d x_d - e_0^* r, \end{aligned} \right\} \quad \dots \quad (23)$$

where

$$z = [r^2 + x_d x_t]^{\frac{1}{2}},$$

$$x_d = \frac{3}{2}\omega l_d,$$

$$x_t = \frac{3}{2}\omega l_t;$$

and substitution into (22) yields

$$pz^2 = Ae_0^{*2} - Be_0^*e_d + Ce_0^*e_t + ae_d^2 - be_d e_t + ce_t^2, \quad (24)$$

where

$$\begin{aligned} A &= -r + c, & a &= -grx_d, \\ B &= x_d - b, & b &= g(x_d x_t - r^2), \\ C &= r - 2c, & c &= grx_t, \\ g &= 3l_\mu \omega / z^2. \end{aligned}$$

Expressing  $e_d$  and  $e_t$  in terms of the bus voltage and relative rotor angle, (24) becomes

$$\begin{aligned} pz^2 &= (x_d - b)e_0 e_0^* \sin \psi + (r - 2c)e_0 e_0^* \cos \psi \\ &\quad + \frac{1}{2}(c - a)e_0^2 \cos 2\psi + \frac{1}{2}be_0^2 \sin 2\psi - [(r - c)e_0^{*2} - \frac{1}{2}(a + c)e_0^2], \end{aligned} \quad \dots \quad (25)$$

This equation, which is a generalization of Hopkinson's formula, is equivalent to the system

$$\begin{aligned} -y &= (r - c)e_0^*/z + pz/e_0^* \\ -y &= \frac{1}{2} \frac{a+c}{z} \frac{e_0^2}{e_0^*} + e_0 \frac{z_1}{z} \sin(\psi + \alpha_1) + \frac{1}{2} \frac{e_0^2}{e_0^*} \frac{z_2}{z} \sin(2\psi + \alpha_2), \end{aligned} \quad \dots \quad (26)$$

where

$$z_1^2 = (r - 2c)^2 + (x_d - b)^2,$$

$$z_2^2 = (c - a)^2 + b^2,$$

$$= g^2(r^2 + x_d^2)(r^2 + x_t^2),$$

$$\alpha_1 = \tan^{-1} \frac{r - 2c}{x_d - b},$$

$$\alpha_2 = \tan^{-1} \frac{c - a}{b}.$$

The first equation of this pair is that of a family of hyperbolas for which  $p$  is the parameter. These are shown on the right in fig. 2, where  $y$  is plotted against  $e_0^*$ .

The second is that of a two-parameter family of prolate and curtate epicycloids given by the loci of points fixed with respect to, and at a distance  $\frac{1}{2}e_0^*z_2/e_0^*z$  from, the centre of a circle of diameter  $e_0z_1/z$ , which rolls on a fixed circle of the same diameter whose centre is  $\frac{1}{2}(a+c)e_0^2/e_0^*z$  below the  $e_0^*$ -axis.

The limits of operability occur where the slopes of the epicycloids are zero. When  $e_0^* > e_0z_2/z_1$ , the epicycloids have no cusps nor loops, and the stable region is on the right-hand side. When the inequality is the other way there are loops on the left-hand side, and a second region of stability exists for segments of the loops between horizontal points. When  $l_d = l_t$ , the epicycloids degenerate to circles. Since the arm of the rolling circle is proportional to  $l_u$ , the diagram shows clearly the tendency of saliency to prevent displacement of the rotor with increasing load.

When the excitation is made smaller and smaller the modulus of the power scale (which is linear) becomes greater and greater, as also does the arm on the rolling circle; in the limit, the outside and inside loops of the epicycloids come together to form a circle, so that a point on one loop for the angle  $\psi$  falls upon the point for the angle  $\psi \pm \pi$  on the other.

The power transmitted at no excitation is

$$p = \frac{1}{2}e_0^2[(a+c) + z_2 \sin(2\psi + \alpha_2)]/z^2,$$

and the limits of operability then are given by

$$\psi = \pm \frac{1}{4}\pi - \tan^{-1} \frac{r(x_d + x_t)}{x_d x_t}.$$

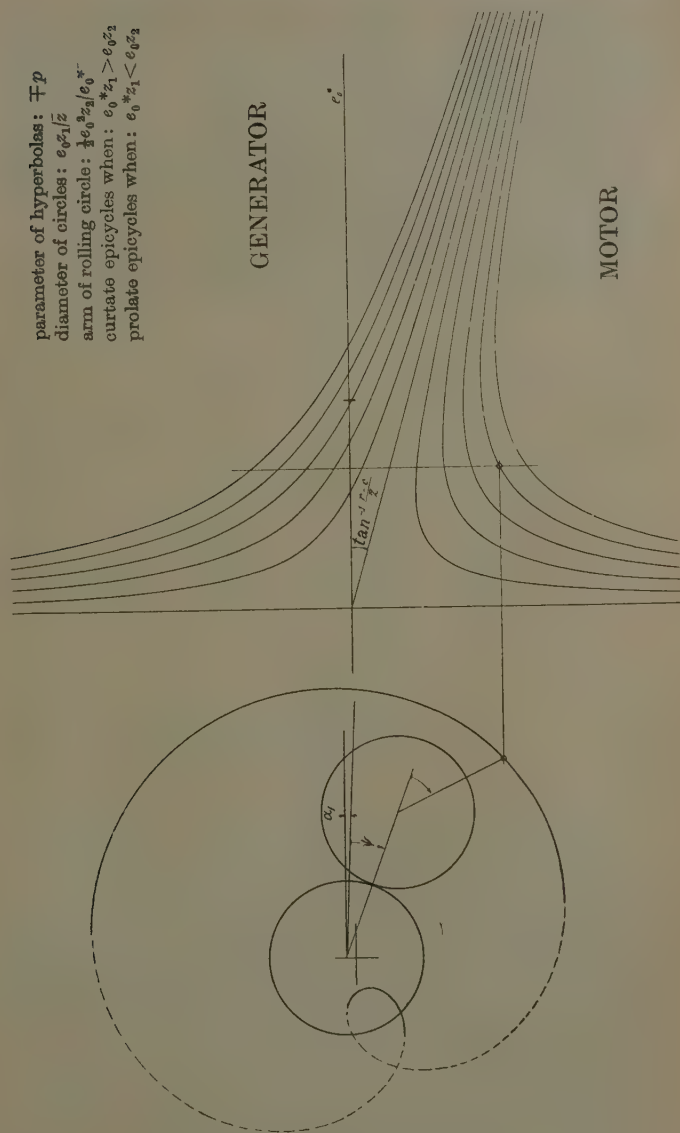
The synchronizing power

$$\delta p_{\text{syn}} \equiv -(\partial p / \partial \psi) \delta \psi$$

is readily computed from (25).

On substituting the value of  $e_d$  and  $e_t$  given by (15) into (24), an equation for the polar locus of the point  $(e_0^*, \psi)$ , with  $e_0$  as pole, is obtained, as illustrated in fig. 3, where the stable part of the locus is indicated by the solid curve and the labile part by the broken curve.

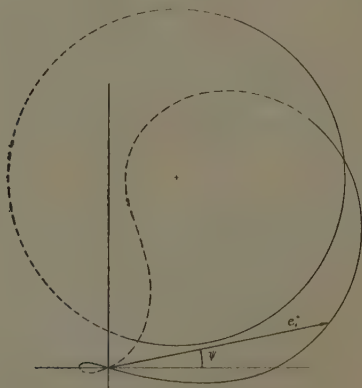
Fig. 2.



The equation has a singular point at the origin in general, and when the curve crosses the origin in cases of pronounced saliency the excitation must be taken, from physical considerations, as reversing in sign at the origin with no discontinuity in the rotor angle. When  $l_\mu$  is written equal to zero in the example illustrated the locus becomes the circle shown  $\dagger$ . For intermediate values of  $l_\mu$  non-symmetrical ovals are obtained which point in a general way toward the origin.

The polar locus of the point  $(q_0, \gamma)$ , with  $e_0$  as pole and  $e_0^*$  eliminated, is a circle of radius  $\frac{1}{2}(e_0^2 - 4rp)r^{-1}$  in the

Fig. 3.



case of the orthocyclic salient-pole machine as well as in the case of the orthocyclic smooth-pole machine.

The polar locus of  $(q_0, \gamma - \psi)$ , with  $e_0^*$  as pole and  $p$  eliminated, is an ellipse in the salient-pole case and a circle in the smooth-pole case. This result has been obtained graphically  $\ddagger$  in the case  $r=0$ , and may be obtained analytically from (21) and the relation  $e_0^2 = e_d^2 + e_t^2$ . The centre of the ellipse, in Cartesian coordinates, is at the

$\dagger$  The circle diagram for non-salient-pole machines is due to Blondel, 'Synchronous Motors and Converters,' p. 44 (1913).

$\ddagger$  Kron, Trans. Am. Inst. Elect. Eng. xlvi. p. 666 (1930).

point  $(-\frac{3}{2}\sqrt{2e_0^*}x/\bar{z}^2, -\frac{3}{2}\sqrt{2e_0^*}r/z^2)$ . The shape, size, and inclination of the major axis of the ellipse is not dependent upon  $e_0^*$ . The length of the major axis, however, is proportional to  $e_0$ . The power corresponding to any point on an ellipse may be obtained graphically by superposing upon the ellipse the family of hyperbolas given by (22). This family has a common asymptote parallel to the  $\eta$ -axis at a distance  $-\frac{3}{2}\sqrt{2e_0^*}(x_d-x_t)^{-1}$ . When  $e_0^*$  is varied the hyperbolas are shifted parallel to themselves along the  $\xi$ -axis and the ellipses are shifted parallel to themselves along a line of centres through the origin whose slope is  $r/x_t$  measured from the  $\xi$ -axis. Since  $(x_d-x_t)^{-1}$  is always greater than  $x_t/z^2$ , the hyperbolas are shifted a greater amount along the  $\xi$ -axis than are the ellipses in that direction for a given change in  $e_0^*$ . For reversed excitation, the ellipses tend to loose contact with the hyperbolas on the positive side of the asymptote mentioned. The hyperbolas on the negative side correspond to operation with the rotor  $180^\circ$  displaced.

The polar locus of  $(\dot{q}_0, \gamma)$  with  $e_0$  as pole is the limaçon of Pascal †. Writing (21) in the form

$$\left. \begin{aligned} -e_0 \sin \psi &= r\dot{q}_0 \sin(\gamma - \psi) - x_t \dot{q}_0 \cos(\gamma - \psi), \\ e_0 \cos \psi &= r\dot{q}_0 \cos(\gamma - \psi) + x_d \dot{q}_0 \sin(\gamma - \psi) + e_0^*, \end{aligned} \right\}$$

substituting

$$\dot{q}_0 \sin \gamma = \chi,$$

$$\dot{q}_0 \cos \gamma = v,$$

and eliminating  $\psi$ , there results

$$\begin{aligned} e_0^*[(r\chi - x_t v)^2 + (e_0 - rv - x_t \chi)^2] \\ - [e_0 - rv - x_t \chi](e_0 - rv - x_d \chi) + (r\chi - x_d v)(r\chi - x_t v)]^2 = 0, \end{aligned}$$

the equation of the limaçon in rectangular coordinates.

The singular point of the locus is given by

$$\chi_0 = e_0 x_t / z_t^2, \quad v_0 = e_0 r / z_t^2,$$

where  $z_t^2 = r^2 + x_t^2$ , and the axis of symmetry makes an angle  $2 \arctan(r/x_t)$  with the  $\chi$ -axis. The centre of the generating circle is at the point

$$\chi_c = \frac{1}{2}(x_t + x_d)e_0 / \bar{z}^2, \quad v_c = re_0 / z^2.$$

† Závada, *Elektrotechnik und Maschinenbau*, xxxvi. p. 348 (1918); Brüderlin, *ibid.* xlivi. p. 781 (1925); Richter and von Timascheff, *ibid.* xliv. p. 185 (1925); Mandl, *Elektrotechnische Zeitschrift*, xlvi. p. 527 (1925); Schammel, *Archiv für Elektrotechnik*, xxvi. p. 28 (1932).

With the singular point as pole and the polar axis along the axis of symmetry, the locus is given by  $\rho = 2r \cos \theta + s$ , where  $r = \frac{1}{2}(x_d - x_t)e_0/z^2$  is the radius of the generating circle and where  $s = e_0^* z / z^2$ .

The polar locus of  $(v_s, \psi)$ , where

$$v = e_0^* + (x_d - x_t)q_0 \sin(\gamma - \psi),$$

is the so-called Joubertian e.m.f., is also known to be a limaçon \*.

**XXIV. A Stroboscopic Jet Method for determining "g."** By  
E. TYLER, D.Sc., M.Sc., F.Inst.P., Lecturer in Physics,  
College of Technology, Leicester †.

[Plate X.]

*Introduction.*

THE utilization of a flashing neon tube as a device for producing stroboscopic vision of a body executing vibratory motion can be well adapted to a liquid jet breaking up into drops ‡.

When such a jet issues horizontally from a nozzle, owing to gravity its path is parabolic, and verification of such affords an interesting exercise for a student of mechanics §.

If, however, the jet is resolved into drops in a definite periodic manner, and at the same time is illuminated with intermittent light of the same frequency, a stationary picture of the detached drops is obtained.

This condition is usually effected by attaching the nozzle to a tuning-fork maintained electrically, and illuminating the jet with light from a steady source cut off periodically by means of a rotating slotted disk, the speed of which is so adjusted until the frequency of illumination is equal to that of fork.

This method does not permit of perfect synchronization for any length of time, owing to possible variation in

\* Léauté, *Comptes Rendu*, clxv, p. 1107 (1917).

† Communicated by the Author.

‡ Tylor, Phil. Mag., Aug. Supplement, 1933, p. 504. Also exhibited at the Leicester Lit. and Phil. Conversazione, Physics Section, British Association Meeting, Sept. 1933.

§ Glazebrook and Shaw, 'Practical Physics,' Section C.

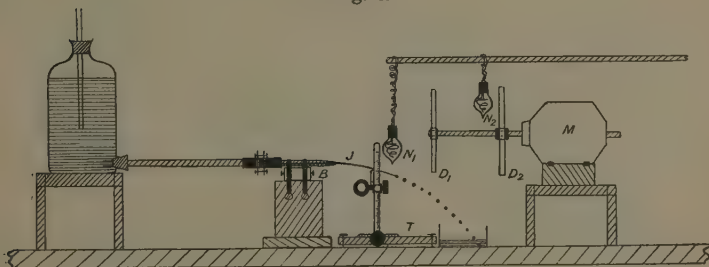
speed of the motor driving the disk. The following arrangement works independently of such a defect and provides an interesting method of evaluating "g" provided the frequency of drop formation is known.

Its adaptation for teaching purposes in the study of bodies falling under gravity may also be found useful, and by virtue of the small distances of fall involved it holds a decided advantage over other methods in which falling bodies are used.

#### *Method and Experimental Arrangement.*

The vibrator, to which is attached a glass nozzle, consists of either (a) a buzzer or electrically maintained fork, or (b) a valve-controlled loud-speaker unit.

Fig. 1.



J=Liquid jet.

B=Electrically maintained vibrator (buzzer, fork, or loud speaker unit).

N<sub>1</sub>=Flashing neon tube, operated at frequency of vibrator.

N<sub>2</sub>=Flashing neon tube, operated at frequency of 50 cycles/sec.

D<sub>1</sub>, D<sub>2</sub>=Stroboscopic disks.

M=Motor driving disks.

T=Travelling microscope (Wilson type).

Illumination of the jet is supplied by a neon lamp, the flashing of which is produced by transformer coupling the lamp to either the primary circuit of the buzzer, or fork electrically maintained, or to the plate circuit of a specially designed valve oscillator.

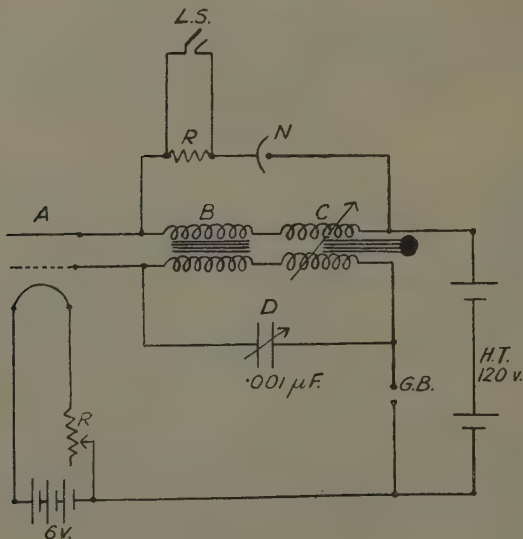
Such arrangements are shown in figs. 1 and 2, the latter being preferred owing to its wide range of available frequencies.

The former arrangement is to be recommended when used by a student, owing to its cheapness and simplicity.

With reference to this method, as a result of coupling the neon lamp to the fork or buzzer circuit the induced voltage in the lamp circuit, at the make-and-break of the primary current operating either the fork or buzzer, is sufficient to cause the lamp to glow, and hence it flashes at a frequency equal to that of the make-and-break primary current.

Now, since the jet is broken up into drops at the same rate as the vibrations of the fork or buzzer, it is illuminated

Fig. 2.



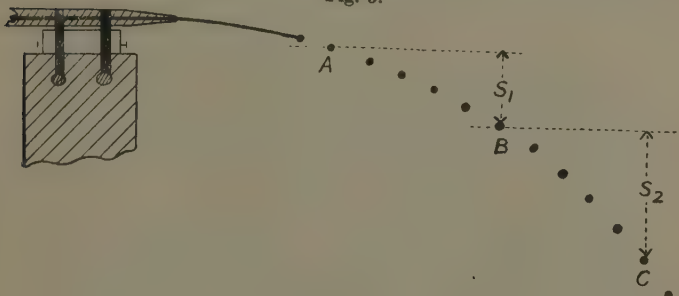
- A = L.S. 5 valve.
- B = Power transformer.
- C = Variable core transformer.
- D = Variable condenser,  $0.001 \mu F$ .
- N = Flashing neon tube illuminating the jet.
- R = Variable resistance.
- G.B. = Grid bias terminals.
- L.S. = Loud speaker unit (vibrator).
- $r$  = Loud speaker shunt resistance.

with intermittent light of the same periodicity, and suitable placing of the lamp behind the jet renders visible a beautiful stationary pattern of the detached drops.

Such a distribution is shown in the spark photograph of fig. 4 (Pl. X.). The pitch of the note emitted by the vibrator is tuned to a similar one produced on a monochord, calibrated with a standard fork, and the detached drops thus provide a suitable time base in studying the vertical fall of the drops.

Alternately the flashing frequency may be ascertained by stroboscopic means, using two disks revolving on a common shaft and illuminated with separate neon lamps, one controlled by the mains A.C. operating at 50 cycles, and the other by the vibrator whose frequency is required. This method is useful with the buzzer as vibrator, and better still with the loud speaker unit.

Fig. 3.



In the second arrangement (fig. 2), using the valve oscillator much better illumination is provided, and it is possible to obtain a stroboscopic photograph with the flashing neon source as the illuminant. A typical one-minute exposure is exhibited in fig. 5 (Pl. X.).

Should the flashing frequency vary during the experiment it is readjusted to a constant value by means of the variable condenser D in the oscillating circuit.

In order to maintain this constancy of flashing the note produced by the loud speaker is kept constant by tuning it to a similar note on a monochord at fixed tension and length.

The double stroboscope arrangement may be also used, but suitable selection of the two sets of markings on the disks is necessary to obtain at the correct motor

speed a stationary pattern on each disk. Stroboscopic synchronization of both motor speed and flashing frequency is thus effected.

Having deduced the frequency of drop resolution by either of the foregoing methods, in order to evaluate " $g$ " it is necessary to measure with precision the vertical spacing distribution of the drops while apparently stationary, and this is done by means of a travelling microscope, with both a vertical and horizontal traverse.

The vertical displacement of successive drops is measured and " $g$ " subsequently deduced.

From such data " $g$ " may be found.

As a verification of this method spark or stroboscopic photographs of the drop distribution may be taken and the spacings measured up afterwards.

### *Theory and Discussion of Results.*

Referring to the trajectory shown in fig. 3, if we select drops at A, B, and C such that there are  $n$  spaces between both AB and BC, then counting the drops successively beyond A, the  $n$ th and  $2n$ th drops occur at B and C respectively.

Let  $S_1$  and  $S_2$  be the vertical displacements between A and B and B and C, and  $N$  the frequency of drop resolution.

Then if  $V_0$ ,  $V_n$ , and  $V_{2n}$  represent the downward vertical velocities of the drops at A, B, and C, the time of fall from A to B and from B to C is  $t$ , where  $t = \frac{n}{N}$ .

Furthermore, neglecting the aerodynamic resistance of the drops, we obtain

$$S_1 = V_0 t + \frac{1}{2} \cdot g t^2,$$

and since  $V_n = V_0 + gt$ ,

$$\therefore S_2 = (V_0 + gt)t + \frac{1}{2} \cdot g t^2.$$

Whence  $S_2 - S_1 = gt^2$ , and, putting  $t = \frac{n}{N}$ , we finally derive

$$g = \frac{N^2}{n^2} (S_2 - S_1),$$

which is the usual expression used for finding " $g$ ."

The accuracy of "g" is thus entirely dependent on the accuracy with which  $N$  and  $S_2 - S_1$  are determined, and the data obtained suffices to give "g" with an error less than 1 per cent.

The following results are typical of the methods employed :—

*Stroboscopic Vision (Neon Tube) and Travelling Microscope Method.*

RESULTS (1).

Vibrator=Loud Speaker Unit. Diameter of Nozzle = 65 mm. Flashing Frequency of Neon Lamp and Drop Formation Frequency,  $N=430$ . (Estimated with Monochord.)

Number of drop.	Microscope readings (vertical) (cm.).	$S_1$ for $n=20$ (cm.).	$S_2$ for $n=20$ (cm.).	$S_2 - S_1$ (cm.).
0	12.940	2.190	—	—
20	10.750	—	4.300	2.110
40	6.450	—	—	—
4	12.698	2.573	—	—
24	10.125	—	4.675	2.102
44	5.450	—	—	—
8	12.380	2.905	—	—
28	9.475	—	5.023	2.118
48	4.452	—	—	—

Average value of  $S_2 - S_1 = 2.110$  cm.;

$$\therefore g = \frac{N^2}{n^2} (S_2 - S_1) = \frac{430^2}{20^2} \times 2.110 = 975 \text{ cm./sec.}^2.$$

## RESULTS (2).

Vibrator=Loud Speaker Unit. Diameter of Nozzle =·65 mm. Flashing Frequency of Neon Lamp and Drop Formation Frequency, N=296. (Estimated with Monochord.)

Number of drop.	Microscope readings (vertical) (cm.).	$S_1$ for $n=14$ (cm.).	$S_2$ for $n=14$ (cm.).	$S_2-S_1$ (cm.).
0	12.935	1.860	—	—
14	11.075	—	4.050	2.190
28	7.025	—	—	—
2	12.790	2.150	—	—
16	10.640	—	4.305	2.155
30	6.335	—	—	—
4	12.630	2.455	—	—
18	10.175	—	4.630	2.175
32	5.545	—	—	—

Average value of  $S_2-S_1=2.173$  cm.;

$$\therefore g = \frac{N^2}{n^2} (S_2 - S_1) = \frac{296^2}{14^2} \times 2.173 = 971 \text{ cm./sec.}^2.$$

## RESULTS (3).

Vibrator=Maintained Buzzer. Diameter of Nozzle=·65 mm. Flashing Frequency of Neon Lamp and Drop Formation Frequency, N=453. (Estimated with Monochord.)

Number of drop.	Microscope readings (vertical) (cm.).	$S_1$ for $n=14$ (cm.).	$S_2$ for $n=14$ (cm.).	$S_2-S_1$ (cm.).
0	11.485	.955	—	—
14	10.530	—	1.880	.925
28	8.650	—	—	—

## RESULTS (3) (con.).

Number of drops.	Microscope readings (vertical). (cm.).	$S_1$ for $n=14$ (cm.).	$S_2$ for $n=14$ (cm.).	$S_2 - S_1$ (cm.).
2	11.425	1.110	—	—
16	10.315	—	2.040	.930
30	8.275	—	—	—
4	11.300	1.225	—	—
18	10.075	—	2.150	.925
32	7.925	—	—	—

Average value of  $S_2 - S_1 = .926$  cm.;

$$\therefore g = \frac{N^2}{n^2} (S_2 - S_1) = \frac{453^2}{14^2} \times .926 = 969 \text{ cm./sec.}^2.$$

## Measurements from Stroboscopic Photograph.

## RESULTS (4).

Pl. X. fig. 5. Time of Exposure=1 minute. Neon Lamp Source. Vibrator=Loud Speaker Unit. Diameter of Nozzle=.65 mm. Flashing Frequency of Neon Lamp and Drop Formation Frequency,  $N=287$ . (Estimated with Monochord.) Magnification =.715.

Number of drop.	Microscope readings (vertical) (cm.).	$S_1$ for $n=10$ (cm.).	$S_2$ for $n=10$ (cm.).	$S_2 - S_1$ (cm.).
0	8.570	1.025	—	—
10	7.545	—	1.910	.885
20	5.635	—	—	—
2	8.435	1.195	—	—
12	7.240	—	2.085	.890
22	5.155	—	—	—

Average value of  $S_2 - S_1$  at .715 magnification =.887 cm.;

Real value of  $S_2 - S_1 = 1.240$  cm.;

$$\therefore g = \frac{N^2}{n^2} (S_2 - S_1) = \frac{281^2}{10^2} \times 1.240 = 979 \text{ cm./sec.}^2.$$

*Measurements from Spark Photograph.*

## RESULTS (5).

Pl. X. fig. 4. Vibrator=Loud Speaker Unit. Diameter of Nozzle=.65 mm. Frequency of Vibrator=248. Magnification=.715.

Number of drop.	Microscope readings (vertical) (cm.).	$S_1$ for $n=8$ (cm.).	$S_2$ for $n=8$ (cm.).	$S_2-S_1$ (cm.).
0	8.580	—	—	—
8	7.485	1.095	1.830	.735
16	5.655	—	—	—
2	8.355	1.280	—	—
10	7.075	—	2.010	.740
18	5.055	—	—	—

Average value of  $S_2-S_1$  at .715 magnification=.737 cm.;

Real value of  $S_2-S_1=1.016$  cm.;

$$\therefore g = \frac{N^2}{n^2} (S_2-S_1) = \frac{248^2}{8^2} \times 1.016 = 976 \text{ cm./sec.}^2.$$

It will be seen that the results for "g" are consistently good when the experimental errors involved are taken into consideration, and compare favourably with other methods in which falling bodies are employed.

The travelling microscope arrangement permits of greater accuracy being obtained, since a wider range of traverse is provided, thus yielding larger differences between  $S_1$  and  $S_2$ .

The photographic results are included merely to illustrate the possibility and novelty of the method.

The stroboscopic photograph (Pl. X. fig. 5) emphasizes clearly the reliability of the steady conditions existing and also merit of the experiment, since during the time of exposure (one minute),  $60 \times 281$  drops actually pass each point, and so build up on the plate a permanent picture of the drops, each drop being well defined.

A further advantage lies in the fact that the vertical displacements of the drops are independent of the horizontal speed of the jet. Should this speed vary during the experiment while traversing with the microscope or taking a photograph, the drops are displaced horizontally

only, and on the plate is produced a horizontal line instead of a drop, similar in character to the exposure shown in fig. 6 (Pl. X.). Maintenance of constant drop formation frequency is, however, essential.

Application of the method for determining the frequency of an electrically maintained fork may be employed, assuming " $g$ ," and, in addition, the existence of overtones of a vibrating diaphragm are readily demonstrated, the characteristic spacing of the drops serving in this respect.

It is not expected that the experiments outlined will supersede the more refined precision methods of measuring " $g$ ," but the novelty of utilizing falling liquid drops to register their own displacement-time trajectories when under the influence of gravity is worthy of recommendation.

#### *Summary.*

A method is described in which a liquid jet, projected horizontally, is resolved into drops at a definite frequency by coupling it to a vibrator consisting of either (*a*) a buzzer or electrically maintained fork, or (*b*) a valve-controlled loud-speaker unit. Employing a neon lamp as a source of illuminant for the jet, and illuminated intermittently at the same frequency as that of drop formation, stroboscopic vision of the detached drops is effected. Under such conditions the apparent stationary drops register their own displacement-time curves, and measurement of such trajectories with a travelling microscope, together with a knowledge of the frequency of drop formation enables " $g$ " to be evaluated. Stroboscopic and spark photographs are also included, from which " $g$ " is also computed.

---

**XXV. Deviations from Paschen's Law.** *By S. P. McCALLUM, M.A., D.Phil., Fellow of New College, Oxford, and L. KLATZOW, D.Phil., Lincoln College, Oxford \*.*

**I**N recent years numerous investigations have been made on the sparking potentials in gases between parallel plates, and in general there has been satisfactory agreement between the results. It has usually been found,

\* Communicated by Prof. J. S. Townsend, F.R.S.

in agreement with the early investigations, that the potential depends on the product of the pressure,  $p$ , and the distance,  $S$ , between the electrodes.

Townsend's theory of the discharge between plane-parallel electrodes is in agreement with this result, provided that the distance,  $S$ , between the plates is small compared with the diameter,  $a$ , of the plates. It is an example of a more general theory, which may be stated as follows \* :—If  $V$  be the potential required to produce a discharge through a gas at pressure  $p$  between two conductors A and B, the same potential difference will produce a discharge through the gas at a lower pressure  $p' = p/k$ , between two conductors A' and B' of the same shape and in the same relative position, but with all the linear dimensions increased in size, so that the distance between points on A' and B' exceeds the distance between the corresponding points on A and B in the ratio  $k : 1$ .

In applying this theorem to the case of plane-parallel electrodes it is seen that, when the pressure of the gas is reduced from  $p$  to  $p/k$ , then in general, in order to maintain the sparking potential absolutely unchanged, not only must the distance between the electrodes be increased from  $S$  to  $kS$ , but also the diameter of the electrodes must be increased from  $a$  to  $ka$ .

In most of the experiments electrodes of constant diameter have been used, and it was found that the potential was the same for different distances between the plates when the pressure is adjusted, so that the product  $pS$  is a constant. This result is in accordance with the theory in cases where the rate of diffusion of the electrons is not very large, as in the diatomic gases.

In the monatomic gases, however, where the rate of diffusion of the electrons is much greater, it is not to be expected that this result would be obtained with the ordinary forms of apparatus unless the diameter,  $a$ , of the plates is large compared with the distance between them. In the experiments on the conductivity of neon †, in which plates of 3·5 cm. diameter were used, it was found that the sparking potential with a large distance between the plates was greater than that with a small distance when the product  $pS$  was constant.

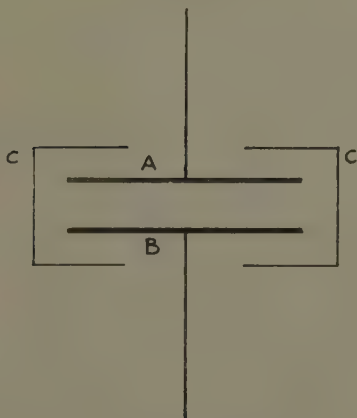
\* 'Electricity in Gases,' p. 365 (Clarendon Press, 1915).

† J. S. Townsend and S. P. McCallum, Phil. Mag. vol. vi. p. 857 (1928).

Recently we have made further investigations of the sparking potentials in monatomic gases with the same apparatus. The arrangement of the electrodes is shown in fig. 1.

The two plates, A and B, were 3.5 cm. in diameter and were fixed inside a metal cylinder, C, 4.5 cm. in diameter, from which they were insulated by quartz rods of rectangular cross-section. The two plates and the cylinder were of nickel. The upper plate was on a spindle which rotated in a micrometer screw, so that it was possible to adjust the distance between the plates

Fig. 1.



Arrangement of electrodes.

to any value from 1 to 12 mm. with the planes accurately parallel.

The results of the experiments are shown by the figures in the following table, where S is the distance between the plates in millimetres,  $p$  the pressure of the gas in millimetres of mercury, the product  $pS$  being a constant equal to 7.4.

With helium the sparking potential was the same with the different distances between the plates, but with neon and argon the potentials increased with the distance S.

The increase depends mainly on the ratio,  $a/S$ , of the diameter of the plates to the distance between them; also to some extent on the diameter of the cylinder, C.

Thus, in neon the potential is 204 volts when the distance,  $S$ , is 3 mm. and the ratio,  $a/S$ , is 11.7, and the potential is 220 volts when  $S$  is 8 mm. and  $a/S$  4.4. Under similar conditions the sparking potential in argon changes from 328 to 358 volts.

These results may be explained by the results of the experiments on the diffusion of electrons in directions perpendicular to the direction of the electric force \*. It was found that the rate of diffusion of electrons in argon and neon was much greater than in helium. This effect was investigated with the apparatus shown in the figure by measuring the photo-electric currents between

### Sparking Potentials in Helium, Neon, and Argon.

Nickel electrodes. $a=3.5$ cm. $pS=7.4$ .					
$S$ .	$p$ .	$a/S$ .	Sparking potential in volts.		
			Helium.	Neon.	Argon.
3.0	24.7	11.7	242	204	328
4.0	18.5	8.7	242	206	338
5.0	14.8	7.0	242	210	343
6.0	12.3	5.8	242	214	347
7.0	10.6	5.0	242	217	352
8.0	9.2	4.4	242	220	358

the plates due to the action of ultra-violet light on a small area at the centre of the upper plate. It was found that there was a small current of electrons to the cylinder, C, when the upper plate was charged negatively and the lower plate and the cylinder were at zero potential.

It is clear, therefore, that an appreciable proportion of electrons leaving the upper plate, A, will be lost to the cylinder, C, due to this lateral diffusion, unless the ratio,  $a/S$ , of the diameter of the electrodes to the distance between them is very large. The number of electrons which leave the cathode and do not arrive at the anode will depend upon the ratio,  $a/S$ , and upon the nature of the gas. The proportion will be greater for an apparatus of which the value of  $a/S$  is small than for one of which this ratio is large, and consequently it would be expected

\* Townsend, 'Motion of Electrons in Gases' (Clarendon Press, 1923).

that in the former apparatus the sparking potential would be greater than in the latter apparatus, although the value of  $pS$  is the same in both cases. This effect would increase with the rate of diffusion of the electrons.

The assumption that the sparking potential is almost independent of the ratio,  $a/S$ , for a given value of  $pS$  has been based on investigations which have been carried out with diatomic gases. In these gases it is known that the lateral diffusion of the electrons is small, and it is not to be expected that the effects of diffusion will be appreciable. In the monatomic gases, argon and neon, however, the lateral diffusion is very large. It is to be expected, therefore, that there would be an increase in the sparking potential of these gases for a given value of  $pS$  as  $S$  is increased. In the case of helium, for which the lateral diffusion is known to be not very much greater than in hydrogen or nitrogen, it is unlikely that the effect will be appreciable. As is seen above the sparking potential in neon is not accurately a function of the product,  $pS$ , unless the ratio  $a/S$  is greater than about 13, and in argon it would appear that the sparking potential is a function of  $pS$  only when the ratio,  $a/S$ , is greater than about 40.

These results are of importance in showing that a comparison of the values of the sparking potentials obtained by different experimenters is possible only if the dimensions of the apparatus used are known. It is clearly insufficient to give the sparking potential of a gas such as neon or argon for a given value of  $pS$  unless the diameter of the electrodes and the distance between them are specified.

Other factors must also be taken into account in the design of a suitable apparatus for the measurement of sparking potentials in a gas. In some forms of apparatus, such as that used by Penning \*, the electrodes are sealed into glass tubes whose diameter is very little greater than that of the electrodes. This arrangement is clearly undesirable as the glass becomes negatively charged, and it is uncertain to what extent this charge affects the uniformity of the field between the electrodes. A considerable proportion of the positive ions and electrons are thus lost by coming into contact with the glass, and an increase in potential between the plates is required

\* F. M. Penning, *Zeit. für Phys.* lvii. p. 723 (1929), and other papers.

in order to compensate for this loss. It is therefore to be expected that with such an apparatus the sparking potentials are higher than those obtained with large plates a short distance apart.

The above considerations apply equally to the design of apparatus constructed to measure the photo-electric current in gases between parallel plates where the distance between the plates is altered and the field intensity is kept uniform. As an example of the errors that may arise in apparatus in which the precautions outlined above have not been carefully observed a further experiment due to Penning and Teves \* may be mentioned. The disposition of their electrodes in the glass tube is given approximately in fig. 2, where the electrode A is illuminated by ultra-violet light. With this apparatus they found that, with a constant force,  $X$ , between the plates and a constant pressure,  $p$ , the current in pure neon

Fig. 2.



decreased as the distance between the two electrodes, A and B, was increased. It is evident at once that the electrons in moving from A to B will diffuse laterally, and their direction of motion may be indicated approximately by the arrows shown in fig. 2. The decrease in current observed can be simply explained in terms of the variation of the electric intensity,  $X$ , between the plates caused by charges diffusing to the glass walls. The effect of the negative charges on the walls of the apparatus is to increase the electric intensity near B and to decrease it near A. A reduction of the electric intensity near A will result in a diminution of the number of electrons emitted from A under the action of the ultra-violet light. It is evident that this diminution in the number of electrons will increase as the distance between A and B is increased.

The results obtained with this apparatus were adduced as evidence that there was no ionization in neon for values

\* F. M. Penning and C. M. Teves, 'Physica,' vol. ix. p. 97 (1929).

of  $X/p$  less than 4. Townsend and McCallum \*, using a properly constructed apparatus, have shown that there is appreciable ionization in neon for values of  $X/p=2$ . It may be mentioned here also that appreciable ionization occurs in the long positive column of neon when the value of  $X/p$  is as low as 0.5.

Since writing this paper more results have been obtained with krypton using the same apparatus. These results show that for a value of  $pS=7.4$  the sparking potential of krypton changes from 346 volts to 382 volts when  $a/S$  changes from 35 to 7.

---

**XXVI. On the Measurement of the Specific Heats of Liquids by a Cooling Method.** By R. W. B. STEPHENS, B.Sc., A.R.C.S., D.I.C., Imperial College of Science and Technology †.

*Introduction.*

IN a previous paper ‡, reference has been made to the suggestion of measuring the specific heats of liquids by observing their rates of cooling when placed inside a hollow cylinder of insulating material, which is itself immersed in a constant temperature bath. Before discussing, however, the development of this work, a brief review of the available methods of finding the specific heats of liquids will serve to indicate their relative advantages and disadvantages. Previous to the advent of accurate thermometry, methods based on change of state (*e. g.*, Bunsen's ice calorimeter) were definitely advantageous when compared, for example, with the method of mixtures, since the indications of the calorimeter are affected only slightly by the external conditions. With the increased accuracy of temperature measurements, however, the method of mixtures received wide application by reason of its simplicity. It is a useful method for obtaining values of mean specific heats over a range of temperature,

\* J. S. Townsend and S. P. McCallum, *loc. cit.*

† Communicated by Prof. H. S. Gregory, Ph.D.

‡ Phil. Mag. ser. 7, xv. p. 857 (May 1933).

but its exactitude is limited considerably by the nature of the corrections involved. In order to reduce these latter to a minimum various devices have been adopted ; in particular, T. W. Richards \* and other workers have devised different forms of adiabatic calorimeters. The apparatus in these cases is designed so that the necessity for correcting for the heat transfer between the calorimeter and its jacket is entirely eliminated. The required condition is obtained in practice by careful adjustments during preliminary experiments, and, consequently, the method is chiefly applicable when a number of observations are to be performed. Electrical methods have undoubtedly advantages from the point of view of ease of control and facility of energy measurement, but usually these methods (*e. g.*, the Callendar and Barnes † continuous flow calorimeter), though extremely accurate, involve considerable care and time in setting up. A recent method, however, described in a paper by Ferguson and Miller ‡, promises to fulfil the dual requirements of accuracy and simplicity of working, albeit measurements have been restricted as yet to the range 20° C. to 50° C. In these experiments it is necessary to determine the electrical energy required to maintain the temperature of a calorimeter at various temperature excesses, the heat dissipated to the surroundings being also estimated by means of a cooling curve.

The remaining class of experiment to come under review is that generally known as the method of cooling, or cooling thermometer method, and it is the type most closely related to the work to be described in this paper. The principle involved is that of a body cooling in a given enclosure, it being supposed that the quantity of heat  $dQ$  emitted in  $dt$  secs. depends only on the excess temperature ( $\theta$ ) of the body above that of the surroundings, and on the extent and nature of the surface of the body, *i. e.*,  $dQ = A \cdot f(\theta) \cdot dt$ , where  $A$  is a function of the surface area of the body and its radiating power. In the determination of the specific heats of liquids by this method, it is usual to employ the same vessel to contain, in turn, approximately equal volumes of the two liquids, whose cooling rates are being compared. In this case

\* J. A. C. S. vol. xxxi. p. 1275 (1909).

† Proc. Roy. Soc. vol. xcix. p. 55 (1902).

‡ Proc. Phys. Soc. vol. xlvi. p. 194 (1932).

A is taken as identical in the two experiments and we may write

$$\frac{m_1 s_1 + w}{m_2 s_2 + w} = \frac{dt_1}{dt_2},$$

where  $m_1$  and  $m_2$  are the masses and  $s_1$  and  $s_2$  are the specific heats of the liquids respectively, and  $w$  is the thermal capacity of the container.  $dt_1$  and  $dt_2$  are the corresponding times for the liquids to cool through the same temperature range.

The obvious advantage of this method is the absence of heat transference or mixing, and it has been used by a large number of early experimenters, e.g., Mayer, Leslie, Dulong and Petit, Regnault, etc. The chief features involved, however, will be clearly evident by a brief consideration of the work of a few observers. In Dulong and Petit's experiments \* the substance under examination was contained in a silver thimble. The outside surface of the latter was kept brightly polished to possess the same radiation powers and prolong the time of cooling. This procedure is the reverse of the modern practice in which it is usual to blacken the outside of the calorimeter, thereby enhancing the radiation losses by comparison with the more irregular convection and conduction losses. The work of Regnault † served to indicate that the cooling method was especially convenient for the determination of the specific heats of liquids available only in small quantities. For accurate work, however, he showed how necessary it is to observe the assumptions implied in the theory, namely, (1) that the cooling surfaces must be identical in the two experiments, and (2) that the liquid must be well stirred to reduce to a minimum the temperature gradient between the outer surface of the calorimeter and the bulk of the contained liquid. R. Mellacœur ‡ is a more recent experimenter, who has given more attention to these details, and he stresses the necessity for making a preliminary experiment, as the various factors controlling the cooling are not constant from day to day. Values are quoted for the mean specific heats of benzene etc. over two ranges of

\* *Ann. Chim. Phys.* (2) vii. pp. 113, 225, 337 (1817).

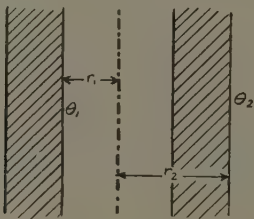
† *Pogg. Ann.* lxii. p. 50 (1844).

‡ *Ann. de Chimie Phys.* vol. xxiii. p. 556 (1911).

temperature (5 to 10) deg. C. and (10 to 15) deg. C., and an error of measurement less than 1 per cent. is claimed.

In the cooling method as ordinarily employed there exists an uncontrollable source of error, due to thermal conduction through the supports of the calorimeter. Consequently this error is kept as small as possible, but in the modification of the method suggested by the author it is to be made the principal heat loss. The rate of cooling of the liquid under test will now be expressed in terms of the specific heat and thermal conductivity of the insulating material forming the cylindrical container. The nearest approach to this idea in previous literature is contained in the work of D. H. Andrews\* on the specific heats of some organic liquids, and he uses the term "calibrated heat conduction" as a means of specifying

Fig. 1.



the method. His experimental procedure is to place the substance under examination in a copper bulb surrounded by a layer of glass wool, through which heat is slowly conducted to it from the outside, while its temperature and the temperature gradient across the wool are measured at frequent intervals. By comparison of this gradient with that observed with a standard substance, the quantity of heat which, in a given interval, flows into the ball can be calculated. The heat capacity of the substance may be now derived from this quantity and from the rise in temperature of the substance during the given time-interval.

#### *Theory of the Method.*

Consider unit length of an infinite cylinder (fig. 1) of an insulating material, where  $r_1$  and  $r_2$  are the internal

\* J. A. C. S. xlvi. p. 1287 (1926).

and external radii respectively and  $\theta_1$  and  $\theta_2$  are the instantaneous temperatures of the internal and external surfaces of the tube. Then if K is the thermal conductivity of the material of the tube in cal. cm.<sup>-1</sup>. sec.<sup>-1</sup>. deg.<sup>-1</sup>, c is the thermal capacity of the material per c.c., and W is the combined thermal capacity of the stirrer and liquid contents per cm. length of the tube, it has been shown in a previous paper \* that

$$\frac{2\pi \cdot K}{\log_e r_2/r_1} = W \cdot \frac{\mu_1 \cdot \theta_1}{(\theta_1 - \theta_2)} + \frac{\pi \cdot c \cdot F}{(\log_e r_2/r_1)^2} \left( \mu_1 + (\mu_1 - \mu_2) \cdot \frac{\theta_2}{(\theta_1 - \theta_2)} \right), \quad \dots \quad (1)$$

where F is a function of  $r_1$  and  $r_2$  only.  $\mu_1$  and  $\mu_2$  are the slopes of the straight lines obtained by plotting time against  $\log_e \theta_1$  and  $\log_e \theta_2$  respectively.

Alternatively we may write

$$\frac{2\pi \cdot K}{\log_e r_2/r_1} \cdot \frac{(\theta_1 - \theta_2)}{\theta_1} \cdot \frac{1}{\mu_1} = (W_L + W_T) + B \cdot \left( 1 - \frac{\mu_2 \cdot \theta_2}{\mu_1 \cdot \theta_1} \right), \quad \dots \quad (2)$$

where  $W_L$  = the mean thermal capacity of the liquid contents per cm. length of the tube,  $W_T$  = the mean thermal capacity of the combined thermometer and stirrer per cm. length of the tube, and B is a factor which may be considered constant for a given temperature range of about 5° C. Now the maximum variation of the term  $B \cdot \left( 1 - \frac{\mu_2 \cdot \theta_2}{\mu_1 \cdot \theta_1} \right)$  for the different liquids used was never greater than 0.0025  $W_L$ , so that it may be considered constant to the required degree of accuracy. It follows immediately from the above equation that  $\frac{(\theta_1 - \theta_2)}{\mu_1 \cdot \theta_1}$  varies linearly with  $W_L$ , so that by plotting these two variables a straight line should be obtained.

#### Description of the Apparatus.

The apparatus was essentially that used for the determination of the thermal conductivity of ebonite †,

\* Loc. cit.

† Loc. cit.

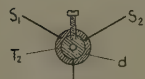
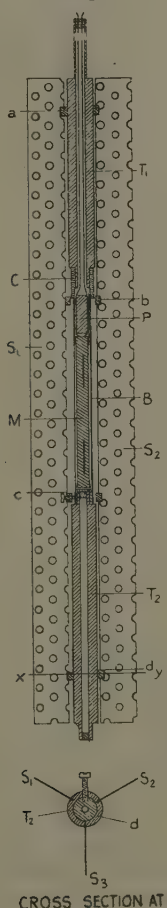
the identical ice-bath being employed in both experiments. The cylindrical form of the insulating material was also retained, but the problem to be overcome was the choice of thermal insulator, which had to withstand immersion in various organic liquids. An obvious solution to this difficulty was a double-walled copper cylinder, with a suitable substance filling the interspace. Such an arrangement, however, involved constructional work which, fortunately, could be avoided by the use of a material known commercially as Bakelite-Dilecto and supplied by the Continental Fibre Company. This material can be obtained in the form of tubes and sheets and is not dissolved by ordinary solvents such as alcohol, benzene, acetone, hot-water, etc.; furthermore, it will withstand a temperature of 100° C. continuously, and even 150° C. for short periods, without change of shape. A tube, nearly 38 cm. long and approximately 7.5 cm. external diameter, was machined and fitted with end plates, of similar design and dimensions as specified in the case of the ebonite tube previously mentioned.

Further comment is only necessary with regard to the method of stirring the contents of the bakelite tube.

A fundamental condition in calorimetric work is that the different portions of the liquid must be efficiently mixed, so that its true mean temperature is registered by the indicating thermometer. The type of stirrer which promotes mixing by an up and down operation suffers from the disadvantage, that the evaporation loss is increased by the continual exposing of fresh surfaces as the stirrer shaft moves in and out of the liquid. In this instance an additional disadvantage results from the fact that the mode of treatment of the problem requires only the temperature of the liquid near the central portion of the cylinder. Consequently, the requisite conditions were best realized by the use of a combined thermometer and stirrer of similar design to that used in the thermal conductivity experiment. A slight modification of this scheme was rendered necessary however, as a number of the test liquids employed were electrolytes. This alteration involved the enclosing of the resistance thermometer in a watertight container, an arrangement which introduced the possibility of thermometric lag. Particular care was therefore taken to keep this factor to a minimum value by reducing the thermal capacity

of the mica web, and using a thin metal tube as the container.

Fig. 2.



CROSS SECTION AT LINE xy

#### *Details of the Thermometer and Stirrer.*

The thermometer (see fig. 2) consisted of a platinum wire wound on the usual form of serrated mica cross, the strips of which, however, were made as small as possible (0.5 to 0.6 cm. wide and 7.5 cm. long). Copper

leads were hard soldered to the platinum wire and set in grooves situated along the bakelite plug P, finally passing upwards through the upper bakelite tube T (external diameter 1.2 cm. approx.). The mica frame M was contained in a thin walled brass tube B, to which was soldered a brass cap C; the latter being fixed to  $T_1$  by a screw thread. A second bakelite tube  $T_2$ , of identical cross-section as  $T_1$ , fitted into a suitable cavity at the lower end of B and hence preserved the desired symmetry of the combined stirrer and thermometer about the centre of the specimen tube. The upper and lower ends of  $T_2$  were closed by tight-fitting copper plugs, and a suitable reduction in the cross-section of the tube at its lower extremity was effected, so that it fitted the bearing surface set in the bottom end plate of the specimen tube. The stirrer consisted of three brass perforated strips ( $s_1, s_2, s_3$ ) soldered into four brass rings  $a, b, c$ , and  $d$ . Set screws passed through holes in these rings, and thus enabled the stirrer to be rigidly attached to the thermometer. The extreme breadth and length of the combined stirrer and thermometer were designed to fit the specimen tube closely, and hence satisfy the necessary requirements for the efficient stirring of the liquid contents.

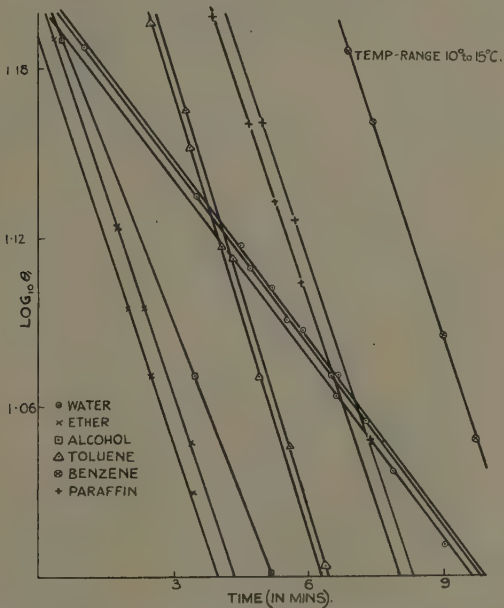
The variation of the combined thermal capacity of the thermometer-stirrer and the liquid contents with the length of the central portion of the tube chosen was negligible. This is evident by considering a particular example, the thermal capacity of the thermometer-stirrer being calculated with sufficient accuracy from the standard values of the thermal capacities of the component parts. For a length of 14.0 cm. the combined thermal capacity per cm. length (with water as the contained liquid) was 30.32 cals./deg. C., whereas 30.26 cals./deg. C. was the corresponding quantity for a length of 18.0 cm.

#### *Experimental Procedure.*

The bakelite tube and necessary apparatus having been adjusted in position, the ice-bath stirrer was set in circulation. After a sufficient period to enable stability of thermal conditions to be attained, the heated test liquid was introduced into the tube, and the speed of rotation of the thermometer stirrer temporarily increased to hasten the efficient mixing of the contents. At a

convenient time this rotational speed was reduced to a suitable value, which was recorded on a chronograph tape throughout the course of the experiment. This automatic recording was effected by the use of a worm on the shaft of the stirrer, and a toothed wheel, which, once every revolution, completed an electric circuit thereby operating a relay. The temperature of the cooling liquid was recorded at suitable time intervals by measuring the resistance of the thermometer with a

Fig. 3.



Callender and Griffith Bridge. Readings of the "wall thermometer," which consisted of a platinum wire wound in close contact with the outer surface of the bakelite tube, were also observed at intervals by means of the same instrument.

#### "Thermal Calibration" of the Bakelite Tube.

The "thermal calibration" of the tube was carried out by the use of a number of suitable liquids of accurately known thermal capacities. These liquids were carefully

chosen so that their different specific heats adequately covered a wide range of values, and they comprised the

Fig. 4.

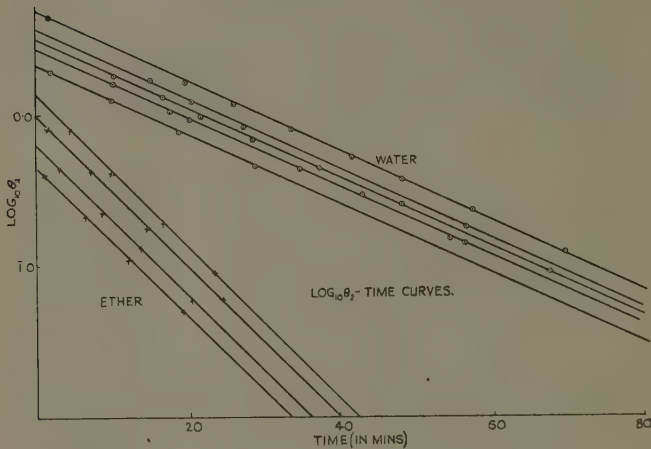
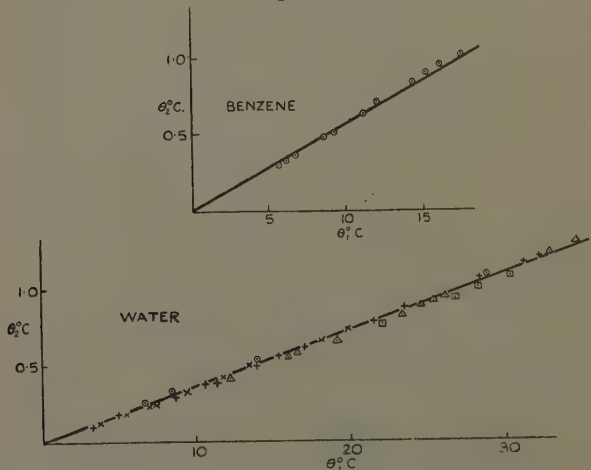


Fig. 5.

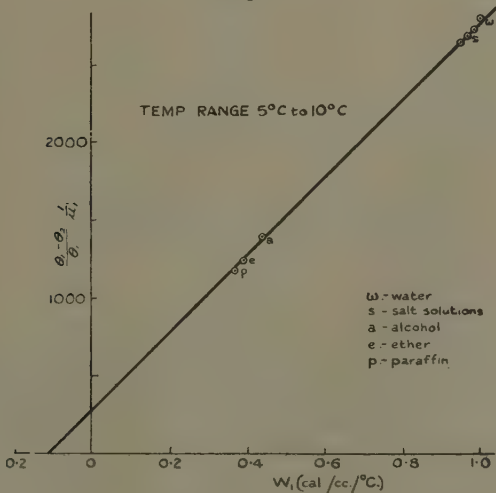


following. Ethyl alcohol, ether (the experimental values of the specific heats of these two liquids as obtained by

different observers showing good agreement), paraffin, distilled water, and sodium chloride solutions. I am indebted for the specimen of paraffin to Dr. H. R. Lang and Dr. R. Jessel, who had determined its thermal capacity by means of the continuous flow calorimeter. The salt solutions were utilized, by reason of their large specific heats, as confirmatory data for the "water reading."

Figs. 3 and 4 are typical log  $\theta$ -time curves, while fig. 5 shows that a linear relation exists between the inside and outside temperatures to the required degree of accuracy, over a restricted temperature range.

Fig. 6.



### CALCULATION OF RESULTS.

Temperature Range (10–15) deg. C.

Benzene :

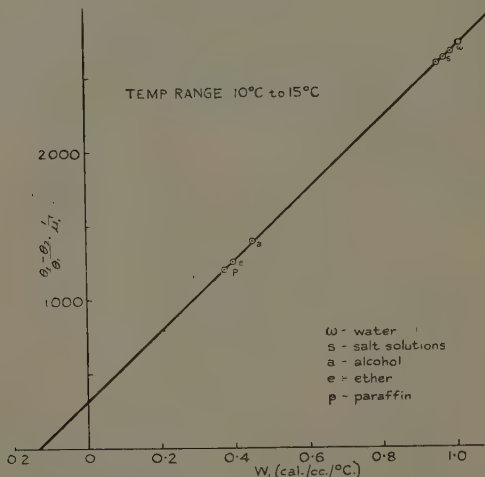
Graphs of  $\log_{10} \theta_1$  (and  $\log_{10} \theta_2$ ) against time were plotted, and from the slopes of the straight lines obtained (see fig. 3)  $\mu_1$  and  $\mu_2$  were deduced.

$$\frac{\mu_1}{2.3026} = 8.268 \times 10^{-4}; \quad \frac{\mu_2}{2.3026} = 8.40 \times 10^{-4}.$$

Corresponding values of  $\theta_1$  and  $\theta_2$  were also plotted, and the expression  $\frac{(\theta_1 - \theta_2)}{\mu_1 \theta_1} \times 2.3026$  calculated to be 1143.

From the graph of  $\frac{(\theta_1 - \theta_2)}{\mu'_1 \theta_1}$  against  $W_1$  (*i.e.*,  $\rho.s$ ),

Fig. 7.



Calibrating liquid.	Temperature range (10 to 15) ° C.		Temperature range (5 to 10) ° C.	
	$\rho.s$ cal. /c.c./° C.	$\frac{(\theta_1 - \theta_2)}{\mu_1 \cdot \theta_1} \times 2.3026$	$\rho.s$ cal./c.c./° C.	$\frac{(\theta_1 - \theta_2)}{\mu_1 \cdot \theta_1} \times 2.3026$
Distilled water . . . .	1.001	2701	1.003	2782
Paraffin . . . . .	0.376	1200	0.374	1176
(a) Ethyl alcohol . . . .	0.449	1396	0.445	1378
(b) Ether . . . . .	0.397	1251	0.398	1243
(c) NaCl solution (1) ..	0.986	2655	0.985	2705
(c) NaCl solution (2) ..	0.972	2631	0.972	2671
(c) NaCl solution (3) ..	0.955	2594	0.954	2635

The values of the specific heats, expressed in terms of the 15° C. calorie, were obtained from the following sources.

- (a) G. S. Parks, J. A. C. S. xlvi. p. 340 (1925).
- (b) Parks and Huffman, J. A. C. S. xlvi. p. 2789 (1926).
- (c) 'International Critical Tables,' ii. p. 327 (1930).

where  $\mu'_1 = \frac{\mu_1}{2.3026}$ , we find the value of  $\rho.s$  corresponding to  $\frac{(\theta_1 - \theta_2)}{\mu_1 \theta_1} \times 2.3026 = 1143$  is equal to 0.353 cals./c.c./deg. C (see fig. 7).

Now the density  $\rho = 0.884$  gm./c.c. at 12.5 deg. C., hence the specific heat of benzene at 12.5 deg. C. is found to be 0.399 cal./gm./deg. C.

### SUMMARY OF OBSERVATIONS.

Liquid.	$\frac{\mu_1 \times 10^4}{2.3026}$	$\frac{\mu_2 \times 10^4}{2.3026}$	Mean temp. ° C.	Specific heat cal./gm./ ° C.
Benzene .....	8.268	8.40	12.5	0.399
Benzene .....	8.160	8.40	8.0	0.402
Toluene .....	8.533	8.71	12.5	0.390
Toluene .....	8.555	8.71	7.5	0.386

The above results are in close accord with those of previous observers, as the following figures indicate :—

### Benzene.

Specific heat cal./gm./ ° C.	Temperature ° C.	Observer and reference.
0.3891	5.0	'International Critical Tables,' 1930.
0.3942	10.0	Accuracy $\pm 2$ per cent.
0.4062	20.0	
0.403	8.1	Huffman, Parks, and Daniels, J. A. C. S.
0.406	13.3	lii. 1930.
0.410	21.9	
0.4095	20.0	Richards and Wallace, J. A. C. S. liv.
		1932.
0.399	22.6	Ferguson and Miller, Proc. Phys. Soc. xlvi. 1932.
0.417	18.0	Marley, Proc. Phys. Soc. xlvi. 1933.

Specific heat cal./gm./° C.	Temperature ° C.	Observer and reference.
0.3856	0.0	' International Critical Tables,' 1930.
0.3986	20.0	Accuracy $\pm$ 1 per cent.
0.394	0.0	Nesselmann and Durdin, <i>Zeitschr. f. tech. physik.</i> xi. 1930.
0.401	10.0	
0.407	20.0	
0.4007	20.0	Richards and Wallace, <i>J. A. C. S.</i> liv. 1932.

It is to be noted that the author's value of the specific heat for benzene at 8.0 deg. C. is higher than that at 12.5 deg. C., which indicates the possible existence of a minimum value in the neighbourhood of these temperatures. This fact could be explained perhaps in the manner suggested by Callendar \* for the similar case of water. He proposed that the increase of specific heat on approaching the freezing-point was due to the presence of a certain proportion of dissolved ice molecules, though there was no obvious guide to the proportion required or to the latent heat of solution to be assumed.

#### DETERMINATION OF THE THERMAL CONDUCTIVITY OF BAKELITE.

If reference is again made to equation (2) it is easily seen that the thermal conductivity ( $K$ ) of the material of the tube may be deduced from the slope of the straight line obtained by plotting  $\frac{(\theta_1 - \theta_2)}{\mu' \theta_1}$  against  $W_1$ .

#### *Experimental Data.*

$$r_1 \text{ (over central } 18.0 \text{ cm. of tube)} = 3.138 \text{ cm.}$$

$$r_2 \text{ (,, ,,, ,,, )} = 3.719 \text{ cm.}$$

\* Phil. Trans. ser. A, excix. p. 147 (1902).

$$W_L \text{ (over central } 18.0 \text{ cm. of tube)} = 29.62 \rho \cdot s \text{ cals./}^{\circ}\text{C.}$$

per cm. length of  
the tube

$$= 29.62 W_1.$$


---

Temperature range ${}^{\circ}\text{C.}$	Slope of graph. $\frac{W_L \cdot \mu_1 \theta_1}{(\theta_1 - \theta_2)}$	K. cal./cm./sec./ ${}^{\circ}\text{C.}$
(5–10) .....	0.02762	$7.47 \times 10^{-4}$ at $7.5^{\circ}\text{C.}$
(10–15) .....	0.02831	$7.62 \times 10^{-4}$ at $12.5^{\circ}\text{C.}$

The following constants of bakelite were obtained by experiment :—

Density at  $15.0$  deg. C. =  $1.335$  gm./c.c.

Linear coefficient of expansion =  $2.5 \times 10^{-5}$  per deg. C.

Specific heat (by Joly's steam calorimeter) =  $0.383$  cal./gm./deg. C.

#### SUMMARY.

The specific heats of benzene and toluene have been measured over two temperature ranges ( $5$ – $10$ ) deg. C. and ( $10$ – $15$ ) deg. C. by an improved form of cooling method, and an accuracy of between one and two per cent. has been attained. By the procedure adopted the accuracy of the measurement can never be greater than that of the assumed specific heats of the "calibrating liquids," consequently it would be desirable to eliminate this uncertainty. An obvious solution of the problem is to use an electrical heating coil immersed in the liquid contained by the cylinder, and determine the electrical energy necessary to maintain steady thermal conditions at various temperatures. In effect this would enable the thermal conductivity K to be determined and, furthermore, by a cooling experiment with water the combined thermal capacity of the thermometer-stirrer and that of the walls of the tube may be evaluated. Therefore, it follows that the only unknown quantity in a cooling experiment with a given liquid will be the specific heat of the latter, which will be thus expressed directly in terms of the specific heat of water.

In the present series of experiments it was impossible to obtain satisfactory readings with the liquids of smaller specific heats, at temperatures above  $15.0^{\circ}$  C., owing to the rapidity of cooling, but this difficulty may be overcome either by choosing a better thermal insulator or altering the radial dimensions of the tube. A further question arises with regard to the existence of a stationary fluid layer on the inner surface of the bakelite tube. The presence of this film would tend to reduce the rate of cooling, and its effect would vary in magnitude with the nature of the contained liquid. Experiments were carried out with the object of detecting the reality of this layer, by determining the relation between the speed of rotation and the rate of cooling. Initial observations appeared to indicate that a minimum speed of stirring was necessary before the rate of cooling became approximately constant. During the present series of experiments the speed was made as large as possible to conform with the above desirable conditions. An inherent disadvantage of open calorimeters and mechanical agitation of the contained fluids is the possible presence of sufficient quantities of dissolved air in the liquids to affect seriously the specific heats. This source of error, however, may be minimized by employing high speeds of stirring and, as in the present apparatus, by reducing the area of the "open" surface of the liquid. The chief advantage of the present experimental procedure over the ordinary cooling method is that the thermal conditions may be quite definite and identical for both the test and the standard liquid. This point is especially important in the case of a liquid which has a large coefficient of thermal expansion, when the assumption that the cooling surface remains invariable with time can be quite erroneous if the ordinary cooling method is employed. In order to exemplify this statement let us take the case of ether, whose coefficient of cubical expansion is  $16 \times 10^{-4}$  per deg. C. It is evident that a change of temperature of only  $6^{\circ}$  C., will produce a variation in surface area of nearly one per cent. This error is avoided by the arrangement adopted in the present experiments, where the temperature of the liquid is observed only at the centre of the cylinder, which is maintained full of liquid.

The thermal conductivity of Bakelite-Dilecto has also been deduced from the experimental data.

*XXVII. Deposits of Elements by High-Frequency Discharge.* By D. BANERJI, M.Sc., Lecturer in Physics, University College of Science, Calcutta, and DIHIRANJOY BHATTACHARYA, M.Sc.\*

[Plate XI.]

### 1. Introduction.

IN a paper recently published in the Philosophical Magazine † a new phenomenon of deposition of mercury on the inside wall of a high-frequency discharge-tube containing the vapour of the element was described. The deposits, which were in the form of symmetrical rings of thin films of the material, were formed on the inside wall not far from the positions occupied by the external sleeve electrodes which fed in the high-frequency current.

The formation of the deposit was attributed to the nature of the distribution of space-potential along the axis of the tube as referred to that along its wall. This introduced radial electric forces which were responsible for driving the positively charged ions of mercury to distinct positions on the wall of the tube. If the above view were correct then ions charged negatively would be expected to form deposits in positions other than those of the positive ions. For instance, with positively charged mercury ions it was found that no deposit was formed immediately under the external sleeve electrodes. With negatively charged ions, therefore, the deposit would be expected to be formed immediately under the electrodes.

In order to verify this hypothesis, experiments were performed with elements which could copiously supply either positive or negative ions in discharge-tubes. Since the atoms of the metals of the first and the second groups of the periodic table of elements part readily with their outer electrons in discharge-tubes and form positive ions, the metals potassium and mercury were chosen for obtaining the supply of positive ions. Again, since the atoms of non-metals of the sixth and the seventh groups in the table, readily form negative ions by attaching electrons to themselves, sulphur and iodine were chosen to supply negative ions in the discharge-tube.

\* Communicated by Prof. S. K. Mitra, D.Sc.

† D. Banerji and R. Ganguli, Phil. Mag. ser. 7, xv. p. 676 (March 1933).

*2. Experiment and Observation.*

Two sets of experiments were performed to obtain the deposits of the elements. In one set the metals, potassium and mercury, and in the other set the non-metals, sulphur and iodine were used. In each of the two sets of experiments two different types of electrodes were used with similar discharge-tubes. In one type the electrodes were of the usual sleeve form as used in our previous experiments with mercury, and in the other type the electrodes were in the form of rings and were made of copper wire (25 S.W.G.). Both the types of electrodes were fitted externally to the tube, the diameter of which was 2 cm. (the corresponding diameter in the experiments previously reported was 2 to 3 cm.). The high-frequency a.c. used in the discharge was of 4000 kilocycles per sec. In order to obtain a copious supply of vapour of the elements in the discharge-tube a small quantity of the element was placed at the bottom of the tube, which was then exhausted to a pressure of about a millimetre of mercury. A slight heating of the tube from outside facilitated the striking of the discharge. The deposits were generally distinctly visible on the inner wall of the tube after a run of about three-quarters of an hour. The deposits obtained with rings were sharper compared with those obtained with sleeve electrodes.

In order to find out the effect of the exciting frequency on the nature of the deposit, three different frequencies were employed in the case of mercury, namely 600, 4000, and 10,000 kilocycles per sec. From the deposits that were obtained no effect of variation of frequency on the shape, size, and the distance between the deposits could be obtained.

The photographs of the deposits that were obtained with the various elements, potassium, mercury, sulphur, and iodine respectively are given in Pl. XI. Figs. 1, 2, 3, and 4 represent the deposits of these elements in succession with broad sleeve electrodes fitted externally to the discharge-tube. Figs. 5, 6, 7, and 8 represent the same in succession but with narrow ring electrodes. The positions and the relative sizes of the electrodes are indicated on the plate by broad arrow-heads in the case of sleeve electrodes and by fine arrow-heads in the case of ring electrodes.

The following points may be noted in the photograph:—  
(1) In the case of metals (figs. 1, 2, 5, and 6) no deposit is formed underneath the electrodes. In the case of non-metals (figs. 3, 4, 7, and 8) the deposit is formed underneath the electrodes. This confirms the hypothesis that the deposits are due to the peculiar nature of the radial electric field in the discharge-tube.

(2) The distance between the deposits formed on either side of the electrodes decreases with the increase of the atomic weight of the element. This is true for both sleeve and ring electrodes.

### 3. Summary.

In the study of the deposits of metallic mercury on the wall of a high-frequency discharge-tube as previously reported, it was suggested that the formation of the deposit was due to the nature of the gradient of potential between the axis and the wall of the discharge-tube. The radial electric force thus developed was responsible for driving the positive ions of mercury formed by the discharge to distinct positions on the wall of the tube. It followed from this that the positions where the deposits of positive ions were formed would be other than those of negative ions. In order to test this view, experiments have been performed with the metals potassium and mercury for positive ions and the non-metals sulphur and iodine for negative ions. The experimental results confirm the correctness of the hypothesis. Photographs of the deposits are given which show that the deposits of metallic ions are formed in positions other than those of non-metallic ions.

It has further been found out that other conditions being the same the distances between the deposits formed on either side of the electrodes decreases with the increase of the atomic weight of the element. This is true for both sleeve and ring electrodes.

In conclusion, we express our best thanks to Prof. S. K. Mitra for his helpful advice and guidance during the course of the investigation.

*Note added in proof.*—Since the paper was communicated, a note by Robertson and Clapp has been published in ‘Nature’ (Sept. 23, 1933) in which some interesting

features of deposit of elements by high-frequency discharge have been discussed. Amongst others, they have been able to obtain ring-like deposit in the case of iodine. The uniform deposit of iodine, recorded by us in our previous paper (*Phil. Mag.* xv. p. 676, 1933), is to be ascribed to an excess of vapour of iodine inside the discharge-tube formed by overheating of the element by outside flame. The ring deposits of iodine were thus hidden by the uniform deposit. It will, however, be noticed that in figs. 4 & 8 (Pl. XI.) we have been able to obtain rings of iodine besides those of mercury, sulphur and potassium.

Wireless Laboratory,  
University College of Science,  
92 Upper Circular Road, Calcutta.

---

### *XXVIII. Notices respecting New Books.*

*High-Frequency Measurements.* By A. HUND. [Pp. 491+xi.]  
(New York : McGraw-Hill Publishing Co., Ltd. Price 5 \$.)

THE development in high-frequency measurement technique has been so rapid in the last few years that even the worker whose main interest lies in this field may well have difficulty in making himself familiar with the latest methods, while the investigator in other subjects who has to make an occasional measurement involving high frequencies will probably be in doubt as to the best way to proceed. A book such as this, which brings together in a handy form the results of the latest researches, should therefore have a warm welcome from all who are concerned with measurements at either audio or radio frequencies.

One finds, as is naturally to be expected, a full account of the well-known bridge methods for impedance determination, but the greater part of the book is concerned with measurements made with the thermionic valve and also with the cathode ray oscillograph. The first chapter presents in convenient form the fundamental properties of resonant circuits, and includes also a discussion on the circuit through the vacuum tube. Then follow chapters on high-frequency sources and the measurement of small currents and voltages. The reader will find in this latter chapter a comprehensive

account of the many ways in which the three-electrode valve may be used for this purpose.

The later chapters of the book are particularly adapted to the requirements of the radio engineer in that the subjects dealt with include the measurement of frequency and modulation and the determination of the constants of aerials and high-frequency feeders.

One of the most valuable sections is that which is concerned with measurements on wave propagation. A large amount of data has been recently published on this subject, and it is convenient to have this excellent summary of the more important methods. The book ends with a useful chapter on piezo-electric apparatus.

As is to be expected in a work of this type, a fair amount of physical and mathematical knowledge on the part of the reader is assumed, but this will not detract from the usefulness of the book to those for whom it is evidently intended. References to original articles are profuse throughout, and this fact, together with the inclusion of many useful tables, will make the book of very great value as a work of reference in the high-frequency laboratory.

*Theory of Thermionic Vacuum Tubes.* By E. L. CHAFFEE, Ph.D. [Pp. 652+xxiii.] (London : McGraw-Hill Publishing Co., Ltd. Price 6 \$.)

THE author of this book is Professor of Physics at Harvard University, and has evidently taken considerable pains to produce as complete an account of thermionic valve theory as is possible at the present time. A survey of the matter included will indicate immediately the success with which this object has been attained, notwithstanding that certain sections of the subject, notably those dealing with large-power valves, gas-filled valves, and rectifiers, have had to be omitted from the present volume, and are promised in a further one.

As the title indicates, the work deals principally with the valve itself rather than with the various circuit arrangements in which it may be utilized, and we find in consequence that considerable space is allotted to the section dealing with the conduction of electricity by electrons *in vacuo*. Thereafter follow chapters dealing with the three-electrode valve both from the design and operation points of view. The triode as amplifier and as regenerator or resistance reducer is then treated, followed by the operation of triodes coupled by resistance and transformer methods.

One of the most interesting chapters is that dealing with the operation of triodes in conjunction with tuned coupled circuits. Three-dimensional models demonstrate very effectively their properties with varying impressed frequency and circuit parameters. Equally important, and of particular interest at the present time, is the treatment in later chapters of the detection of modulated signals both by diodes and triodes and with large and small impressed voltages. The concluding chapter contains a useful account of the action of tetrodes and pentodes, including such special types as the variable- $\mu$  tetrode and the electrometer valve.

A list of symbols employed throughout the book is conveniently placed at the beginning, and although the list looks rather formidable as to its length, the symbols are carefully explained as they are introduced in the text, and do not interfere with the very readable characteristics of the book as a whole. The book can be confidently recommended to those requiring an exceptionally thorough treatment of the thermionic valve.

*Thomas Young, F.R.S.: Philosopher and Physician.* By FRANK OLDHAM, M.A. [Pp. 159, with portrait.] (London: Edward Arnold & Co., 1933. Price 6s.)

An excellent little book, giving "a concise account of the life and work of one who was both a scientist and a philosopher." The book is an outcome of a suggestion made by Lord Rutherford during one of his lectures in the Cavendish Laboratory. Young received a medical training; nevertheless he was Professor of Natural Philosophy at the Royal Institution for two years, after which he went back to medicine, diversified with other pursuits, such as exploration into the interpretation of Egyptian hieroglyphics. But it is as a natural philosopher that he is best known and has the highest reputation. This book gives a very interesting account of what he achieved, particularly in regard to the nature of light and colour. Perhaps a little too much space is given to Brougham's animadversions in the 'Edinburgh Review'; but the reader can pass lightly over these.

*Introduction to Physical Chemistry.* By ALEXANDER FINDLAY, Professor of Chemistry in the University of Aberdeen. [Pp. vi+492, with 124 figures.] (London: Longmans, Green & Co. Price 7s. 6d.)

THE aim which the author has had in view in writing this book was to provide a textbook which should not only serve

as an introduction to physical chemistry but should also carry the student on to such a point that he can read with profit the numerous special monographs which are now available. Numerous references are given to original literature, so that supplementary information can always be obtained by the teacher or student.

The writer has a clear style, and his account of the matter should give students a sound introductory knowledge which takes into account even some of the most recent work. Now and then lapses take place. For example, Joule and Kelvin never discovered the inversion point of their effect in connexion with the expansion of gases. It was Olszewski who found it. All that the original investigators found was that while the effect was positive, *i.e.*, cooling, in the case of air, it is negative in the case of hydrogen (*i.e.*, warming) under the conditions of their investigations.

The book covers a very wide ground. It is doubtful whether it is wise to cover so wide a range in introductory teaching. It has the advantage, however, that the teacher or reader can select the portions with which he is specially concerned.

*Handbook of Mathematical Tables and Formulas.* Compiled by R. S. BURINGTON, Ph.D. [Pp. 251.] (Handbook Publishers Inc., Sandusky, Ohio, 1933. Price 2 dollars.)

IT is claimed that the scope of this handbook is sufficiently inclusive to meet the needs of workers in such sciences as chemistry, physics, and engineering, but this must be understood in an elementary sense. The first section consists of formulæ in algebra, geometry, and calculus, but does not include any differential equations. It is attractively arranged and contains very useful tables of indefinite and definite integrals covering altogether about 29 pages out of 86. The second section contains the usual tables of the elementary functions (some to four and some to five places and including trigonometric functions to radians) and some additional ones such as short tables of the error integral (form in  $e^{-x^2}$ ), elliptic integrals and the gamma function, and a few actuarial tables. Special mention may be made of the trigonometric tables to five places at one minute interval,  $\log x$  to five places for  $x=10(1)1109$  and  $\log_{10} x$  to ten places for primes under 1000.

As regards the essential features of reliability and facility of use, the book seems satisfactory after a short trial. It is of a convenient size (5½" by 8"), the cover is flexible and the book stays open anywhere, the printing is clear and well-spaced on good paper, and there is an efficient index. The

type used in the tables is not as now usually recommended, but is uniform and easily legible, and care has been taken over details. No attempt at complete checking of the tables has been made, but examination of portions of several showed only one mistake ; p. 240, for  $\sin^{-1} k = 6^\circ$ , K should be 1.5751. One or two misprints noticed in the text are of no importance.

*The Hollerith and Powers Tabulating Machines.* By L. J. COMRIE, M.A., Ph.D. [Pp. 48.] (London : Printed for Private Circulation, 1933. Price 2s.)

THIS is a revised edition of a valuable article first published in 1930 in the 'Transactions' of the Office Machinery Users' Association and includes recent developments which were described in the author's Newmarch Lectures early in 1933. It provides a unique study and comparison of these two important types of punched-card using machines, with a full discussion from the user's point of view of their capabilities, costs, necessary equipment and labour, speed of working, and so on. There are 41 excellent illustrations and skeleton diagrams, and details are included not only of the standard machines, but also of the smaller and less expensive types which have been introduced to meet the needs of a wider class of user.

The whole is written from the standpoint of the author's experience as Director of the 'Nautical Almanac,' and he has also published an account of the application of the Hollerith machine to a special problem ('Monthly Notices' R. A. S. xcii. p. 694 (1932)). Anyone interested in the possibilities of easing the mechanical labour of numerical work would be well advised to obtain a copy of this pamphlet from the author at the Royal Naval College, London, S.E. 10, and so familiarise himself in an easy and pleasant manner with the machines before consulting the makers. Dr. Comrie's work in developing the scientific possibilities of commercial calculating machines, as well as in the actual production of standard mathematical tables, needs only to be known to be appreciated.

[*The Editors do not hold themselves responsible for the views expressed by their correspondents.*]

URISON.

Phil. Mag. Ser. 7. Vol. 17. Pl. VIII.

FIG. 1.



FIG. 2.



FIG. 3.





FIG. 4.

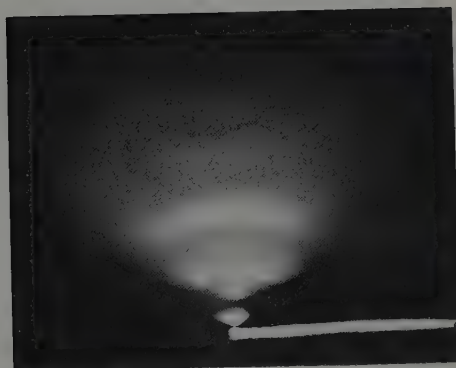


FIG. 5.

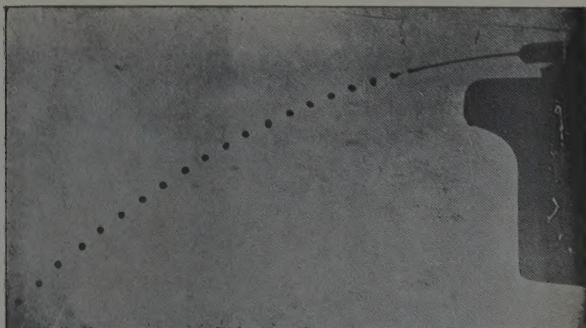


FIG. 6.



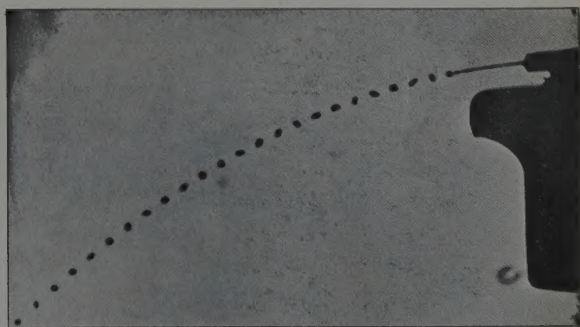


FIG. 4.



Spark photograph. Water jet in air.  $d=65$  mm.  
Drop formation frequency = 248. Magnification = .715.

FIG. 5.



Stroboscopic photograph. Water jet in air.  $d=65$  mm. Flashing neon lamp source. Drop formation frequency = 281. Exposure = 1 minute; constant jet speed. Magnification = .715.

FIG. 6.



Stroboscopic photograph. Water jet in air.  $d=65$  mm. Exposure =  $\frac{1}{2}$  minute, constant frequency of drop formation = 281; variable



FIG. 1.

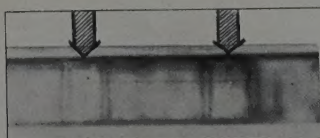


FIG. 2.

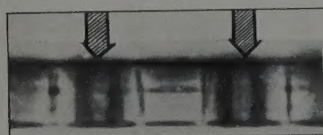


FIG. 3.

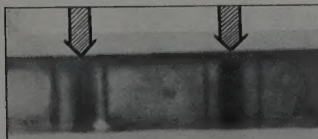


FIG. 4.



FIG. 5.

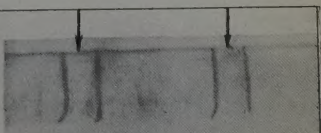


FIG. 6.

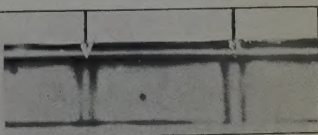


FIG. 7.

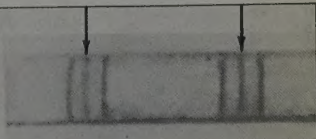
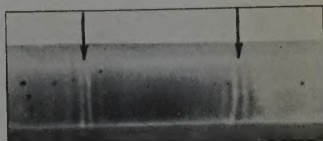


FIG. 8.



Illustrating deposits of elements by high-frequency discharge.

Figs. 1 & 5, Potassium ; figs. 2 & 6, Mercury ; figs. 3 & 7, Sulphur ; figs. 4 & 8, Iodine. Figs. 1, 2, 3, & 4 are with "sleeve" electrodes and figs. 5, 6, 7, & 8 are with wire electrodes.

The positions and the relative widths of the electrodes, which are in the form of rings and are fitted outside the discharge-tube, are indicated by arrow-heads. Broad arrow-heads are for sleeve electrodes and narrow arrow-heads are for wire electrodes. Note that in figs. 1, 2, 5, & 6 (metals) there is no deposit underneath the electrodes, while in figs. 3, 4, 7, & 8 (non-metals) there is deposit immediately underneath every electrode.

